# Research Experiences for Undergraduates Program

## 1998 Program Report

National Radio Astronomy Observatory

# Research Experiences for Undergraduates Program
# 1998 Program Report

National Radio Astronomy Observatory

# Table of Contents

# National Radio Astronomy Observatory
# REU Program Report

## Overview

Nineteen undergraduates participated in the 1998 Research Experiences for Undergraduates Program sponsored by the National Science Foundation, at the NRAO. Research initiated in previous years by some students and their mentors continues, giving the program a continuing impact even for students who have departed. In this report we divide the narrative into four main sections, each of which covers activities in the program and research conducted at one of the four main NRAO sites; Charlottesville, Socorro, Green Bank and Tucson. In an Appendix, we include the reports which many of the students wrote as part of their experience. Seven of the research projects will be presented at the 193rd meeting of the American Astronomical Society in Austin, Texas, in January, 1999. All of these presentations are expected to be published in astronomical journals during 1999.

Several students were supported by non-REU funds--graduate students, graduating seniors, or foreign students. They are included in this report for completeness. Specifically, these students include: Ronak Shah, Charlie Silver, Josh Bloom, Andreea Petric, and Laura Woodney. Ms. Petric and Mr. Silver were 1997 REU students who returned to pursue their research. NRAO policy is not to support the same student from REU funds for more than one summer.

There were 87 applicants to the program, of whom 35 (40%) were women. There were 23 positions which were filled, of which 19 were funded from under REU guidelines. Of these 23 positions, 13 (57%) were filled by women. Of the REU positions, 11 (58%) were filled by women. Since the REU program was planned before funding actually arrived, only 15 of the 19 students were actually supported by REU funds directly from NSF for this purpose; the remaining students were funded from other sources.

# 1998 Research Experiences for Undergraduates Program

## National Radio Astronomy Observatory

## Research Projects by NRAO Site

- Charlottesville
- Socorro
- Green Bank
- Tucson

## Charlottesville, Virginia (NRAO Headquarters)

There will be four students in the 1998 NSF Research Experience for Undergraduates (REU) program at NRAO-Charlottesville. Highlights of the program will include a series of introductory level lectures on aspects of astronomy, particularly radio astronomy, spread over a few weeks. These lectures are intended to aquaint the students with the research which various staff members carry out.

Summer students from Green Bank and Charlottesville met at a get-together with mentors and lecturers in Charlottesville.

Many of the students in the NRAO-Green Bank program will visit Charlottesville for a tour of the Central Development Laboratory , and of the University of Virginia's facility for the fabrication of the Semiconductor-Insulator-Semiconductor detectors used in millimeter wave receivers, the Semiconductor Device Laboratory.

The students enjoy an informal get-together with astronomers from the University of Virginia and NRAO at lunch. followed by a visit with graduate students from the University's Astronomy Department.

1998 Summer Students (L-R):Kjersten Bunker, Greg Stinson, Laura Woodney, Andrew West and Jessica Golub at the controls of the 43m telescope. Water is the dominant consitituent of comets but is unobservable owing to the earth's atmosphere. However, its photodissociation product OH can be observed with the 43m telescope. Unfortunately, not by us--we only established upper limits to the molecular loss rate.

1998 Summer Students and others launch a rocket from the NRAO-Green Bank airstrip (L-R): Andrew West, Greg Stinson, bystander, J. Wootten and L. Stone.
Later in the summer, the Charlottesville students visited Green Bank to use the NRAO telescopes located there, to meet members of the Green Bank staff, and to attend the annual picnic. The students wrote a Target of Opportunity proposal to measure OH in comets which was awarded time.

The students gave a series of 15 minute talks on their projects during a lunch symposium in Charlottesville before they begin leaving for the summer. They produced short reports describing their summer research.

One highlight will be the placing of the backup structure onto the Green Bank telescope ( GBT ), the world's largest steerable telescope. It is an offset paraboloid, 110m across the longest axis, incorporating

16 million lbs of steel in the moving structure. The surface is more than half complete on the structure; during the rest of the year it will be completed. We went go to Green Bank for observations, and watched the process.

During the course of the summer, the students conducted several short observing sessions in Green Bank on the 43m telescope, and toured the Green Bank Telescope, in a final phase of construction this summer. The 40 ft telescope there is a student telescope, open for any project which students would like to carry out on it (though its instrumentation is limited). If there is interest, we may carry out, probably remotely, a project on the VLA or 12m telescope in Tucson.

We're very excited about the Millimeter Array, which was selected as the top priority for a new astronomical instrument in the 90s back at the beginning of the decade by the Astronomy Survey Committee. Funding has been approved and should begin in June 1998.

# CV Summer Student Schedule, Summer 1998

| **Date** | Person | **Item** | **Location** | **Time** |
|---|---|---|---|---|
| 5 Jun | open | Public Night at McCormick Observatory | at the Observatory | 9pm |
| 7-8 Jun | Wootten | Observing on 43m Telescope, Green Bank | NRAO, Green Bank | 1am for 25 hrs |
| 15 Jun | Wootten | Introduction | NRAO,Room 317, Stone Hall | 9am |
| 19 Jun | open | Public Night at McCormick Observatory | at the Observatory | 9pm |
| 26 Jun | McMullin | 43m observations: OH in Comet Soho | Observing on 43m Telescope, Green Bank | |
| 3 Jul | open | Public Night at McCormick Observatory | at the Observatory | 9pm |
| 8 Jul | Garwood | AIPS++ | NRAO,Room 317, Stone Hall | 9am |
| 10 Jul | Kellerman | Accidental Radio Astronomy | NRAO,Room 317, Stone Hall | 9am |
| 13 Jul | Turner | Interstellar Molecules and Their Chemistry | NRAO,Room 317, Stone Hall | 9am |
| 17 Jul | open | Public Night at McCormick Observatory | at the Observatory | 9pm |

| | | | | |
|---|---|---|---|---|
| 22 Jul | Wiseman | Young Stars | NRAO,Room 317, Stone Hall | 9am |
| 23 Jul | Bradley | Central Development Lab Introduction | Rm 228 Ivy Road | 9am |
| 23 Jul | Bradley | Tour of Central Development Lab | Rm 228 Ivy Road | 10am |
| 23 Jul | | Lunch with U. Va. | NRAO,Room 317, Stone Hall | 12pm |
| 23 Jul | Bradley | Tour of U. Va. Device Fabrication Facility | U. Virginia | 1:20pm |
| 23 Jul | Wootten | BBQ for CV, GB REUs and mentors | Wootten Home | 6pm |
| 24 Jul | Wootten | Dense Clouds; Interstellar and Cometary | NRAO,Room 317, Stone Hall | 9am |
| 1 Aug | | CV REUs -> Green Bank Picnic | Green Bank, W. Va. | noon |
| 3 Aug | Wells | The Green Bank Telescope | NRAO,Room 317, Stone Hall | 9am |
| 7 Aug | Simon | The Millimeter Array, Extrasolar Planets, and Zodiacal Light | NRAO,Room 317, Stone Hall | 9am |
| 7 Aug | open | Public Night at McCormick Observatory | at the Observatory | 9pm |
| 10 Aug | McMullin | 43m observations: OH in Comet Giacobini-Zinner | 43m telescope, GB | 9am |
| 14 Aug | Students | REU research presentations | Rm 317, | high noon |
| 21 Aug | open | Public Night at McCormick Observatory | at the Observatory | 9pm |
| 22 Aug | McMullin | 43m observations: OH in Comet Giacobini-Zinner | 43m telescope, GB | 9am |

**Ronak Shah of The University of Virginia works with Al Wootten on**

## Deuterated Molecules in Star-Forming Regions

The quest of star--formation studies involves observing and modelling systems forming Solar--analog stars. This proposal undertakes an investigation of deuterated molecules as an alternative method of examining such objects. Cold gas--phase and grain--surface fractionation enhances the abundance of deuterium in molecules above the canonical D/H ratio (1-2 x 10^5). Recent NH2D observations of infall signatures towards protostars, such as NGC 1333 IRAS4A, show agreement with data on CS, N2H+ and HCO+. These results indicate that deuterated species can underscore the kinematic and chemical evolution of low--mass protostars forming Solar--analogs. This proposal's goal encompasses understanding the dynamics of star--forming material, and the coeval physio--chemical effects denoted in spectra of deuterated molecules. This will be accomplished with single--dish and interferometric observations, and archived infrared and X--ray data in order to address protostellar evolution models. This may eventually aid in understanding the evolution of the Solar Nebula.

This work was presented at the 193rd AAS Meeting Session 71

**Greg Stinson, of Carleton College**
**and Kjersten Bunker, of North Carolina State University**
**work with John Hibbard**
**on**

## Merging Galaxies

# Greg Stinson's Summer: Interacting Galaxies

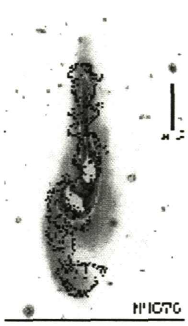

Galactic mergers are some of the most dynamic events in the universe. Tidal (just gravitational) forces strip stars and gas out of a galaxy into elegant tidal features while other material is compressed causing copious star formatio n. The fact that all these effects are the result of simple gravity is astonishing.

For many years, scientists did not believe that the features seen in peculiar galaxies could possibly be the result of Newton's simple gravitational law, Fg = G M m / r^2. (Newton, 1726, Royal Academic Society) There were various theories that related these features to the jets seen in distant radio objects. Looking at **Figure 1** (left), a picture of NGC 4676, or "The Mice", one can understand where they would get such an impression. The northern tail extends straight out from the top, why shouldn't that be a jet?

Astrophysicists were led back to simple gravity by Alar and Juri Toomre in 1972 (ApJ 178, p. 623). The Toomres ran 3-body code to simulate galactic mergers. The three bodies are two galactic potentials and one test particle that moves at the behe st of these combining potentials. In one simulation, it is possible to have multiple test particles. Each particle tests a different starting position. On the order of 100 test particles were thrown into these potential wells.

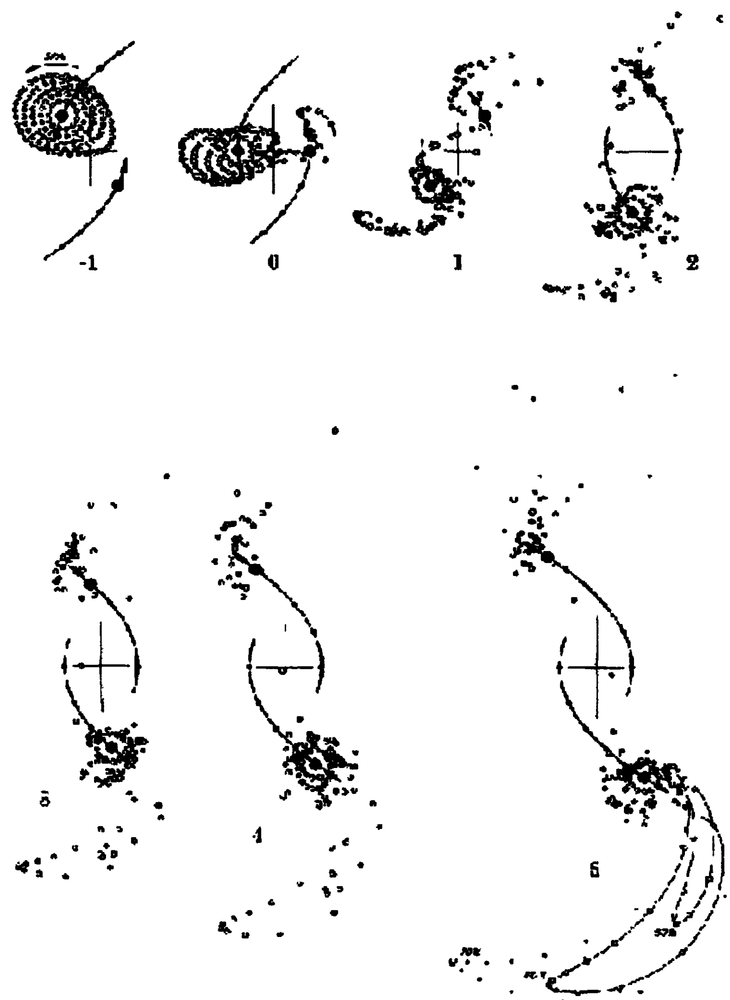


**Figure 2:** Evolution of interacting galaxies using 3-body method, note development of "tails" and "bridges" (Toomre & Toomre 1972)

The features that formed by running the model were arcs streaming out of the interacting galaxy as shown in figure 2. The Toomres called these arcs "tails". They also noticed similar features coming out the other side of galaxies which they called "anti-tails", but which are commonly called "bridges" because they appear to be material connecting two galaxies. The Toomres' found that they could manipulate the size of these tidal features by altering the interaction geometry. There are four main parameters, the size of the orbit (or distance between the two galaxies), the ellipticity of the orbit, the inclination angle of each galaxy in relation to the orbital plane, and the amount which you rotate each galaxy about the axis perpendicular to the orbital plane, or argument of periapse. This geometry is shown in figure 3.

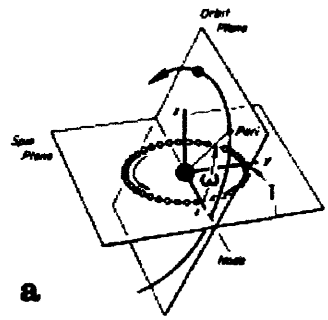

**Figure 3:** Encounter geometry, note "i" = inclination angle, "w"=argument of periapse (Toomre & Toomre 1972)

In general, the tail will be ejected in the plane of the galaxy, so if the galaxy is inclined to the orbital plane, the tail will come out at that inclination angle. As the inclination angle becomes greater (that is, as the galaxy's plane become s more perpendicular to the orbital plane, assuming one starts with the galaxy rotating in the same direction as it is orbiting the other galaxy), the tail decreases in size. And then as that inclination angle becomes greater than perpendicular (the gala xy is rotating the direction opposite to the orbital direction), no tail is formed.

The other angular parameter with which one can fiddle, the argument of periapse, does not have as large an effect on the creation of the tidal features. The main effect is in viewing angle or the angle at which the tail appears to be in relationship t o the other galaxy's tail. This is useful in the case where tails are coming out of both galaxies in an interacting system and one needs to have the two tails relate to one another at a certain angle. A much slighter effect is a widening of the tai 1 when the argument of periapse is increased.

It should be noted that the Toomres' were not the first to use computers to simulate the gravitation effects on interacting galaxies. Nine years earlier, Pfleiderer (1963, Zs.f.Ap, 58, 12), a single grad student was unsuccessful in the formation o f tidal features because his galaxies moved past one another faster than they could have interacted.

Using all these tools, the Toomres' were able to match the morphology (visual shape) of galaxies. They matched four systems: two with spirals and companion, Arp 295 and M51 (the "Whirlpool Galaxy"), and more typical early stage mergers, NGC 4038/ 9, "the Antennae", and NGC 4676, "the Mice".

At the time these matches were done, there was only good morphological data. Techniques for obtaining kinematics (velocity) data were confined to one-dimensional long slit spectra. These could only give kinematics in especially bright regions and the re only along a line. Today, Fabry-Perot interferometers can be used for bright optical sources while spectral line data collected by radio interferometers can be used for regions rich in neutral Hydrogen gas. Both of these techniques provide velocity i nformation for each point on an image. Thus, one can know the velocities at which points in the tail are moving relative to one another.

This information has made it possible to match more than morphology. My project stemmed from this desire to match n-body simulations to detailed observations. Several systems have already been matched using kinematics data including a rematch of NGC 4676 and NGC 7252. One might wonder at the need to rematch what the Toomres' have already matched. It turned out that this additional exploration lead to the discovery that material in tails that is closer to the galaxy has a smaller apocenter than material farther out in the tail. This return of tail material to the merging body may cause fine gas structure in the resulting elliptical galaxy.

After matching such relatively simple interactions, there was a desire for something more challenging. In a survey of 14 interacting systems using the VLA, three particularly odd systems were found. Arp 299 was one of these. Using optical images, this galaxy looks like a relatively normal interacting system, with one galaxy producing a tail. But, when the VLA gas data was laid over the optical, the gas tail appeared separate from the optical. Reasons for this were guessed at: A) A superwind, created by the outflow from the numerous supernovae ignited by the galactic interaction could have created a hot, gaseous medium that would ram pressure strip the gas out of the tail, leaving the stars as an optical remnant. While this seems reasonable, the two tails seem like fully formed tidal features, each having been created on it's own. This leads to a second possibility, B) The two tails are actually one very wide tail, that appears to be two because of projection effects. In this case, an explanation for the separation of materials needs to be found. In the Toomres' model, outer rings of test particles begin the formation of the tail, followed by inner rings of test particles. Thus, the outside parts of tails are composed of the material from the outside of a galaxy while the inside of tails is from further in the galaxy. In the disk of spiral galaxies, optical surface brightness falls off exponentially, while the gas density falls off at a much less precipitous rate. Combining these two observations, it seems plausible that the outer part of a tail would be composed of primarily gas while the inner part would have a higher optical content. Then, if the galaxy were oriented towards us just right, we would see this disparity between tails.

It was this second possibility that led to my investigation of n-body simulations. What needed to be determined was whether or not just gravity could create a wide tail with different makeups at different locations. To do this, we first needed to run gravitational n-body simulations. The code that we used was created by Josh Barnes and uses a tree as a data structure to hold the particles that make up the galaxy. With this method, it is possible to quickly run a true n-body simulation. What separates an n-body simulation from a three-body simulation is the changing of potentials. In a three-body simulation, the potentials of the two massive bodies remain constant, while the third particle is effected by the changing summation of these 2 constant potentials. But, in an n-body, the potential energy contours are recalculated with each iteration based on the location of all n particles. The n-body method is better able to model the intricate gravitational effects than 3-body simulations.

The first step in running any simulation is to narrow parameter space by making assumptions based on observations. In our case, we knew that one of the galaxies did not create a tail. From the Toomres', we know that this galaxy must be spinning with a retrograde orientation or be perpendicular to the orbital plane. A couple of initial attempts showed that the perpendicular orientation produced the proper morphology. The separation of the galaxies at periapse also needed to be determined. At too great a distance the galaxies would barely interact, too close and the interaction would happen too quickly producing an undersized tail. One-half of a scale unit was determined to be the proper distance. The remaining parameter to be manipulated was the angle at which the tail-forming galaxy should be to the orbital plane. This parameter could not be so easily determined. The tails formed by almost every inclination angle, except for extreme values (i > 50s), formed a tail with approximately the same morphology. fairly intense investigation of various inclination angles paired with various arguments of periapse did not produce significant variation. The most important piece of information found in this trade study was that none of the orbit al parameters created a wide tail. This finding is not yet a conclusion, though. The galaxy models that we were using contained hollow centers. It may be that these centers are what creates the tail width. The piece of evidence supporting this is Figu re 4 which is a much larger simulation that includes the central disk particles which were left out of the simulations I ran this summer. The large particles represent those from the outer half (?) of the disk, while the small particles are those from th e center of the disk. The greater tail width and separation of inner and outer disk particles is noticeable. Thus, a larger simulation needs to be run.

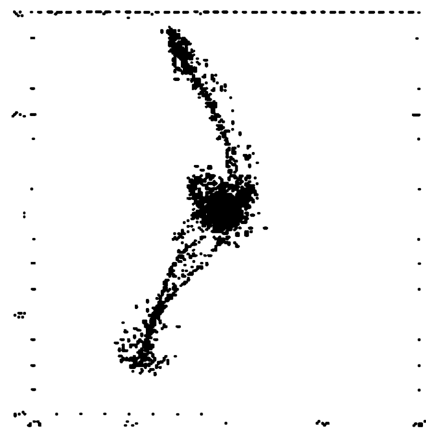

**Figure 4:** 64K particle Simulation. Small particles are from inside of disk, large from outer portion

If a larger simulation is not successful, there is another possibility for modeling Arp 299. Many disk galaxies that have been observed have a warp, meaning that a given ring of particles has a different inclination than more inner rings, and as a result is projected onto a different plane. While doing these simulations, we came to realize that a number of the 14 tailed systems had much less drastic bifurcated or parallel features, and that this might be a common phenomena. It seems plausible tha t a warp would cause a split tail, each component having a slightly different observable make up.

The viewing of these 6 dimensional simulations (3 spatial and 3 velocity components) is not a trivial matter. A program to do this viewing had been created prior to my arrival at NRAO, but its controls were cumbersome. To alleviate this problem, I a dded a graphical user interface to control the rotation, scaling, and other properties of the model. The experience in graphical user interface programming was invaluable.

The modeling of interacting galaxies has advanced since the days of Toomre and Toomre. Now we can examine kinematics data rather than just morphological and make more accurate models. We have also found out details about the process of galactic inter action which are critical to our understanding of the evolution of all types of galaxies.

- Arp 299 HI data
- Model match to outer filament
- Model match to inner filament

2) Gas-dynamics in Tidal Tails in collaboration with J. Hibbard (NRAO) and J. C. Mihos (CWRU) We frequently find significant displacements between the gaseous (as mapped by HI) and stellar tidal features. One possibility is that gas dynamical effects play a role during the formation of tidal features, giving the gas slightly different kinematics and

hence a slightly different dynamical history. This project involves a detailed comparison between SPH and non-SPH simulations of the NGC 7252 encounter modeled by Hibbard & Mihos (1995). The simulations have already been run, and the student would be expected to examine how the different components develop and establish methods to evaluate what effects are playing the deciding role.

3) Tidal Dwarf Formation in Tidal Tails in collaboration with J. Hibbard (NRAO) It has long been known (eg Schweizer 1978) that clumps of star formation with properties similar to dwarf galaxies exist within tidal features. Some of these features show enhancements also in the underlying stellar light and in the neutral gas column density and line-profile width, leading to the suggesting that they will evolve into independent dwarf galaxy satellites. This suggestion is supported by detailed numerical simulations which demonstrate that self-gravitating structures can indeed develop in tidal material torn of during galaxy interactions. However, tidal features which simultaneously exhibit enhancements in the HI column densities, HI line widths, optical surface brightness, and H-alpha emission are rare. This has not deterred many investigators from applying a Jeans-mass criteria and some reasonable range of M/L to any and all HI or optical enhancements, and claim such features are Tidal Dwarfs. There is never any mention made whether other non-enhanced regions of the tail satisfy the same requirements. The goal of this study is to see if the Jeans criteria is generally satisfied within tidal features, or if it only occurs at regions with an underlying optical condensation. In this project, the student would use my existing data on 14 tailed systems and use the HI momO, moml maps and calibrated B+R images to evaluate the Jeans mass and MHI/L of various features, to see if their are indeed any special regions within the tails. These data include 4 well studied tidal dwarfs as well as plenty of other knots and such which can be intercompared. http://deneb.physics.carleton.edu:8080/people/greg/summer.html

4) The Local Environment of Star Forming and Active Galaxies in collaboration with J. Hibbard (NRAO) and perhaps J. Condon (NRAO) In this project, the student would correlate the IRAS and NVSS data bases with the Tully Atlas of nearby bright galaxies - a volume limited catalog of galaxies brighter than Mb<-16 within 40 Mpc. In particular, we are interested in whether IR or Radio bright galaxies prefer certain types of environments, as measured by the local density parameter listed by Tully. Other density measures should also be examined. We would also examine morphologically peculiar galaxies in the Tully Atlas and examine if these are distributed differently than the radio or IR bright galaxies.

**Andrew West , of Haverford College**

**works with Ken Kellerman**
**on**

## Application of the Angular Size Redshift Relation

The NRAO Very Long Baseline Array (VLBA) has been used over a period of 4 years to obtain repeated images of a large sample of quasars and active galactic nuclei (AGN) at 15 GHz. The resolution is better than 1 milliarcsecond (mas) and we are able to located the relative position of small features with an accuracy better than 0.01 mas. This corresponds to about 0.1 parsecs at cosmological distances (H = 65 km/sec/Mpc). Thus we are able to determine component motions even for sources with apparent subluminal velocities.

In most quasars and AGN, features appear to propagate away from the central engine along a well collimated radio jet with apparent transverse velocities between zero and 10c. The median observed apparent velocity is about 5c, corresponding to a typical intrinsic velocity of about 98 percent of the speed of light oriented about 10 degrees to the line of sight. There is some evidence for accelerations along the jet, but no evidence of infall into the central engine As indicated by previous studies, (Vermeulen & Cohen 1994, ApJ, 430, 467; Vermeulen 1995, PNAS, 92, 11385) consideration of the effects of Doppler boosting suggests that the distribution of apparent velocities is not consistent with simple ballistic models or that there is a significant spread in intrinsic velocity.

We have examined the apparent angular velocity-redshift relation which offers a potentially powerful test of world models. Our data are consistent with standard Friedmann models and somewhat favor a deceleration constant between 0 and 1/2 for a zero cosmological constant. Further observations of a bigger source sample, especially at large redshift, along with an increased time base, may lead to more precise constraints on world models.

This work was presented at the 193rd AAS Meeting Session 107

# NRAO/Socorro 1998 Research Experience for Undergraduates (REU) Program

The summer REU program at NRAO/Socorro in 1998 consists of 4 main categories of activity:

1 - student research projects, in collaboration with an NRAO advisor
2 - lectures to the students by NRAO staff members
3 - a joint student project, involving observations with the Very Large Array (VLA)
4 - guided tours of the VLA, given by the students on weekends

The 1998 REU program at NRAO/Socorro is under the direction of James Herrnstein , and Tim Bastian. Dr. Herrnstein is a Jansky Postdoctoral Researcher at NRAO/Socorro, and Dr. Bastian is a member of the scientific research staff.

## Student Research Projects

Each of the REU students will work with one or more advisors on one or more projects throughout the summer. This is the main focus of the program, and the majority of the students' time will be spent on these research endeavors. These projects involved observing, data reduction and analysis, equipment development, and theoretical studies. At the end of the program, each student gave a lunch talk explaining the main project(s) he or she worked on during the summer. The possibility exists for the students to present their original research at scientific meetings deemed appropriate by their advisor(s). Following is a detailed list of the specific projects carried out by the NRAO/Socorro REU students:

**Melissa Nysewander of Agnes Scott College**
**works with Miller Goss**

**on**

## The Distant HII complexes NGC 3576 and NGC 3603

NGC 3576 ($l = 291.3^o$, $b = -0.7^o$) and NGC 3603 ($l = 291.6^o$, $b = -0.5^o$) are optically visible, luminous HII regions located at distances of 3.0 kpc and 6.1 kpc, respectively. We present 3.4 cm Australian Telescope Compact Array (ATCA) observations of these two sources in the continuum and the H90alpha, He90alpha, C90alpha and H113beta recombination lines with an angular resolution of 7" and a velocity resolution of 2.6 km $s^{-1}$. All four recombination lines are detected in the two sources. Broad radio recombination lines are detected in both NGC 3576 ($dV_{FWHM} > 50$ km $s^{-1}$) and NGC 3603 ($dV_{FWHM} > 70$ km $s^{-1}$). In NGC 3576 a prominent N-S velocity gradient (~30 km $s^{-1}$ $pc^{-1}$) is observed, and a clear temperature gradient (6000 K to 8000 K) is found from east to west, consistent with a known IR color gradient in the source. In NGC 3603, the H90alpha, He90alpha and the H113beta lines are detected from 13 individual sources. The Y+ (He/H) ratios in the two sources range from 0.07+/-0.01 to 0.21+/-0.05. The H113beta/H90alpha ratio in NGC 3576 is close to the theoretical value, suggesting that local thermodynamic equilibrium (LTE) exists. This ratio is enhanced for most regions in NGC 3603, which may be the result of high optical depth or stimulated emission. We compare the morphology and kinematics of the ionized gas at 3.4 cm with the distribution of stars, 10micron emission and $H_2O$, OH, and $CH_3OH$ maser emission. These comparisons suggest that both NGC 3576 and NGC 3603 have undergone sequential star formation.

This work was presented at the 193rd AAS Meeting Session 16

**Joshua Eisner of Harvard University**
**works with J. Herrnstein**
**on**

## The High Mass Star Forming Region W51-IRS2 in W51

This past summer, I worked with James Herrnstein, Lincoln Greenhill and Karl Menten on the W51IRS2 star formation region. The region is particularly interesting in that it is only one of three star formation regions where an SiO maser source has been detected (in comparison, SiO masers have been detected around tens of late-type stars). The summer research consisted of the reduction of VLA data from March 1998, and some data from

July 1998. We had data at 22 and 43 GHz, and we has both continuum and spectral line data at each of these wavelengths. I spent the first 6 weeks or so of my time reading the current literature, and reducing the data using AIPS, IDL and IslandDraw. The remaining 6 weeks were spent in analyzing the results of the data reduction. This analysis was very fruitful, and there is much more to be done, because of the richness of the data set: the final images contained H2O masers, SiO masers, a compact HII region, and an ultracompact HII region. We found that the dominant region of water maser activity, which also corresponded to the location of the SiO maser source, was not coincident with any of the radio continuum sources, nor was it coincident with any IR point sources. We attempted to come up with models to explain this result, and the best model we have come up with thus far involves an outflow from a protostar (or possibly multiple protostars).

This work was presented at the 193rd AAS Meeting Session 71

**Scott Schnee , of Columbia University**
**works with Rick Perley**
**on**

## Array Studies

Last summer I worked with Rick Perley on the flux density scale. I learned to edit and calibrate continuum data in AIPS. I worked with about 15 sources, mostly quasars and Seyferts, but also four planets. The data was taken in all bands from 90 cm to 7 mm. From the calibrated data I made images of the sources to determine the measured flux density of these calibrators. By determining the ratios of the flux densitiies of these secondary calibrators to 3C295 and using the results from a paper by Baars et al to calculate the absolute flux density of 3C295 we were able to determine the true flux densities of the secondary calibrators. By comparing these values to those determined in previous years by Rick Perley we checked for variability in these calibrators.

**Charlie Silver , of Columbia University**
**works with Greg Taylor**
**on**

## The Nucleus of NGC 1275

During the summer of 1997 Charlie Silver worked with Taylor on a low-frequency study of 3C84 using the VLBA. The surprising result from those observations was the discovery of a steep-spectrum "milli-halo" surrounding the parsec-scale core and jets (Silver, Taylor \& Vermeulen 1998, ApJL, submitted). The relativistic particles that produce the milli-halo may diffuse out from the core and jets, or may originate in Supernovae. Charlie and I plan to search for "milli-halos" in starbursting systems like Arp220 \& Mrk231 (where a structure that might be a milli-halo has been reported by Carilli, Wrobel \& Ulvestad 1998), and in a few other nearby AGN. We hope to work on this project this summer, although the observing time for it has not yet been granted.

Our primary research project for summer 1998 will be the study of 5 intra-day variable (IDV) sources. These compact extragalactic radio sources are known to exhibit variability on time scales as short as hours (Heeschen \etal 1987; Wagner \etal 1990). The fundamental nature of these variations is uncertain, including the question of whether they are intrinsic to the source or caused by extrinsic propagation effects. If intrinsic, these variations challenge the conventional beaming models that explain the origin of the radio emission. Existing observations have been mostly confined to single-dish monitoring of flux density and polarization at centimeter wavelengths, often combined with simultaneous optical photometry. In the fall of 1996 we observed 5 IDV sources over 8 days with the VLBA (project BK32), the 60" optical telescope at Palomar, and the ROSAT X-ray telescope. The VLBA data, which includes polarimetry, should allow us to discriminate between intrinsic and extrinsic mechanisms. Charlie will lead the reduction of the VLBA data. The goal of this project is a publication in the ApJ.

**Jane Rigby, of Penn State University,**
**works with K. Anantharamiah**
**on**

## Recombination Lines in Active Galactic Nuclei

Jane R. Rigby, of Penn State University worked with K. Anantharamaiah Recombination Lines in External Galaxies The student learned about Seyfert and starburst galaxies, synthesis imaging, and radio recombination lines (RRLs). She then searched two galaxies for radio recombination lines, which probe ionized gas in nuclear regions. Radio recombination lines are produced in ionized gas. In a few percent of collisional recombinations, the electron is captured into a very excited state. The electron then cascades down, quantum level by quantum level; these small energy changes resul t in emission of radio photons. Though these lines are weak, they are largely unaffected by dust; therefore, they can be used to probe the conditions and kinematics of ionized gas, particularly in the nuclear regions of starburst and Seyfert galaxies, re gions which are optically obscured. Observing extragalactic recombination lines is an observation challenge because it requires high dynamic range spectral line observations. The student reduced, calibrated, and analyzed spectra from two galaxies: ultraluminous IR galaxy Markarian 251 ( a Seyfert 1); and elliptical galaxy NGC 1052. Both have bright nuclei, which could produce stimulated emission of recombination lines. In Mrk 231, a "hole" in HI absorption against the central core, combined with a turnover in the nuclear spectrum, suggested the existence of radio recombination lines. However, at X and L bands, detection is uncertain (sensitivity of ~0.5 mJy.) For the observed emission measure of EM = 10^7, if the observed spectral turnover were due to free-free absorption, for any temperature, we would have seen RRLs from the central VLBI core component. Since we saw no strong lines, we conclude that the observed sp ectral turnover must be due to syncrotron self-absorption, not free-free absorption. For the southern VLBI core component, we conclude that the gas density is above 10^3 cm^-3. We also looked for recombination and OH lines in elliptical galaxy NGC 1052. No elliptical galaxy has been searched for RRLs, because elliptical galaxies have little gas. However, NGC 1052 has good evidence for ionized gas: it is known to have an inne r, ionized gas disk; it has strong, extended Halpha, OII, and NII emission; and it has water megamasers. We searched for recombination lines at X band in NGC 1052, but found none down to a sensitivity of ~2 mJy. We also searched for OH emission in NGC 1052 at L band and found a possible detection at v=1600 km/s. (NGC 1052 is receeding at 1500 km/s.) VLA observations to confirm this observation were recently made. If this line is real, we have detected molecul ar gas falling into the center of NGC 1052 at 100 km/s, presumably feeding the AGN.

**John W. Weiss , of Carleton College**
**works with Tim Bastian and Ketan Desai**
**on**

## The Nature of Microturbulence in the Solar Wind

My time at NRAO was spent researching scattering inthe ISM and solar wind. Usually, scattering would be an annoyance to astronomers, since it degrades images. However, if one is interested in the scattering medium (in our cases, the ISM and solar wind), scattering can give us a great deal of information on the medium. Among other things, once can learn about how the turbulent pockest are distubted in terms of their sizes, the alignment of anisotropies and the density of the medium. This is how I spent my summer. With Ketan Desai, I examined scattering in the ISM by looking at quasar 2050+365, a double source. In this case, we are taking images taken a few years apart an measuring how the seperations change. This differential wander measurement may allow us to reject or support certain models of the turbulence in the ISM. With Tim Batian, I looked at the scattering of quasar (point) sources as they passed through the solar wind. By measuring the amount of scattering, we were able to get a measurement of the power of the scatter, as well as picking up some density and anisotropy information. My summer was spent, then, learning about synthesis imaging, learning the specifics needed for scattering (by no means an easy field, but that's what made it so exciting!), and doing the anove research. It was an enlightening, fun, and well-spent summer.

**Michael Crawford, of New Mexico Tech**
**works with Bob Hjellming**
**on**

## The Appearance of Highly Relativistic Radio Sources

The project will be primarily computational in nature, with a very specific astronomical application: taking models for radio sources moving at highly relativistic speeds (0.9-0.99c, not the really extreme cases - as yet) and computing/predicting their appearence to an observer. The application is to the highly relativistic galactic jets in GRO J1655-40, GRS 1915+105, and Cyg X-3, but we want to explore the general problem with the goal of producing interactive programs to see the way these sources would appear for different geometries and underlying physical models.

**,Josh Bloom of Caltech**
**works with Dale Frail**
**on**

## Radio Afterglows from Gamma-ray Bursters

The goal is the detection of long-lived afterglows from gamma-ray bursters at radio wavelengths. The study of these afterglows in the radio yields unique diagnostics not obtainable by any other means. In particular radio observations give the size and allow one to infer the expansion of the relativistic fireball that is produced in the burst.

A student might be expected to work on several things including (1) the monitoring of known radio afterglows (2) searching for radio emission from new bursts, (3) modeling the flux evolution of the synchrotron-emitting fireball, (4) developing observing/reduction code to simplify the process of obtaining radio data on GRBs. Depending on the student's talents I can see this as a pure observing project, a theory project or a partial software project. The detection of an afterglow would almost certainly involve the publication of paper.

**Andreea Petric, of Columbia University and NMIMT**
**works with Michael Rupen**
**on**

## Line Widths and the Universal HI Profile in NGC 1058

We use HI observations to trace the vertical motions of the neutral gas in the face-on spiral galaxy NGC 1058. The combination of high sensitivity and low inclination permits the accurate measurement of line profiles at high spatial and spectral resolution, virtually uncontaminated by planar motions associated with disk rotation or spiral density waves. Although the width of the line profile varies from one beam to the next (FWHM= 14 -- 30 km/s), some global trends are evident. The lines are broader in the central 1.5arcmin, where the star formation is most vigorous. However, outside this region the linewidths are uniformly smaller in the spiral arms than in the interarm regions; and there is a general anticorrelation between H$\alpha$ emission and broad profiles. The line profiles are not Gaussian, and hence cannot solely be determined by single-temperature thermal broadening. The surprise is that the observed shape does seem to be universal, in the sense that the line profiles at every pixel, when scaled by their FWHMs, appear identical. This implies that whatever mechanism determines the relative distribution of kinetic energies operates in the same fashion throughout the galaxy -- both within and beyond the stellar disk, in quiescent regions and in regions with active star formation.

This work was presented at the 193rd AAS Meeting Session 8

## Lectures, etc...

Several lectures about radio astronomy and interferometry will be presented, allowing the students to obtain a good understanding of the technique. Talks were also given on general topics in astronomy, presented by members of the scientific staff. The astronomy talks were designed to give the students an understanding of what sort of research goes on at NRAO, and in radio astronomy in general. The detailed list of lectures and events for the summer is in the following table.

# 1998 Calendar of Events -- New Mexico

This is the list of student lectures and other organized events for the summer students. Many of the future events are only tentatively scheduled.

## June 1998

June 17, 8:30 am: Sixth Summer School in Synthesis Imaging begins at Workman Center.
June 23, 8:30 pm: Sixth Summer School in Synthesis Imaging ends at Workman Center.

## July 1998

July 10, 1000 Radiative Transfer Bryan Butler
July 14, 1000 Scattering Ketan Desai
July 16, 1000 Radio Galaxies Frazer Owen
July 21, 0900 HI in Galaxies Michael Rupen
July 24, tbd Gamma Ray Bursters Dale Frail
July 28, tbd Recombination Lines Anantha
July 30, tbd Masers Jim Herrnstein

## August 1998

Aug 4, tbd Galactic Sources Bob Hjellming

Last Modified on **Jan 15, 1999**

*J. Herrnstein (jherrnst@nrao.edu) FAX: (505)835-7027*

# Green Bank, West Virginia (NRAO 43m and 100m Telescopes)

Students conducting their research at the NRAO Green Bank Site in West Virginia included the students in the list below, along with others. The program at Green Bank is under the direction of Dr. Ron Maddalena.

1998 Summer and co-op Students (L-R): Marc Apgar, Jennifer Lockman, Steve Hicks, Naomi Bates, Lisa Wray, and Nicole Wiersgalla

1998 Summer and co-op Students and NRAO staff members after a caving trip (L-R): Frank Ghigo, Jennifer Lockman, Pat Matheny, Ron Maddalena, Nicole Wiersgalla, and Steve Hicks.

# 1998 Calendar of Events -- West Virginia

The following lists the scheduled activities for the GB students:
May 7, 12, and June 2 -- Student Orientation and tours

## June 1998

June 1 - 5 -- Future VLBI Missions from Space (workshop)
June 14 - 27 -- Teacher's Institute
June 12: Mark Clark: M&C architecture
June 17: Toney Minter: Turbulence
June 26: Lisa Wray: Radio Astronomy Receivers
June 29: Frank Ghigo: Earth Wobble

## July 1998

July 1: Dan Pedtke: OVLBI

July 7: Jim Braatz: Active Galactic Nuclei
July 9: Rick Fisher: Antennae
July 14: Dana Balser: Radiative Processes
July 16: Joe McMullin: Spectroscopy
July 21: Ron Maddalena: Holography
July 22: Jay Lockman: HI in the Milky Way
July 23: Gary Anderson: History of Radio Technology
July 27 - 29 -- Workshop on Science with the Green Bank Telescope (workshop)

The dates might vary slightly from the above. The time and place might also vary but will usually be at 3:00 in the conference room in the new wing.

**Naomi S. Bates, of Princeton University**
**works with Ron Maddalena**
**on**

# Extragalactic Hydrogen Wings

The project concentrates on the analysis and interpretation of observations of the wings of HI profiles of galaxies. The project attempts to characterize the component of gas that has a higher velocity dispersion than the gas typically attributed to galaxies. That is, the project attempts to study what in our galaxy would be called high-velocity clouds or a warm/hot component to the neutral ISM.

**Nicole Wiersgalla, of the University of Minnesota**
**works with Dana Balser and Tony Minter**
**on**

# Turbulence in HII regions and the Diffuse Ionized Gas (DIG)

The student will use both observations and models to explore the role of turbulence in classical HII regions which are usually confined to the galactic plane and the diffuse ionized gas (DIG) which pervades the galaxy. The observations will consist of both single-dish and interferometric radio recombination line data. Additional observations have been proposed using the Virginia Tech Spectral Line Imaging Camera (SLIC) which the student may use to measure the [SII]/H alpha abundance ratio; these measurements can constrain possible heating mechanisms. A computer program called CLOUDY will be used to simulate the physical conditions of the ionized gas. Depending on the student's background a specific aspect of the project could be emphasized.

**Laura Woodney, of The University of Maryland**
**works with Joe McMullin**
**on**

# Chemistry in Comets

Laura Woodney worked on two separate projects while at Green Bank. The first was finishing a paper for submission to Icarus on flashes off of Jovian satellites during the D/Shoemaker-Levy 9 impact. It was predicted that these flashes would be quite bright, however, nothing but tentative detections was reported from various observers around the world. In this paper Woodney examines her own possible detections, and discusses the physical implications the weak or non-existent reflections of light from the impacts have on the impact conditions.

Woodney's main project was to examine the morphology of the relationship of HCN and CN in Comet Hale-Bopp. Hale-Bopp is the first comet for which there has been simultaneous high resolution imaging of this parent and daughter pair, so that this is the first time the morphology of their relationship can be examined. A greater understanding of the HCN/CN relationship will place constraints on the much disputed nature of other proposed CN parents. Of particular interest is what these HCN images can reveal about the nature of the association of the nuclear HCN source with the CN jets since there is enough spatial resolution to detect HCN jets.

The HCN maps of the J=1-0 transition at 3mm were made with the Berkeley-Illinois-Maryland Association (BIMA) Array in Northern California, with a beam size of ~ 9''. The maps have been create so that they are phased with the rotational period of the comet to reduce the smearing of any spatial features seen in the maps. At each phase examined, data spanning several days has been summed both to increase the signal to noise ratio and give more complete uv coverage than a 1 to 2 hour observation would provide on its own. When these maps are compared to similarly phased narrowband CN images obtained at Lowell Observatory taken near or at the same time as the HCN images it is clear that at least some of the CN jets are a product of HCN jets, but that there is probably a secondary source. A likely candidate for this secondary source is dust, however more exotic parent molecules such as $C_2N_2$ as suggested by Festou et al. (1998) are also possible.

**Keri Eberhardt, of The University of Nebraska**
**works with Glen Langston**
**on**

# Highly Redshifted Molecular Lines

Speakers at the high redshift radio line symposium in Green Bank WV highlighted the importance of systems exhibiting absorption features. Also they noted that there are relatively few objects to study. Our summer student will reduce data from observations made with the 140ft for search for absorption features in a sample of 27 high redshift radio sources with $3.35 < z < 3.83$. This redshift range was chosen to place limits on the absorption in the H_2O (22.2 GHz), HCN (88.6 GHz) and CO (115.3 GHz) lines. Sources with redshifts in this range may be observed with existing Cassegrain receivers at the 140ft. Since these sources are relatively bright, reasonable absorption limits may be placed in only a few hours observations. We will observe 10 days, examining these 27 sources at 3 frequencies. Sample Selection Optical absorption lines seen in the spectra of high redshift QSOs may originate from different types of objects. Absorptions lines of MG II, heavy elements and the damped Lyman-alpha lines most likely originate in normal galaxies (cf. Bergeron and Boisse 1991, A. and A., vol 243, page 344). If absorption lines are produced by material in the galaxy containing the quasar, the lines are important for studying the formation and evolution of that galaxy. Because the galaxies are distant, it is difficult to obtain information about their global properties from emission studies. (There are important exceptions such as for IRAS 10214+4724, Brown and Vanden Bout, 1992 Ap. J. Letters, vol 397, page 19.) Our quasar sample was selected from the NED astronomical data base from IPAC at Caltech. The criteria for inclusion was that source was a radio source with known redshift. The sample redshift range was chosen to allow the water line to be detected in C-band, HCN to be detected in K-band with 18 to 22 GHz feed and CO to be detected with the K-band 22 to 26.5 GHz feed. A primary interest in the high radio line symposium was the chemistry of the high redshift absorbing clouds. The occurance of a single line does not strongly constrain the system, due to uncertainties in the spin temperature and filling factors. It is the relative abundance of the elements that is of interest. The HCN, HCO^+, HNC, and CS observations of Wilklind and Combes (1997, A. and A., vol 324, page 51) of Centaurus A show strong molecular absorption features. Their results indicate that the relative molecular abundances in the absorbing clouds of Centaurus A are consistent with measurements in the galaxy. Different molecular abundances are expected for galaxies at high redshift, although Lucas and Lizst (1993, A. and A., vol 273, L33) present observations toward BL Lacertae which are under-abundant in HCN compared with predictions.

**Marc Apgar, of West Virginia University**
**works with Wes Grammer**
**on**

# Green Bank Telescope Diagnostics

Mr. Apgar will work on developing enhancements to a DOS-based Green Bank Telescope hardware diagnostic program.

**Jennifer Lockman, of**
**works with Jay Lockman**
**on**

# Hydrogen Emission in the Milky Way

The student would participate in the final phases of a very large survey of Hydrogen emission in the Milky Way. The student's work would involve use of the 140 Foot Telescope for several days to observe the 21 cm line of hydrogen, reduction of that data including calibration, correction for atmospheric and instrumental effects, and checks for interference or other bad data, and assemblage of that data and previous data into large maps. As a final phase, the data will be examined for evidence of shells of HI that might result from assemblages of supernovae or the impact of high-velocity clouds on the galaxy.

**Jessica Golub, of Vassar**
**works with Jim Braatz**

**on**

## Water Masers in Nearby Galaxies

1. Galaxies which have been searched for H2O masers, but not detected, tend to get lost in people's work and go unpublished. As there are many groups now searching for masers, it would be useful to have a list of all undetected galaxies. The student could solicit such lists from each research group, organize it and distribute it back to them. I have actually started this already, and I think it would be a good short-term project to complete it.

2. Conduct a study of nearby, edge-on galaxies. I have two interests in such sources. One, they may be candidates for new maser searches, but it would be ideal to identify any signs of activity (compact radio cores, IR excess, ...) in them before targeting them for observation. The second, I have found an unusual discrepancy in the inclination angle distribution of AGNs, and it could be compared to other galaxy populations.

3. To calibrate, reduce, and organize several rounds of 140-ft observations done in the past year. I've done preliminary reduction already, but I'd like to have some more detailed spectra and studies done on several H2O maser observations. This would involve some unipops work.

This work was presented at the 193rd AAS Meeting Session 6

# Tucson, Arizona (NRAO 12m and VLBA Telescopes)

Students conduct their research at the NRAO Tucson Site in Arizona. The program in Tucson is under the direction of Jeff Mangum. As the NRAO offices are across the street from KPNO/NOAO offices, the REU group shares in the activities of the NOAO REU program there.

In addition to the general activities carried out at the KPNO/NOAO offices, the NRAO and KPNO/NOAO REU students participated in two group activities organized by the NRAO staff. The first was a night at the 12 Meter Telescope, where the REU students spent a day at the 12 Meter Telescope. Following a tour of the telescope and lab facilities, where the students were introduced to the instrumentation used in millimeter wavelength astronomy, the students were given the opportunity to participate in some actual millimeter wave astronomical observations. With this experience the students got an introduction to the observing techniques used in millimeter wavelength astronomy.

The second general activity was a lecture series on millimeter wavelenth astronomy given by members of the NRAO scientific staff. Three lectures were given. Jeff Mangum gave a presentation on millimeter wavelength research into the properties of objects in the Solar System and molecular clouds. Darrel Emerson gave a lecture on millimeter wavelength observing techniques. Finally, to complete the survey of millimeter astronomy, Simon Radford gave a lecture on extragalactic astronomy at millimeter wavelengths.

Three REU students conducted research at the NRAO Tucson site in Arizona during the summer of

1998.

The following are detailed reports describing the work done by each REU student at NRAO Tucson.

**Beth Biller, of Swarthmore College**
**works with Tamara Helfer**
**on**

# The Physical Conditions and Structure of HCN and CS Emission in the Milky Way Plane

In a recent study of the large-scale HCN and CS distribution and emission properties as a function of location in the Milky Way, Helfer \& Blitz (1997) used the NRAO 12m to observe the 3 mm emission from HCN, CS, and CO along 30 positions in the first quadrant of the Milky Way. Emission from HCN and CS is surprisinly common; however, the lines are relatively weak, which suggests that either the transitions are subthermally excited or that the filling fraction of dense clumps is small. This REU project is divided into two parts, either of which could satisfy a completed project should time pressures prevent combining the two: (1) An analysis of NRAO 12m CS J=3-2 observations towards selected lines of sight; these observations are to be combined with the CS J=2-1 data in order to model quantitatively the physical conditions in the emitting gas. (2) The reduction and analysis of BIMA observations of HCN, CS, and CO toward one line of sight, in order to determine whether the sprectral feature comes from compact, dense subclumps that have relatively low filling fractions on pc scales, or whether it comes from a smooth distribution of gas at relatively low density.

For the main part of this REU project, Beth compared NRAO 12m observations of the 2 mm CS J=3-2 emission along 9 lines of sight in the Milky Way plane to their 3 mm counterparts from Helfer \& Blitz (1997). This involved retrieving the raw CS J=3-2 spectra, fitting baselines to emission-free regions of the spectra, and averaging together 4-point cross observations to compare to the existing 3 mm data. Beth then learned how to run a Large Velocity Gradient radiative transfer model to interpret the CS J=3-2 to CS J=2-1 line ratios over the pc-scale features. We derived molecular hydrogen densities of $<$ 10$^5$ cm$^{-3}$ for features at all lines of sight, with most of the derived densities in the range 2.5 $\times$ 10$^4$ to 1 $\times$ 10$^5$ cm$^{-3}$. These densities are about an order of magnitude lower than those derived from CS observations of cloud cores in M17, S140, and NGC2024 by Snell et al. (1984), and they are one to two orders of magnitude lower than the densites derived using HC$_3$N observations of cores in Orion, M17 and Cepheus A (Bergin et al. 1996). In addition to the radiative transfer study, Beth learned some basic techniques of millimeter interferometry by reducing CO, CS, and HCN BIMA observations along one line of sight. While the CO emission was extremely complex, the CS and HCN emission was concentrated on size scales of about half a parsec, a scale comparable to the size of starforming cores in nearby GMCs. Beth has written a report to summarize many of the details of her work this summer, and she plans to attend the January 1999 AAS meeting in Austin to present our results.

This work was presented at the 193rd AAS Meeting Session 71

**Alexis Johnson, of The University of Virginia**
**works with Jeff Mangum**
**on**

# Molecular Spectral Line Images of Comet Hale-Bopp

Images of the CO, HCN, HCO+, and CH3OH emission from Comet Hale-Bopp were obtained near perihelion passage of this famous celestial visitor in spring 1997. These images were obtained using the On-The-Fly (OTF) observing technique at the 12m telescope. Alexis concentrated on the analysis of these data to (1) derive the spatial and spectral correspondence between the molecular emission distributions; (2) measure the spatial and temporal variations in the abundances of these molecules within the comet; (3) study the kinematic structure of the comet as traced by each species. Alexis spent most of her time developing a set of analysis tools using the IDL analysis package. The results of this work will be presented at the AAS meeting in Austin, Texas in January 1999.

This work was presented at the 193rd AAS Meeting Session 11

**Laura A. Snyder, of Iowa State University**
**works with Simon Radford**
**on**

# Study of Chajnantor and Other High Astronomical Sites

The NRAO has proposed to build the Millimeter Array (MMA), which will be substantially more powerful than any existing telescope for astronomical observations at millimeter and submillimeter wavelengths. At these wavelengths, atmospheric water vapor can limit the observational sensitivity and resolution. As part of MMA development, therefore, NRAO has conducted an extensive site test campaign. For the last three years, we have studied a high altitude (5000 m) site near Cerro Chajnantor in the Andean altiplano on the eastern edge of the Atacama desert in northern Chile. Autonomous instruments record the atmospheric transparency at 225 GHz and 350 um, the atmospheric stability at 12 GHz, and meteorological parameters. The NRAO and other groups have also operated similar instruments at other sites, notably Mauna Kea and the South Pole, where existing (NSF supported) telescopes are located.

These data clearly demonstrate Chajnantor is a world class site for astronomy at millimeter and submillimeter wavelengths. This conclusion is based, however, on a relatively simple statisical analysis. The data are rich enough to support more detailed investigations such as correlations with meteorolgy databases.

Ms. Snyder completed the following studies of the site:

Cloud cover: Ms. Snyder analyzed surveillance images of the Chajnantor site's southwestern horizon for the nine 9 months, 1997 June to 1998 February. From these images, she determined the average cloud cover and its diurnal and monthly variations. An MMA memo is in preparation.

Subsurface temperature: Ms. Snyder analyzed data from a subsurface temperature probe for the six months, 1997 June to October. She determined the thermal diffusivity of the soil, the diurnal and monthly temperature fluctuations in the subsurface temperature, and the properties of subsurface freezing and melting episodes, including the effective soil salinity. An MMA memo is in preparation.

Digitized maps: Ms. Snyder measured published contour maps to extend a digital elevation model of the site. This will be used as input for hydrodynamic modeling of wind flow over the site.

El nino correlations: Ms. Snyder investigated possible correlations between sea surface temperature indexes and conditions measured at the site. The data hint at an influence of the El Nino/Southern Oscillation, but no definite conclusions were reached.

**Michael Crawford, of New Mexico Tech**
**works with Bob Hjellming**
**on**

# The Appearance of Highly Relativistic Radio Sources

Under the supervision of Robert Hjellming, Michael Crawford worked on a project to compute, and display as images, the appearence of sources moving at relativistic speeds. It was part of an ongoing effort the compare models of Galactic jet sources assocatiated with X-ray binaries and transients with VLA, VLBA, Merlin, and ATCA radio light curves and images.

The source models combined precessing jet kinematics to compute the apparent location of jet material, Doppler boosting of the intensities to predict the apparent surface brightness of the jet; and convolution with elliptical beams to smear the predicted image to the resolution of instruments like the VLA or the VLBA. All the computations were done on a PC using MathCAD. Once the computations were being done correctly, Michael was able to predict the correct general appearance of the jets in SS433 and the Feb. 1997 one-sided jet ejection during an 11 Jy flare in Cyg X-3. The resulting programs allow one to predict the appearence of adiabatically expanding relativistic jets for any values of the kinematic parameters.

The next stage of the project was to compute the radio light curves of the sources modeled in this way, but that was just begun when the 12 weeks ended. The light curve computation has since been completed by Robert Hjellming, and is being successfully applied to transient events in a large number of Galactic X-ray binaries and transients.

# Appendix
# Student Presentations at the 193rd AAS Meeting
# Austin, Texas

Biller, B. A. (Swarthmore College) and Helfer, Tamara (NRAO) Session 71.05

DePree, C.)Nysewander, M. C. (Agnes Scott College) and Goss, W. M. (NRAO Session 16.01

Eisner, J. A. (Harvard University), Herrnstein (NRAO), Greenhill, L. J. (CfA) and Menten, K. M. (MPIfR) Session 71.13

Golub, Jessica S. (Vassar College) and Braatz, J. A. (NRAO) Session 6.12

Johnson, A. M. (University of Virginia) and Mangum, J. G. (NRAO) Session 11.21

Petric, A. O., (NMIMT) and Rupen, M. P. (NRAO) Session 8.18

West, A. A. (Haverford College), Kellerman, K. I., Vermeulen, R. C. (NFRA), Zensus, J. A. (MPIfR) and Cohen, M. H. (Caltech) Session 107.03

Copies of the abstracts follow.

---

# [71.05] The Density and Structure of CS Emission in the Milky Way Plane

*B.A. Biller (Swarthmore College), T.T. Helfer (National Radio Astronomy Observatory)*

In an earlier survey of CS(J=2--1) emission in the plane of the Milky Way, Helfer & Blitz (1997) found that emission from this high dipole moment molecule was more commonly detected in the Galactic plane than in solar-neighborhood Giant Molecular Clouds, albeit at a weaker level than in starforming cores in GMCS. Here, we present observations of CS(J=3--2) and CS(J=2--1) from twenty-one pc-scale ''features'' along nine lines of sight in the first quadrant of the Milky Way plane. Using a Large Velocity Gradient (LVG) radiative transfer model of the observed line temperatures, we derive moderate (log $n(H_2)$ $cm^{-3}$ = 3--5) densities for the features. The moderate densities suggest that these features are not cloud cores; they may instead be similar to the envelopes around starforming cores. For one line of sight that was specially selected for strong molecular emission, we derive a density of log $n(H_2)$ $cm^{-3}$ = 5.4; this special position appears to be the only core candidate in our sample. We also present interferometric observations of one of the cloud features; these observations place limits on the size scale of the emitting region.

---

The author(s) of this abstract have provided an email address for comments about the abstract:
beth@merlin.swarthmore.edu

---

# [16.01] NGC 3576 and NGC 3603: Two Luminous Southern HII Regions Observed at High Resolution with the Australia Telescope Compact Array

*C. G. De Pree, M. C. Nysewander (Agnes Scott College), W. M. Goss (NRAO)*

NGC 3576 (l = 291.3°, b = -0.7°) and NGC 3603 (l = 291.6°, b = -0.5°) are optically visible, luminous HII regions located at distances of 3.0 kpc and 7.7 kpc, respectively. We present 3.4 cm Australian Telescope Compact Array (ATCA) observations of these two sources in the continuum and the H90\alpha, He90\alpha, C90\alpha and H113\beta recombination lines with an angular resolution of $7^{\prime\prime}$ and a velocity resolution of 2.6 km $s^{-1}$. All four recombination lines are detected in the integrated spectra of the two sources. Broad radio recombination lines are detected in both NGC 3576 ($\Delta V_{FWHM} \geq$ 50 km $s^{-1}$) and NGC 3603 ($\Delta V_{FWHM} \geq$ 70 km $s^{-1}$). In NGC 3576 a prominent N-S velocity gradient (~30 km $s^{-1}$ $pc^{-1}$) is observed, and a clear temperature gradient (6000 K to 8000 K) is found from east to west, consistent with a known IR color gradient in the source. In NGC 3603, the H90\alpha, He90\alpha and the H113\beta lines are detected from 13 individual sources. The Y+ (He/H) ratios in the two sources range from 0.07±0.01 to 0.21±0.05. The H113\beta/H90\alpha ratio in NGC 3576 is close to the theoretical value, suggesting that local thermodynamic equilibrium (LTE) exists. This ratio is enhanced for most regions in NGC 3603, which may be the result of high optical depth or stimulated emission. We compare the morphology and kinematics of the ionized gas at 3.4 cm with the distribution of stars, 10\micron emission and $H_2O$ and $CH_3OH$ maser emission. These comparisons suggest that both NGC 3576 and NGC 3603 have undergone sequential star formation.

---

---

# [71.13] SiO Masers, Water Masers, and Outflow in the W51-IRS2 star-forming region

*J. A. Eisner (Harvard University), J. R. Herrnstein (NRAO), L. J. Greenhill (Harvard-Smithsonian CfA), K. M. Menten (MPIfR)*

The W51-IRS2 star-forming region is one of only three in which SiO maser emission has been detected. In contrast, SiO maser sources occur in the circumstellar envelopes of tens of late-type stars. We present the results of sensitive, high angular resolution observations of W51-IRS2 made with the VLA in its two largest configurations, at 7 mm and 1 cm wavelengths. The SiO maser emission is coincident with a known luminous cluster of water masers, although no corresponding radio continuum source is detected. The SiO emission has a linear spatial structure and may trace an outflow from an obscured protostar, on scales of approximately 200 AU. The proposed model in consistent with the morphology of the brightness distribution of water masers.

---

The author(s) of this abstract have provided an email address for comments about the abstract: jeisner@cfa.harvard.edu

---

# [6.12] Continuum Emission from Megamaser-Detected Active Galaxies

*J. S. Golub (Vassar College), J. A. Braatz (NRAO)*

Currently there are 18 galaxies known to harbor water megamasers, all of which are associated with an active galactic nucleus (AGN). Using data taken with the VLA in B configuration, we mapped the X-, C-, and L-band radio continua of four of these galaxies: Markarian 1210, IC 2560, IC 1481, and TXFS 2226-184. The radio structures are unresolved by the VLA in each case. High resolution (VLA-A or VLA-B) radio data are now available for 13 of the maser-detected galaxies, and we used this data to investigate whether these galaxies tend to have greater nuclear radio luminosity than a sample of undetected AGNs. Nonparametric statistical tests from the ASURV software package were used to compare the galaxies. The results from the new data suggest that megamaser-detected galaxies in fact do tend to have greater radio luminosity. This trend may be a result of physical processes occuring in the accretion disk of the black hole in the AGN.

---

The author(s) of this abstract have provided an email address for comments about the abstract: jegolub@vassar.edu

**AAS Meeting #193 - Austin, Texas, January 1999**
*Session 11. Observatories, Telescopes and Instruments*
*Display, Wednesday, January 6, 1999, 9:20am-6:30pm, Exhibit Hall 1*

[Previous] | [Session 11] | [Next]

---

# [11.21] Analysis of Spectral Line Data Cubes with IDL

*A. M. Johnson (University of Virginia), J. G. Mangum (NRAO)*

To aid in the extraction of the useful information from a three-dimensional observational data set, we have developed a set of IDL macros which extract linewidth information. These tools were developed to analyze any three-dimensional (RA, Dec, Velocity) data cube. In particular, these tools are being used to analyze the linewidth characteristics of a set of molecular spectral line images of Comet Hale-Bopp obtained with the NRAO 12 Meter Telescope in late March of 1997. These macros will in the future be supplemented with other IDL macros which will allow analysis of the spatial and spectral properties of the molecular spectral line emission from objects such as molecular clouds, evolved stars, and external galaxies.

This work was supported through the NSF Research Experience for Undergraduates (REU) program.

---

[Previous] | [Session 11] | [Next]

**AAS Meeting #193 - Austin, Texas, January 1999**
*Session 8. Galactic Morphology and Stellar Populations*
*Display, Wednesday, January 6, 1999, 9:20am-6:30pm, Exhibit Hall 1*

[Previous] | [Session 8] | [Next]

---

# [8.18] Line Widths and the Universal HI Profile in NGC 1058

*A.O. Petric (NMIMT), M.P. Rupen (NRAO)*

We use HI observations to trace the vertical motions of the neutral gas in the face-on spiral galaxy NGC 1058. The combination of high sensitivity and low inclination permits the accurate measurement of line profiles at high spatial and spectral resolution, virtually uncontaminated by planar motions associated with disk rotation or spiral density waves. Although the width of the line profile varies from one beam to the next (FWHM= 14 -- 30 km/s), some global trends are evident. The lines are broader in the central 1.5arcmin, where the star formation is most vigorous. However, outside this region the linewidths are uniformly smaller in the spiral arms than in the interarm regions; and there is a general anticorrelation between H\alpha emission and broad profiles. The line profiles are not Gaussian, and hence cannot solely be determined by single-temperature thermal broadening. The surprise is that the observed shape does seem to be universal, in the sense that the line profiles at every pixel, when scaled by their FWHMs, appear identical. This implies that whatever mechanism determines the relative distribution of kinetic energies operates in the same fashion throughout the galaxy -- both within and beyond the stellar disk, in quiescent regions and in regions with active star formation.

---

[Previous] | [Session 8] | [Next]

---

# [107.03] Kinematics of Quasars and AGN

*A. A. West (NRAO \& Haverford College), K. I. Kellermann (NRAO), R. C. Vermeulen (NFRA), J. A. Zensus (MPIfR), M. H. Cohen, (Caltech)*

The NRAO Very Long Baseline Array (VLBA) has been used over a period of 4 years to obtain repeated images of a large sample of quasars and active galactic nuclei (AGN) at 15 GHz. The resolution is better than 1 milliarcsecond (mas) and we are able to located the relative position of small features with an accuracy better than 0.01 mas. This corresponds to about 0.1 parsecs at cosmological distances (H = 65 km/sec/Mpc). Thus we are able to determine component motions even for sources with apparent subluminal velocities.

In most quasars and AGN, features appear to propagate away from the central engine along a well collimated radio jet with apparent transverse velocities between zero and 10c. The median observed apparent velocity is about 5c, corresponding to a typical intrinsic velocity of about 98 percent of the speed of light oriented about 10 degrees to the line of sight. There is some evidence for accelerations along the jet, but no evidence of infall into the central engine As indicated by previous studies, (Vermeulen & Cohen 1994, ApJ, 430, 467; Vermeulen 1995, PNAS, 92, 11385) consideration of the effects of Doppler boosting suggests that the distribution of apparent velocities is not consistent with simple ballistic models or that there is a significant spread in intrinsic velocity.

We have examined the apparent angular velocity-redshift relation which offers a potentially powerful test of world models. Our data are consistent with standard Friedmann models and somewhat favor a deceleration constant between 0 and 1/2 for a zero cosmological constant. Further observations of a bigger source sample, especially at large redshift, along with an increased time base, may lead to more precise constraints on world models.

---

If you would like more information about this abstract, please follow the link to http://www.cv.nrao.edu/2cmsurvey. This link was provided by the author. When you follow it, you will leave the Web site for this meeting; to return, you should use the Back comand on your browser.

# Project Reports
# 1998 REU Students

Marc Apgar (West Virginia University)

Naomi S. Bates (Princeton University)

Keri Ann Eberhardt (University of Nebraska)

Jennifer Lockman (College of Charleston)

Patrick B. Matheny (West Virginia University)

Nicole Wiersgalla (University of Minnesota)

Andrew A. West (Haverford College)

# Summer REU program project report

**Marc Apgar**
**National Radio Astronomy Observatory**
**9/1/98**

The following details my work performed over the course of the twelve week REU program. I participated in the program during the summer of 1998 at the National Radio Astronomy Observatory in Green Bank, WV. I worked on two different projects: a software upgrade for the 85 foot telescopes and the design/construction of a local oscillator for the 40 foot telescope. The following report discusses both projects separately.

# Programming upgrade summary for the 85 foot telescopes.

Advisor: Frank Ghigo


Summary:
The previous control system for the 85 foot telescopes was written in Pascal. The code needed to be converted to C and be made to operate on a Linux machine rather than DOS.


Objectives:
1. To convert existing Pascal code into a C program with similar functionality.
2. Software must read position encoders and run motors appropriately.
3. It must be Linux compatible. The previous program ran on a DOS environment.
4. The user interface screens must be telnet and Xterm compatible.
5. The program must continue accepting input while running the antenna motors.

Solution:
After some deliberation, I decided to rewrite most of the code while ignoring much of the previous Pascal code. The code was lengthy and many of the Pascal statements had no direct translation to C. A Pascal to C converter program was tried but had difficulty with many parts of the program including cursor locating, assignment to variables in structures and various looping constructs. The global variables were easier to translate but direct conversion of the rest of code was abandoned. All of the globals were defined in a single file. This file was translated with ease and provided insight on the how the previous program operated. The practice of keeping all variables global was appropriate for this situation and was retained. Also, the appearances of the previous menus were retained except for the underlying method of cursor placement and update. Other sections of the old source code were contained in about ten other files and were ignored.

To best perform screen update, the curses library was used. This C library allows for cursor positioning, boldfacing, and keystroke scanning. It is robust enough to output to Xterm and telnet sessions and performs efficiency optimized screen updates. Some extra coding was necessary to verify the window was large enough to display the menus.

The program was written without any blocking routines. Since the program must continuously monitor and adjust the antenna(s), it cannot get hung up on user input. So all user input was taken in one key at a time. The program would adjust the antennas twice a second while waiting for a keystroke. The curses library has a function that will scan the keyboard and return a null character when nothing is pressed. All user input was attained with this function to keep the program cycling continuously.

The movement of the 85-foot antenna movement is physically limited in declination and hour angle. The hour angle limits are narrower at lower declinations (Figure 1). The antenna is moved with eight different motors including two slew motors. Since the slew motors are capable of moving the antenna 25° per minute, care was taken in the design of the algorithm that controlled it. A "No Slew Zone" was created inside the movement boundaries, which was a zone where the program would not allow certain slew motors to run. Even if the antenna were operated past a limit, it would coast down to a speed slow enough to not cause damage. Slewing was allowed in this zone only when it was in a direction that takes it *away* from the boundary. This zone prevented the operator from manually controlling the slew motors and violently running the antenna into a limit. Also, the adjustment process occasionally overshoots a target position so the zone ensured the program was "extra careful" when adjusting near a limit. All movement was prevented in the "No Movement Zone", even when the motors were manually controlled.

All limits were defined in a text file that was not compiled with the code. It was read every time the program was started so the operator could easily make adjustments without having to recompile. A help file was created that also can be modified by the operator and read at any time while the program is running by pressing H.

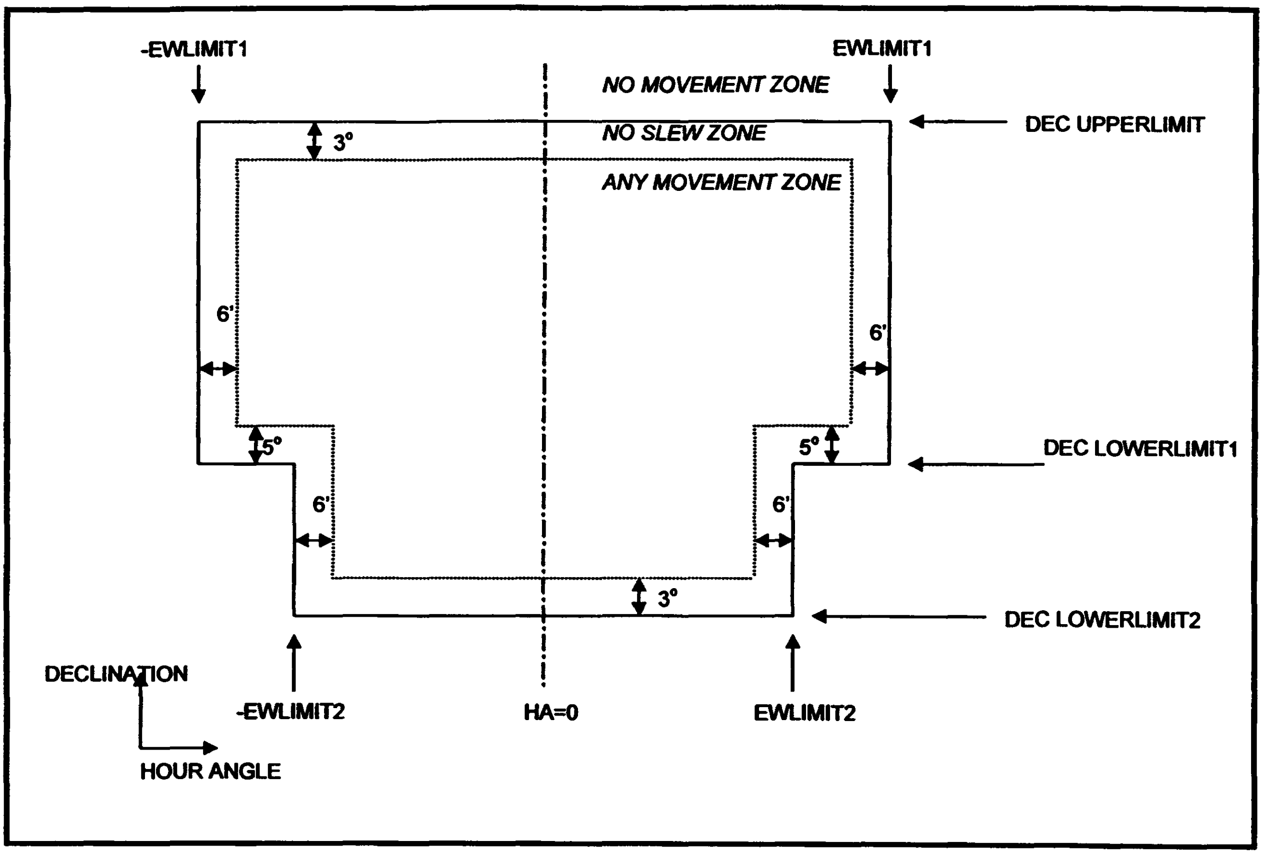


Figure 1 – Adjustment boundaries

The program was written to operate the antenna in five different modes:

1. Stop – All rates zero.
2. Manual – Rates specified by the user in the manual menu.
3. Positioning – Pointing telescope to commanded declination and hour angle. When positioned, the program enters stop mode automatically.
4. Tracking – Pointing telescope to commanded declination and right ascension.
5. Automatic – Not implemented. Read commands from a file and execute them at the times specified.

The structure of the program was set up so it can be easily understood and modified. The **Main** routine contains calls to functions that do not block execution(Figure 2). All of the functions return control to **Main** immediately except **BackgroundChar** which waits for a keystroke. While **BackgroundChar** waits for a keystroke, it repeatedly calls **Send, Recieve** and one of the menus. This ensures that the screen is always updated, the antenna is monitored and adjustments made if necessary. The user can choose from various actions by using the up arrow and down arrow keys. At any time, one action will be highlighted on the menu. When enter is pressed, the selected action is executed. When left or right arrows are pressed, the menu is changed and a new set of action functions take effect. This means that the user has different actions available for each menu. The method for calling the menus and actions was designed to allow for easy addition of more actions and menus.

The only function that turns the slew motors on is **Kickstart**. **Kickstart** is called by any action routine that commands antenna movement. It is also called during the special case of "crossing the corner".

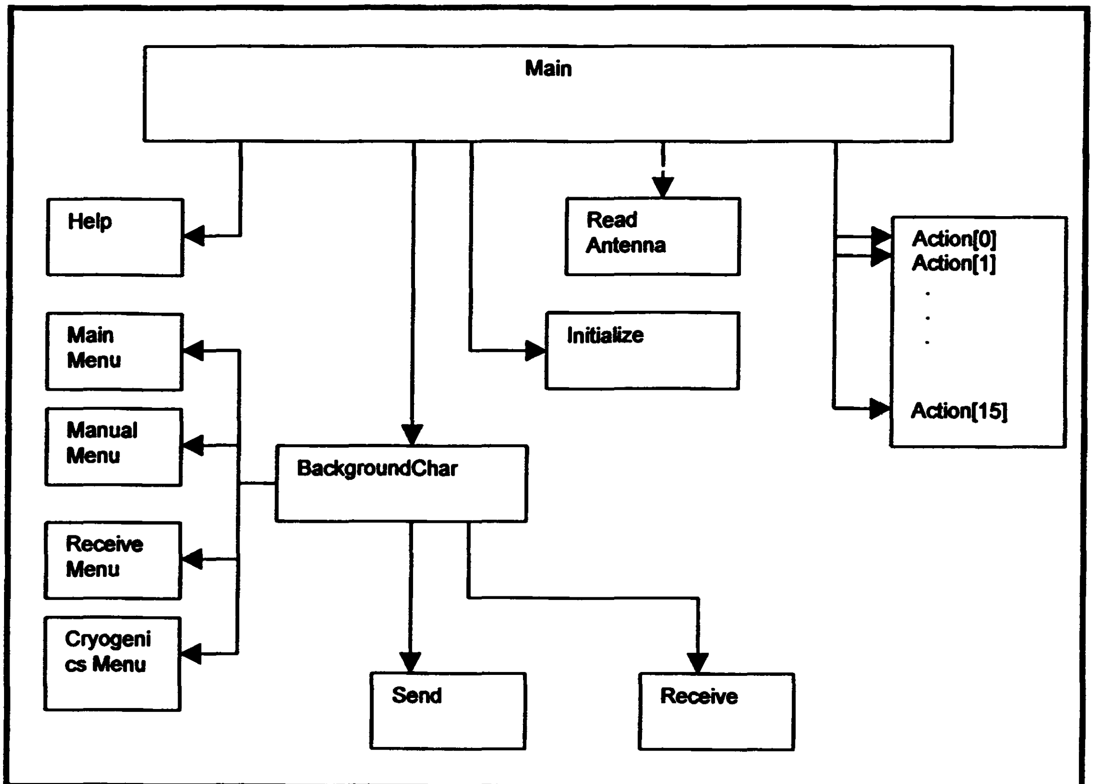

Figure 2 – Functional Block Diagram

The upgrade consisted of five files:

1. Menus.h – This include file contains all of the menus available to the user, all highlightable fields, and corresponding actions.
2. Vars.h – This include file specified all globals, structure and constants used in the program. All antenna variables including, position, limits and rates are global.
3. Tel85.c – This is the main program which is compiled with menus.h and vars.h. It also calls the functions Ant85Req, Ant85Set, Ant85Init, GetSidereal and GetUTTime which were created by Frank Ghigo.
4. Antennas.txt – This file contains the operating parameters for up to 4 antennas. It is read by Tel85 in the beginning of execution. Parameters include, motor controller specifications, limits, predefined positions, etc.
5. Help.txt – This help file can be read and modified by any text editor. It is available while tel85 is running by pressing H on any screen. Antenna adjustments will continue in the background while reading help.

Conclusions:

1. The antenna control software is now more robust, portable and easier to maintain.
2. The control system can now be connected over the internet via xhost or telnet.
3. Slow network connections or a slow system will not hinder the operation of the program. The antenna positioning algorithm compensates for slower sampling rates. The curses library tries not to overflow slow terminals.
4. When the connection to the motor controller is broken, the program simply beeps until the connection is reestablished. When reestablished, the program recovers without error.

# 40 foot local oscillator

Advisor: Wes Grammer

Summary: To finish the design and construction of a new local oscillator for the 40-foot telescope.

Objectives:
1. Create a LO with a 1.2 to 2.0 GHz frequency range.
2. The design should be made of several changeable modules.
3. Control via a keypad or remotely with a serial port.
4. Synchronized to 5, 10, or 100MHz reference.
5. Step function that allows a step size to be defined and buttons to change the frequency by the predefined step.

Solution:
1. Digitally controlled phase locked loop. *
2. Liquid crystal display. *
3. Use a PC/104 embeddable controller for the digital control. *
4. Connect the display, frequency control to the PC/104 bus. Connect a frequency selector switch and keypad to TTL(8255) ports.

* The asterisk denotes things designed by Wes Grammer. My role was to become familiarized with his general design and work out the details for digital control.

The PC/104 used in this project contained an 80188 processor running at 12 MHz which is easily capable of controlling all of the components. The display used was the Hitachi LM038 which has a single line of twenty liquid crystal characters and a Hitachi controller. A DDS was used to divide the incoming reference by an adjustable integer. The PC/104 adjusted this integer based on input from the keypad. The Keypad was connected to one of the PC/104 TTL ports. A standard 4X4 row/column scan was done to detect which of the sixteen keys were pressed. The qualcomm Q3236 was used for the PLL frequency synthesis. It contains a divider that was controlled by the PC/104 via the bus.

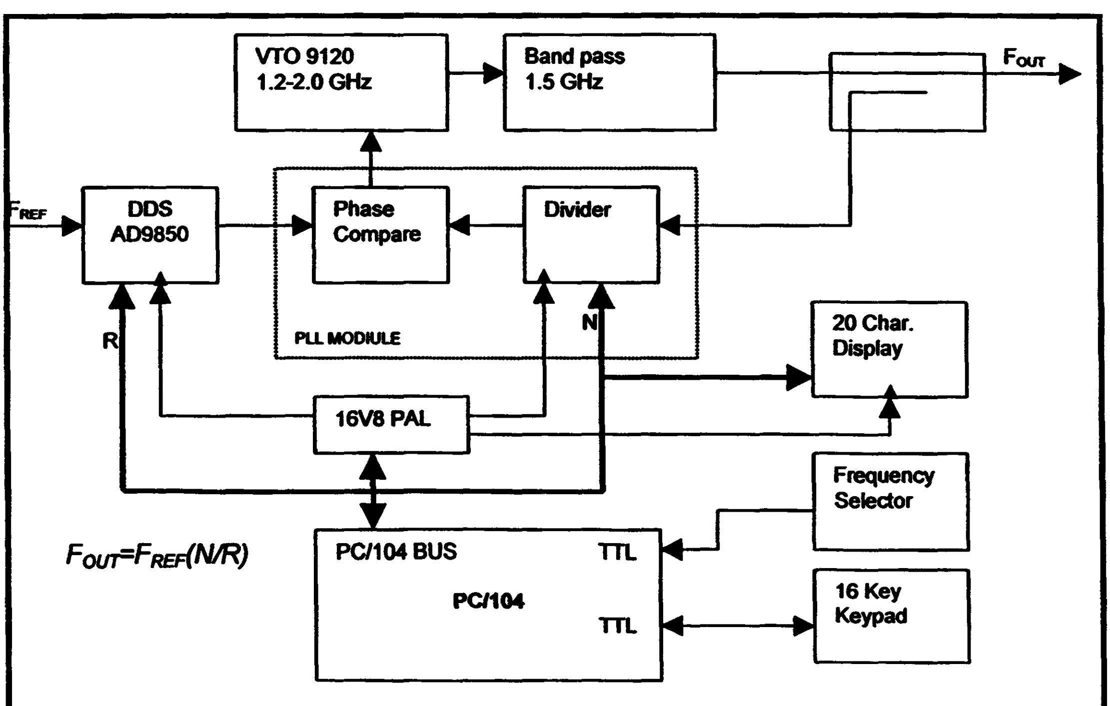


Figure 3 - 40-foot LO block diagram

A 16V8 PAL was needed for address decoding. It was programmed to output enables for specific addresses. Enable signals were needed for the PLL, DDS, and the LCD. The addresses assigned to these were arbitrarily chosen as follows:

| Pin | Port Address | PC/104 name | External device |
|---|---|---|---|
| | XX00 | Offboard I/O | LCD busy flag. Read only. |
| | XX01 | Offboard I/O | LCD instruction. Write only. |
| | XX02 | Offboard I/O | LCD data write. |
| | XX03 | Offboard I/O | LCD read as internal operation. |
| | XX08 | Offboard I/O | PLL AWR |
| | XX0C | Offboard I/O | PLL M1WR |
| | XX10 | Offboard I/O | PLL M2WR |
| | XX14 | Offboard I/O | PLL HOPWR. Load A, M1, M2. Data ignored. |
| | XX18 | Offboard I/O | DDS FQ_UD Update frequency. Data ignored. |
| | XX1C | Offboard I/O | DDS W_CLK |
| | FE00 | Watchdog | |
| | FE40 | 8255 Data A | Input from frequency switch. |
| | FE41 | 8255 Data B | Unused (output) |
| | FE43 | 8255 Data C | Keypad rows(PC0-PC3) + columns(PC4-PC7) |
| 1 | | System clock | |

The PC/104 was loaded with compiled C code. The source is shown below:

```
#include <stdio.h>
#include <conio.h>
#include "188regs.h"


/*ports for lcd display*/
#define IR_WRITE 0x00
#define IR_READ  0x01
#define DR_WRITE 0x02
#define DR_READ  0x03

/*PLL parameters*/
#define VCO_DIVIDE 1024.0
#define A_WRITE    0x08
#define M1_WRITE   0x0C
#define M2_WRITE   0x10
#define HOP_WRITE 0x14

/*User limits*/
#define MAXFREQ 2.0E9
#define MINFREQ 1.0E4
#define MAXSTEP 1.0E7



/*
Keypad scans a 16 button keypad and returns an
integer.
The keys are assigned values as follows:
           +-------------------------+
           |                         |
           |                         |
           |   {1}  [2]  {3}  [10}   |
           |                         |    ^
           |                         |   /|\
           |   {4}  {5]  {6}  [11}   |    |
           |                         |    |
           |                         |    |
           |   [7]  [8]  [9}  [12]   |    | Top
           |                         |
           |                         |
           |   {13] [0]  {14] {15]   |
           |                         |
           |                         |
           |                         |
           +-------------------------+
                      |_______|
*/


int printd(line)
  char line[20];
  {
  int place;
  long int x;
  while(inp(IR_READ)>0x80);
  outp(IR_WRITE,0x02);
  for(x=0;x<1000;x++);
  while(inp(IR_READ)>0x80);
  for(place=0;(place<20)&&(line[place]>0x0F);place++){
    outp(DR_WRITE,line[place]);
    while(inp(IR_READ)>0x80);
    for(x=0;x<100;x++);

    }
  return(0);
  }

int InitDisplay(){
  'long int x;
  char Test[20]="XXXXXXXXXXXXXXXXXXXX";

  outp(IR_WRITE,0x30);
  for(x=0;x<9000;x++);
  outp(IR_WRITE,0x0C);
  for(x=0;x<9000;x++);
  outp(IR_WRITE,0x01);
  for(x=0;x<9000;x++);
  outp(IR_WRITE,0x06);
  for(x=0;x<9000;x++);
  outp(IR_WRITE,0x14);
  for(x=0;x<9000;x++);
  if(inp(IR_READ)<0x80){
    printf("Display initialized.\n");
  printd(Test);

    for(x=0;x<90000;x++);
    return(1);
    }else{
    printf("Display error. \n");
    return(0);
    }
  }


int Previous=-1;


int Keypad() {
  long int x;

  int  Code[16]={0x11,0x21,0x41,0x81
,0x12,0x22,0x42,0x82
,0x14,0x24,0x44,0x84,0x18,0x28,0x48,0x88  };
  int Key[16]=  {1   ,2   ,3   ,10   ,4   ,5   ,6
,11   ,7   ,8   ,9   ,12  ,13  ,0   ,14  ,15  ];

  int Now;

  while(1){
    for (x=0;x<1000;x++);
    outp(DPORTC,0xF0);
    Now=(inp(DPORTC)&0xF);
    if(Now!=0){
      outp(DPORTC,0x10);
      if(inp(DPORTC)!=0x10)Now=Now|0x10;
      outp(DPORTC,0x20);
      if(inp(DPORTC)!=0x20)Now=Now|0x20;
      outp(DPORTC,0x40);
      if(inp(DPORTC)!=0x40)Now=Now|0x40;
      outp(DPORTC,0x80);
      if(inp(DPORTC)!=0x80)Now=Now|0x80;
      outp(DPORTC,0xFF);

      if((Previous!=-1)&&(Previous!=Now)){
          if(Previous>0){  /*Rollover routine. (Non-
essential)*/

if((Previous&0x0F)!=(Now&0x0F))Now=Now&(~(0x0F&Previou
s));

if((Previous&0xF0)!=(Now&0xF0))Now=Now&(~(0xF0&Previou
s]];

            for(x=0;(Now!=Code[x])&&(x<16);x++);
            if(x<16){
              Previous=-1;
              return(Key[x]);
              }
            }else{
            for(x=0;(Now!=Code[x])&&(x<16);x++);
            if(x<16){
              Previous=Now;
              return(Key[x]);
              }

            }
          }
      }else{
      Previous=0;
      }
    }
  }

double Adjust(Freq)
  float Freq;
  {
  float Clock=5.0E6;
  float DDSStep;
  int x;
  char Temp[20]="                    ";
  union DDS_load{
    unsigned long int Full;
    char Word[4];
    }DDSAccum;
  printf("\nDesired frequency    : %8.1f Hz.
\n",Freq);
  DDSStep=Clock/4294967296.0; /*4294967296=2^32*/
  printf("DDS step frequency   : %8.6f
Hz.\n",DDSStep);
  DDSAccum.Full=(unsigned long
int)(0.5+Freq/(VCO_DIVIDE*DDSStep));
  printf("DDS accumulator input: %lX (%lX)\n
",DDSAccum.Full,DDSAccum.Word[0]);
  printf("DDS output frequency : %8.1f
Hz.\n",((float)DDSAccum.Full)*DDSStep);
  printf("Sythesized VCO output: %8.1f
Hz.\n",((float)DDSAccum.Full)*DDSStep*VCO_DIVIDE);
  printf("VCO resolution        : %8.3f
Hz.\n",DDSStep*VCO_DIVIDE);
  outp(0x1C,0x04);/* Reset DDS.*/
  for (x=0;x<1000;x++);
```

```
  outp(0x18,0x00);
  for (x=0;x<1000;x++);
  printf("%02X ",outp(0x1C,0x00)); /*Phase and control
word*/
 .for (x=0;x<1000;x++);
  printf("%02X ",outp(0x1C,DDSAccum.Word[3]));
  for (x=0;x<1000;x++);
  printf("%02X ",outp(0x1C,DDSAccum.Word[2]));
  for (x=0;x<1000;x++);
  printf("%02X ",outp(0x1C,DDSAccum.Word[1]));
  for (x=0;x<1000;x++);
  printf("%02X ",outp(0x1C,DDSAccum.Word[0]));
  for (x=0;x<1000;x++);
  outp(0x18,0x00);
  sprintf(Temp,"%12.6f MHz.
",(((float)DDSAccum.Full)*DDSStep*VCO_DIVIDE+0.5)/1.0E
6);
  printd(Temp);
  return(((float)DDSAccum.Full)*DDSStep*VCO_DIVIDE);
  }

double Step(){
  int place=5;
  double entry=0.0;
  long int x;
  int key;
  char Display[20]="Step-              ";
  printd("Enter step size.      ");
  while(place<20){
    key=Keypad();
    switch(key){
      case 10:
          printf("\n");
          sscanf(Display,"Step=%lf",&entry);
          sprintf(Display,"%15.6f MHz",entry);
          printd(Display);
          for(x=0;x<200000;x++);
          return(entry*1.0E6);
          break;

      case 11:
          printf("\n");
          sscanf(Display,"Step=%lf",&entry);
          sprintf(Display,"%15.9f GHz",entry);
          printd(Display);
          for(x=0;x<200000;x++);
          return(entry*1.0E9);
          break;

      case 12:break;
      case 13:
          place=5;
          printf("\n");
          sprintf(Display,"Step=              ");
          break;
      case 14:
          Display[place]='.';
          printf(".");
          place++;
          break;
      case 15:
          return(0);/*abort frequency entry*/
          break;
      default:
          Display[place]=key+48;
          printf("%ld",key);
          place++;
      }
    printd(Display);
    }
    return(10.0);
  }

double Center(){
  int place=7;
  double entry=0.0;
  int key;
  char Display[20]="Center=            ";
  printd("Enter center.          ");
  while(place<20){
    key=Keypad();
    switch(key){
      case 10:
          printf("\n");
          sscanf(Display,"Center=%lf",&entry);
          return(entry*1.0E6);
          break;

      case 11:
          printf("\n");
          sscanf(Display,"Center=%lf",&entry);
          return(entry*1.0E9);
          break;

      case 12:
          return(0); /*abort frequency entry*/
          break;
      case 13:
          place=7;
          entry=0;
          printf("\n");
          sprintf(Display,"Center=             ");
          break;
      case 14:
          Display[place]='.';
          printf(".");
          place++;
          break;
      case 15:break;
      default:
          Display[place]=key+48;
          printf("%ld",key);
          place++;
      }
    printd(Display);
    }
  return(0.0);
  }

main(){
  long int x;
  double StepSize=1000.0;
  double Freq=1.0E6;
  double Want;
  InitDisplay();
  outp(DCMDR,0x91); /*Initialize keypad*/
  Adjust(1.0E6);
  while(1){
    switch(Keypad()){
      case 10:
          if((Freq+StepSize)<MAXFREQ)Freq=Freq+StepSiz
e;
          Adjust(Freq);
          break;
      case 11:
          if((Freq-StepSize)>MINFREQ)Freq=Freq-
StepSize;
          Adjust(Freq);
          break;
      case 12:
          Want=Center();
          if((Want>MINFREQ)&&(Want<MAXFREQ))Freq=Adjus
t(Want);
            else Adjust(Freq);
          break;
      case 15:
          Want=Step();
          if(Want<MAXSTEP)StepSize=Want;
          Adjust(Freq);
          break;

      }
    }
  }
```

Figure 4 – C code to be loaded into the PC/104

Conclusions:

The project could not be completed so it was brought to a state where is can be taken over by someone else. All testing and diagnostic tools were documented as well as what has been finished and what needs to be done. The following has been completed:

1. Keypad interfaced and tested. A routine was written to scan the keypad and return keystrokes to software.
2. Frequency selector switch interfaced.
3. Display interfaced and tested. A routine was written to write strings to the display.
4. DDS interfaced and tested. The mathematics for loading the DDS was written and works correctly.
5. Two voltage regulators were soldered into a circuit board and tested.
6. The bus cables (bold lines in figure 3) were built and tested. Connection to the DDS works fine but the PLL connection is untested.
7. Simple user interface allows a user to type on the keypad, view the entry on the display and see the corresponding adjustment on the DDS.

Still to finish:

1. PLL needs to be assembled, plugged in and tested. The DB-25 connector cable is already built.
2. RF assembly and testing.
3. Building an enclosure and final assembly.

# A Survey to Detect Galaxies with High-Velocity Gas

Naomi S. Bates (Princeton Univ./NRAO)

HI observations of 70 near face-on galaxies with the NRAO 140 ft telescope detected numerous galaxies that show significant evidence of high velocity gas (HVG), most of which have not been previously reported to have such gas. The observed HVG may be a warm component of the ISM, gas accelerated to high velocities, or gas external to the plane of the galaxy.

The chosen galaxies typically have sizes < 20', velocities < 1600 km $s^{-1}$, and HI fluxes > 50 Jy km $s^{-1}$. About half of the galaxies are irregulars and the rest are spirals. Our observations are well suited to detecting HVG since they have both high sensitivity and good velocity resolution (1 or 2 km $s^{-1}$). The work is part of a project to study how the properties of galaxies (e.g., galaxy type, star formation or supernovae rates, and IR emission) and HVG are related.

Since the galaxies are nearly face on, their HI profiles show only slight, if any, rotational broadening. To model the rotational broadening as well as to identify the existence of HVG, we used a non-linear, least-squares routines and a physical model similar to that Schulman used in his thesis (1995, University of Michigan). Typically, the detected HVG has a velocity dispersion twice that of the normal (cold) ISM, regardless of the dispersion of the cold ISM. HVG makes up 10 to 50% of the HI mass in these galaxies.

High Redshift Molecules:
My 1998 Summer Experience at NRAO-Green Bank

by Keri Ann Eberhardt

working under astronomer Glen Langston

Over the course of three months, Glen Langston and I worked together on numerous projects, from observations with the 140' telescope to repairing the tour center's on-site solar system model to compiling galactic data with the 45' tracking station. I thank Glen for his patient teaching and constant smile, and I also thank all of the NRAO staff for their dedication to us students. I am so grateful to have met and worked with all of you.

## High Redshift Molecules

Knowing which molecules were present near early galaxies and quasars is crucial, for within this knowledge lie clues to the universe's overall structure and history. Questions like, "Was the universe as molecularly complex at its birth as it is now?" can be answered as certain species are and are not detected. Also, previous molecular detections at high redshift (i.e. Omont et al, 1996) show that the detection of early molecules, despite the high sensitivity required for these measurements, is possible when and if a certain molecule is present.

NRAO astronomers Glen Langston and Robert Brown chose a redshift range of $3.35 < z < 3.83$ for our source sample so that the molecules H2O (rest frequency, 22.2 GHz) , HCN (88.6 GHz) and CO (115.3 GHz) might be observed using the existing Cassegrain receivers on the 140' telescope. Their final list of 27 sources was approved for 10 days of observing using the Green Bank 140' telescope on C and K band receivers.

When I arrived, I had only three days to learn radio astronomy basics before our observing began. In this time, Glen and the 140' engineers showed me the auto correlator and harmonic mixers, as well as the receivers inside the Cassegrain house. Not only was this profitable for me educationally, but also it specifically enhanced the observing because I could better imagine what was physically happening between the received signal and the data output.

As a side experiment, Glen wanted to process the data using both the 140' auto-correlator and the GBT (Green Bank Telescope) spectrometer. We had to use time-tagged data which synchronized with the 140' nutation and mod-focusing because the telescope and GBT spectrometer were not operating with the same software. Resultingly, I kept track of when the 140' was on and off source so that we could find out which data from the GBT spectrometer was usable (that is, which data was not taken in between nutation cycles).

Our observations started on May 22, 1998. We first tested the telescope on the Orion KL region by detecting certain hydrogen recombination lines and the water line. The data from both the auto-correlator and the GBT spectrometer showed up well for the H20 (22.2 GHz) observations, but the hydrogen recombination lines were not good due to unusually high noise levels. After changing a bad card in the auto correlator and a configuration on the local oscillator, the noise was severely reduced and our tests continued successfully. From that time onward, we observed for ten days under the same general process: initially testing using either Orion KL or SGR B2 as sources, then pointing the telescope with radio bright objects (like 3C286), then observing one of our 27 sources for two hours, then pointing again, then observing a source again for two hours, and so on until our time was up.

The double beam switching technique (DBLBO) was used for most of our observations. This technique not only modulates the focus of the receiver, but also switches back and forth between ON source and OFF source positions at regular intervals (for our observing, each interval was six minutes long). As a result, we end up with four possible spectra (ON source at one focus, ON source at another focus, OFF source at one focus, OFF source at another focus). The 140' first local oscillator was set to 13.32 GHz (.347 X 48 X .8) and the second local oscillator was set to 15.8 GHz. For the GBT spectrometer data, we altered the second LO frequencies for each source in order to center any absorption features present along the 800 MHz wide line. For the 140' auto-correlator data, the channel width was 0.625 MHz (80 MHz/ 128 channels) with two polarizations. For the GBT spectrometer data, the channel width was 0.195 MHz (800 MHz/ 4096 channels) with one polarization.

On the fifth day of observing, source B1422+2309 (z=3.62) became much more interesting after we found that damped Lyman-alpha forests had previously been detected near it (Bechtold and Yee, 1995). Using the observed wavelengths of the Lyman-alpha forests and the rest frequencies of neutral hydrogen and other molecules, we could determine at what frequencies other molecules might be detected to a much greater accuracy. Also, knowing that neutral hydrogen had been detected near B1422+2309 increased the possibility of finding more complex molecules near the same source, especially compared to other sources with no known molecular clouds. The fact that B1422+2309 is gravitationally lensed was attractive as well, because the images we received from it were magnified.

Thus, what started as observations of a sample of 27 high redshift sources was eventually narrowed down to one source of particular interest. We observed B1422+2309 on both May 26 and June 3 of 1998, and ended up with a total integrated observing time of 14:00:00 (14 hours) for CO and 00:48:00 (48 minutes) for HCN. Neither the 140' auto-correlator nor the GBT spectrometer plots showed significant absorption features for this source.

By not observing significant features for B1422+2309, we can set an upper limit for the amount of CO near B1422+2309 based upon column-density models used by Wikland and Combes in their study of PKS 1413+135 (z=0.247) (1997). That is, at our sensitivity, there cannot be anymore CO or HCN beyond some number X (which we have, as yet, to determine), because, otherwise, we would have detected it at our level of sensitivity.

References

Bechtold J., Yee H., 1995, AJ, V110, 5
Omont et al
Wikland T., Combes F., 1997, A&A, 328, 48

# H I Survey of the Milky Way

Jennifer Lockman
College of Charleston

This summer Jennifer Lockman worked with Dr. F. J. Lockman on a survey of neutral hydrogen, or H I, in the Milky Way Galaxy. The entire survey covers $\ell = 65°$ to $185°$ and $b = \pm 10°$. Over two observing runs this summer and many others over the past few years, the bulk of the data has been obtained for the survey.

Observations were conducted at the 43m telescope at Green Bank, WV at 1420 MHz. The student aided Dr. Lockman in the process of reducing the data which involved discovering the proper baseline for the data set, performing an atmospheric correction and determining whether the system temperature varied as a function of time of day and hour angle. The student also learned the process of observing with the 43m telescope which involved planning the observations and writing the observing program files that command the telescope.

The data were taken as scans for the most part, where the telescope scanned at a constant latitude over a 10° longitude strip. In the scan mode, the signal was integrated every 20 seconds, meaning that a spectrum was obtained every $8'$ giving full Nyquist sampling. Care had to be taken in areas of the Milky Way where the continuum changed significantly over small angular sizes. The noise tube firing the calibration signal could be misinterpreted by the electronics from one firing to the next, offsetting the calibration by the amount the continuum was changing. In this case, the telescope moved every $8'$ and stopped and the spectra were taken individually.

NATIONAL RADIO ASTRONOMY OBSERVATORY

POST OFFICE BOX 2 GREEN BANK, WEST VIRGINIA 24944-0002
TELEPHONE 304 456-2011 FAX NO. 304 456-2271

To: David H. Parker
From: Patrick B. Matheny
Date: September 4, 1998
Subject: REU Summer Student Report for May 11 - August 21, 1998

I worked for the Green Bank Telescope (GBT) Antenna Metrology Group for my summer assistantship. I worked on a variety of projects ranging from the GBT rangers to a hydrostatic level. My main project was the hydrostatic level. It was somewhat functional when I arrived, but had plenty of modifications and new tasks that needed to be completed.

During the first weeks of my stay I helped my coworkers with work being performed on the rangers. We tested rangers, that were in place around the GBT, for their pointing accuracy. I was taught how to run the ZIY program, the program used to point the rangers, by Jason Ray who is a Co-op student at NRAO. We performed this at night to help us in seeing where the lasers were hitting. At the beginning of the summer the lasers were not pointing as accurate as they could. We re-surveyed all of the points that we used as targets and performed the pointing test again. By mid summer we had the lasers pointing pretty well, we could get a ranger to point to another rangers retro on the left and turn it to point to another rangers retro on the right and get roughly the same amount of return. This told us that the rangers could be adjusted to point where they are supposed to.

I also worked with my coworkers on the GEO-SAR project. The GEO-SAR project is a laser ranger for Jet Propulsion Labs (JPL). It had to be designed to the size that JPL requested. This brought several restrictions into play when the design was being drawn up. They also needed the laser beam to be roughly 10 inches in diameter at 10 meters. This meant that a lens had to be used to expand the beam. I learned that optics can play a big role in the transmitted laser beam. The laser comes out of the laser unit at roughly 3 mm and goes through an expanding lens that at 10 meters will give a 10 inche diameter circle. Once the laser is reflected back to the ranger unit it goes through another lens that focuses the laser on the detector. We found out that by expanding the laser also meant that the laser unit had to have a uniform beam. If the beam wasn't uniform it would make it impossible to get accurate results. By the end of my stay a unit had been built and was in the process of being tested.

My main project was the hydrostatic level. Bill Radcliff helped me set up the hydrostatic level and get what was done, at that time, working. When I started, the level ran two probes, took the reading of the water level and stored the data in a file. There were several things that needed to be added. Temperature sensors needed to be incorporated, a water system that could pump water and keep it where needed, a way to tell if the probes were in the water or not when the program was started and the program had to be modified to run the new hardware.

After I became familiar with programming in Basic and the commands to control the bits of the DGH modules, the first thing I worked on was to fix the program so that if the water touched the probe more than once, on a given reading, that the computer wouldn't mess up. Next, I wrote a loop to check and see if the probes were in the water when the program was started. To do this I added a connection to the interface boards that would either be a high voltage or a low voltage depending on whether the probe was in the water or not. If the program decided that a probe was in the water it executed commands that would drive the probe up out of the water.

Another modification was to add in thermistors. There were three thermistor that needed to be incorporated into the hydrostatic level. I added the commands to the program that would take temperature readings and display them on the screen of the computer. By doing this the user could see what the temperatures were at the respective thermistor. I also added a loop to circulate water in the system. The temperature reading were a part of the loop along with turning valves and pump on or off. This loop had to be written to control the valves and pump in a given order so that you wouldn't pump unwanted water into the beakers or drain it out. I also had to keep as much air out of the lines as possible, so I kept the water locked in the lines until the pump was started. Circulating the water allows the temperature of the water to be kept constant at both beakers. After this circuit was built, the valves and pump had to be connected. I designed an aluminum plate to hold the six valves and a power strip. I then connected the controlled AC lines to the power strip and then connected the valves and pump to their respective line. Two thermistors were used to monitor the temperatures of the water, one in the supply line and one in the return line.

I also had to build a circuit that would allow the six valves and pump to be controlled by the computer. To do this I used solid state relays, which would allow me to control 120VAC by turning a bit of the DGH module on or off. I also put the pump in a reservoir, so that the level could be used for demonstration.

I gave a talk on the hydrostatic level to the NRAO staff. In the talk I explained what it was going to be used for, a general idea of how it worked, why it was better than optical levels and demonstrated the hydrostatic level. I also showed a graph that demonstrated the levels accuracy. The data was taken over thirty minutes and showed the evaporation of water over that period of time.

During my last week, I went with Jason Ray up on the GBT surface to run a test on the panel setting tool. The test was to see how accurate they could adjust the test panels that were in place on the GBT. The test also gave us an opportunity to find any problems that needed to be fixed.

NATIONAL RADIO ASTRONOMY OBSERVATORY

POST OFFICE BOX 2 GREEN BANK, WEST VIRGINIA 24944-0002
TELEPHONE 304 456-2011 FAX NO 304 456-2271

There were a few problems that were encountered and later fixed by Jason. Another test was scheduled for the next week to try the unit with the problems fixed.

I would like to thank David H. Parker and the Metrology group, National Science Foundation and NRAO for giving me the opportunity to work with the GBT Antenna Metrology group. I found the work to be very interesting and knowledgeable and gained valuable experience during the time I spent at NRAO.

Sincerely,

Patrick B. Matheny

Turbulence in HII regions
Summer Research Project 1998
NRAO REU Program
Nicole Wiersgalla
advisors: Dana Balser and Toney Minter

I have been studying one HII region, W43 so far this summer. In order to determine if there is actually turbulence present, we need to look at:

*density fluctuations (really observing emission measure so it is the density squared)

*velocity fluctuations over the region

The start with the density fluctuations, we have been looking for a power law with a slope that would signify turbulence.

I have written a C program that reads in the UV data from the region. I then plot the data by log (amplitude squared) vs. log (uv distance), with one plot per channel. We have then fit a line to the points to get the slope of the power law.

So far, it looks like there is turbulence by the slope of the line, which fits the formula:

power spectrum = 10^6 * (uv dist.)^ -2.1

*where the power spectrum is the amplitude squared.

The velocity fluctuation part of the project is where most of the useful information will come from.

I have taken the spectral line data, and fit a guassian to the line for each pixel across the region. I then made a map of the center velocitie to see if there was any sort of motion present. (To do this line fitting, I used a program called GIPSY, Groningen Image Processing System)

The center velocity data was also written to a data file, and Toney computed the structure function. So far, we have not come to any real conclusions about what the structure function tells us about the region. But, this is something I will work on this next year.

The next step is to start with another HII region, NGC6334. I will follow the same procedure with the next region. When I work on my thesis, Toney and Dana plan to have me look at more regions, and then see if there is any sort of correlation between turbulence and other characteristics of the HII regions (size, density, age, etc.)

# Compact Extragalactic Radio Sources

Andrew A. West
Haverford College
NRAO Summer Student 1998
Advisor: Ken Kellermann

**Abstract**

Using the Very Long Baseline Array (VLBA), 132 active galactic nuclei (AGN) which contain compact radio sources were imaged at a wavelength of 2 cm. The resolution of less than 1 mas in some cases has allowed for cosmological tests to be performed. Using the theory for standard rods and standard velocities in a Friedmann cosmology, relations of angular size and proper motion were respectively compared to the redshift of the object. Because the theory for AGN and jet physics is not clear, challenges have arisen in reducing the scatter of the data. Although neither test seems to constrain a particular universe or value of q at the time of writing, there is evidence that the proper motion-redshift test may yield significant results in time.

## 1. Introduction

### 1.1 Compact Radio Sources

Compact Extragalactic Radio Sources are considered the central engines of AGN. They are powerful emitters and have peak brightness temperatures approaching or at $10^{12}$ K. Using the VLBA interferometer, high resolution images are made which show structure on a couple of parsec scales. The resolution is so good that a dime could be imaged at a distance of 3500 km (if it were radio bright.) Although these compact sources have been studied for many years, there are still many mysteries. The physics of these objects is not well understood. It is believed that the bright central component is produced by self absorption of the relativistic electrons traveling out of the core or black hole along the magnetic field lines. This is believed to happen when the brightness temperature is around $10^{12}$ K. These relativistic electrons also produce the jet structure seen. When observed over a period of time, the jet components appear to move. A good example of this movement can be seen in the source 1226+023 (Figure 1.) There are several theoretical models for the movement of these side components along the small scale jets.

However, they will not be discussed in this paper and are considered not well understood.

The standard model of a radio galaxy is an object with a core component, collimated jets and large side lobes. This large scale structure can approach hundreds of kiloparsecs. However with the parsec scale used in this study, small scale jet structure can be seen. Sometimes the jets are seen to align with their large scale counterparts and other times there seems to be a collimated jet that does not align but instead twists and turns before reaching a straight path. Again, there is little understanding of either phenomenon.

There are many interesting things that can be learned from these compact sources. A better understanding of the Jet physics, AGN unification and cosmology are just three areas that can stand to gain from these powerful giants. This paper focuses on two of the cosmological tests that can be performed with the use of these compact sources. They are the angular-size redshift test and the proper motion redshift relation. Cosmological tests are believed to be an excellent use of compact sources because of the small effect that universe evolution plays on these objects. Their small size in comparison to their host galaxies and other extragalactic objects make them almost if not totally unaffected by changes in things like the intergalactic medium. Their lifetimes of tens to hundreds of years are very short in comparison to age of the universe and thus they should be similar to one another at a variety of different redshifts. This of course holds only in the case where the physics of these objects is the same. Currently, this is the common agreement.

### 1.2 Angular Size- Redshift Relation

It is possible for compact radio sources to be considered standard rods. As mentioned above, because of their small size, large energy output and subsequent short lifetimes, compact source linear size may be virtually constant and independent of epoch. If so, compact radio sources could serve to answer one of astronomy's current questions, what type of universe do we live in? Basic Friedmann cosmology assigns parameters to the geometry of the universe. If compact radio sources do possess the quality of standard rods than it will be possible to solve for these parameters by looking at the angular size of the sources at different epochs. It may not be possible to isolate a specific cosmology but constraints can be put on some of the cosmological parameters. Our task will be to devise a method to measure the angular size of the compact radio sources and plot our results against the redshifts.

The equation for angular size of an object based on its epoch can be expressed by,

$$\theta = \frac{H_0}{c} \frac{q_0^2 (z+1)^2}{q_0 z + (q_0 - 1)(\sqrt{2 q_0 z + 1} - 1)} L \qquad \textbf{(1)}$$

where H is Hubble's constants, q is the deceleration parameter, z is the redshift, c is the speed of light and L is the linear size of the source. A theoretical curve for 3 different values of q is given in Figure 2.

### 1.3 Proper Motion-Redshift Relation

As discussed above, many compact radio sources appear to have small jets coming from them. Individual components can be measured with VLBI technology. It has been found that these components are moving away from the central core of the radio source. Original measures of the velocities put these speeds well over the speed of light. They were thus dubbed superluminal radio sources. As we know, it is impossible to break the universal speed limit of light, and thus an explanation is in order. One of the more convincing models is that the jets are beamed at a very small angles to the line of sight. The model also suggests that the components of the jets are moving at or close to the speed of light. Therefore the components are emitting radio light as they move at high speeds towards us and hence relativistic effects must be taken into account. The geometry of the situation is fairly trivial and can be demonstrated to find that the superluminal velocities arise from a time delay in the light travel time of the core component as the moving component "catches up" to the emitted core light.

It is also important to note that the probability of seeing something beamed close to the line of sight is small. But due to the fact that the beaming dramatically increases the observed emission by Doppler Beaming, we most likely only see components from high z objects that are beamed towards the line of sight. Therefore the sources can be considered self selecting. Basically, the objects far away are impossible to see unless they are beamed close to the line of sight and so we only see those sources. If a jet's emission is strengthened along the line of sight, then the other, opposite to the line of sight, will be diminished. This enables us to see mostly sources with one jet coming out of them. We do see some two jet objects. These are found at low z and will help us in determining the angle to the line of sight as well as Hubble's constant. With the phenomenon of Doppler beaming creating a selection effect, it can be assumed that all of these objects are undergoing the same physics processes and can be considered standard velocities or standard javelins.

As one might assume when the redshift of the object gets higher, cosmological effects start to appear. Assuming that all of the jets are beamed along the same angle and that they all are moving at about the same velocity ~c, then we can measure their apparent motion along the sky and solve for a cosmology. Like the angular size-redshift relation, there may be too much scatter to solve for a specific cosmology and we may settle for constraining some of the important constants. If the theory discussed above is correct, then we can fit our data using the relation,

$$\mu = \frac{\beta_{app} H_0 (1+z)}{z} \left[ \frac{1+(1+2q_0 z)^{\frac{1}{2}}+q_0 z}{1+(1+2q_0 z)^{\frac{1}{2}}+z} \right] \qquad \textbf{(2)}$$

where q is the deceleration parameter, H is Hubble's constant, μ is the proper motion in the sky and β is the apparent transverse velocity in multiples of c. A theoretical curve for three different values of q is shown in Figure 3.

## 2. Observations

The data consists of 2 cm observations made by Kellermann, Vermeulen, Zensus and Cohen using the VLBA interferometer. It is an unbiased and very complete data set of extragalactic sources. In the past, people studying compact radio sources have looked at a couple of sources that were exotic or fast moving. People who were interested in looking at all of the sources as a whole were forced to use other people's data and deal with the fact that the sample was biased. In the Kellermann et al. (1998) data there are 132 total sources which have been observed multiple times starting in August of 1994. At the time of writing, the last observations were made in March of 1998. There are scheduled observations for the fall of 1998. Later writings will include the data from these runs.

## 3. Analysis

### 3.1 θ vs z

The challenging part of this test was deciding how the size of each object would be measured. But before that could be done, it was thought important to have a beam size that was a similar linear size for all of the sources. Using a q of 0.5 and a H of 65 km/sec/Mpc, the images were all convolved in AIPS to obtain a linear beam size of 0.008 X 0.004 pc. It was thought to be important to smear out the objects at smaller redshifts because of the finer structure that would be observed due to their close proximity.

It was decided to measure the distance from the core to the component farthest from the core at 1% of the core's flux. This was decided because less than 1% created too much noise on many on many of the images and more than 1% eliminated too many sources. Other techniques that were considered and may be used in the future were looking at all of the closest components, the brightest components or the furthest components. Using basic AIPS procedures, measurements were made of all of the sources with components at 1% of the peak flux. It was determined that sources with luminosities below $10^{25}$ W/Hz should not be included because below this luminosity the physics are predicted to be different than other sources. The measured angular distances were plotted using Microsoft Excel in a angular size vs. Redshift plot. (Figure 4) Sources were then binned and the result can be seen in Figure 5. Error bars were not included in either of the plots. Because of the large scatter, constraining a cosmology or any cosmological parameters appears to be far off. This test shows little promise. It is possible that another way to measure the angular size of these objects may be found in the future.

### 3.2 $\mu$ vs z

The measurements for the sources in the proper motion redshift relation were straight forward. Gaussian fits were made of the core and all of the side components. Distances from the core to the side components were calculated in each of the epochs. Each component's angular distance from the core were then plotted versus time and a least square fit (LSF) was used to fit a line to the data points. The resulting slope calculated was the proper motion in miliarcseconds (mas) per year. (Figure 6) Using the Excel function LINEST, errors in the slope were calculated.

Sources were eliminated based on four criteria. In order to be included in the study, sources had to have a measurable redshift, at least one side component, a well defined side component and a slope error of less than 50% of the value of the slope. After eliminating many sources, the data consisted of ~100 sources. These sources were used to make a plot of proper motion versus redshift (Figure 7.) From this plot, it was apparent that cosmological effects were present but the scatter of the data points would not constrain any cosmological parameters.

In order to reduce the scatter of the data, several characteristics of each source were looked at. One of the things was the luminosity. As mentioned above, sources with low luminosity are most likely exhibiting different physical phenomenon. In fact, there is a good chance that these low luminosity sources have similar processes going on but are not beamed at angles along the line of sight. The reason we can still see them is because they are at low values of z and therefore much closer. The limit we used for this test was $3.5 \times 10^{25}$ W/Hz. All sources below this limit were not included. Figure 8 shows a histogram of the distribution of apparent velocity when we limit the luminosity of the sources. H of 65 km/s/Mpc and a q of 0.5 were used to calculate the apparent velocity. It can be seen that there is a peak in the distribution around a value of 5 or 6c. Figure 9 shows the apparent motion versus z plot after binning the sources. It is possible to see that there is a trend in the fall off of this plot that may constrain values of q if the errors can be reduced.

Another characteristic that was looked at in limiting the source data and decreasing the scatter is the source type. There are conflicting views on what the relationship between different types of AGN are. In this study it appears that the quasar population has less scatter than that of the Bl Lac or Radio galaxy populations. This can be seen in Figure 10. Figure 11 shows the distribution of apparent velocity for quasars. Again we see a peak in the distribution around a value of 6c. This is encouraging. Binning the data and plotting the proper motion versus redshift (Figure 12) yields a distribution with less scatter and a higher chance of constraining some of the cosmological parameters.

The last characteristic that has been looked at is gamma ray production in these AGN. There is limited data on Gamma ray production in AGN. That which is available has shown to be promising (Figure 13) and yields a similar distribution in apparent velocity (~6c.) However, more data is needed to make any valid claims.

## 4 Conclusions

### 4.1 Summer Results

As seen from the various figures and text above, nothing conclusive has been determined as of yet. The angular size redshift relation has not proven promising in the work done this summer. The scatter it too great and although at lower redshifts we see a 1/z fall off which is to be expected, the data scatters at $z > 0.8$. However, because the hypothesis of the compact sources as standard rods continues to make good sense, there are perhaps different techniques that can be applied to this data set in order to yield an answer to this cosmological question.

On the other hand, the proper motion vs redshift relation has shown good evidence of promising results. Although nothing can be said for sure at the time of writing, one can see how limiting certain factor in the data has produced less scatter in the distributions. The addition of new data from a fall of 1998 observing run as well as more thought on limiting factors that might reduce the scatter in the distributions of apparent velocities, might lead to constraints on the value of q.

It is especially important to make observations of many objects at high z. One epoch of these high z observations have already been made. Subsequent runs will give us a better understanding of this relation at higher z where the cosmological effects become drastically more important.

## 4.2 Future Work

Some of the future work planned has already been discussed. More data and a better understanding of the theory and physics of the compact radio sources will help to better constrain cosmological parameters. The study of these sources will also break somewhat from questions of cosmology and look into specific questions of the sources. There is a plan to look at the sources variability and how that corresponds to the movement and ejection of the side components. There is also a plan to look at the surface brightness of each of the objects in order to make an observational study of the Tolman relations.

There is still a considerable amount of knowledge that can be gained from the study of these extragalactic compact radio sources. The work completed this summer has but scratched the surface of all that is possible. With each new observing run, we hope to gain a superior understanding of these powerful monsters of space and use them to help us better understand the shape, history and beginnings of our universe

## 5. Acknowledgments

I would like to thank Ken Kellermann for taking the time to listen, and teach me so patiently this summer. He has been a great influence in my starting on a new intellectual adventure. I would also like to thank Al Wootten for his help in making the summer fascinating and refreshing by complimenting our research with talks and observations. And thanks to the NSF for funding the NRAO REU program. It has been a valuable step in my continuing process of edification.

## References

Cohen et al. 1988 ApJ 329 1

Gurvits 1994 ApJ 425 442

Kellermann, K. Preprint

Kellermann, K. I & Pauliny-Toth, I. I. K. 1981 Ann Rev A&A 19 373

Kellermann, K. I. 1993 Nature 361 134

Kellermann et al. 1998 AJ 115 1295

Mukherjee et al. 1997 ApJ 490 116

Neeser et al. 1995 ApJ 451 76

Vermeulen, R. C. & Cohen, M. H. 1994 ApJ 430 467

Zensus, J. A. 1997 Ann Rev A&A 35 607

Captions

Figure 1: Side Component Motion in source 1226+023

Figure 2: Theoretical curves for 3 different values of q in Angular Size (mas) vs. redshift relation.

Figure 3: Theoretical curves for 2 different values of q in Proper motion (mas/year) vs. redshift relation.

Figure 4: Raw Data Angular size (mas) vs. Redshift

Figure 5: Binned Data for Angular Size (mas) vs. redshift relation.

Figure 6: Angular Size (mas)vs. time (years) Least Square Fits for source 1226+023. Different letters represent the different components.

Figure 7: Proper motion vs. redshift for all components. Error bars are from linear fit errors.

Figure 8: Distribution of apparent velocity for sources with luminosity > $10^{25}$ W/Hz.

Figure 9: Binned Data for proper motion vs. redshift luminosity selected sources

Figure 10: Proper motion vs. redshift separated by AGN type.

Figure 11: Distribution of apparent velocity for quasars.

Figure 12: Binned data for proper motion vs. redshift quasar selected sources.

Figure 13: Distribution of apparent velocity for sources with gamma ray emission.

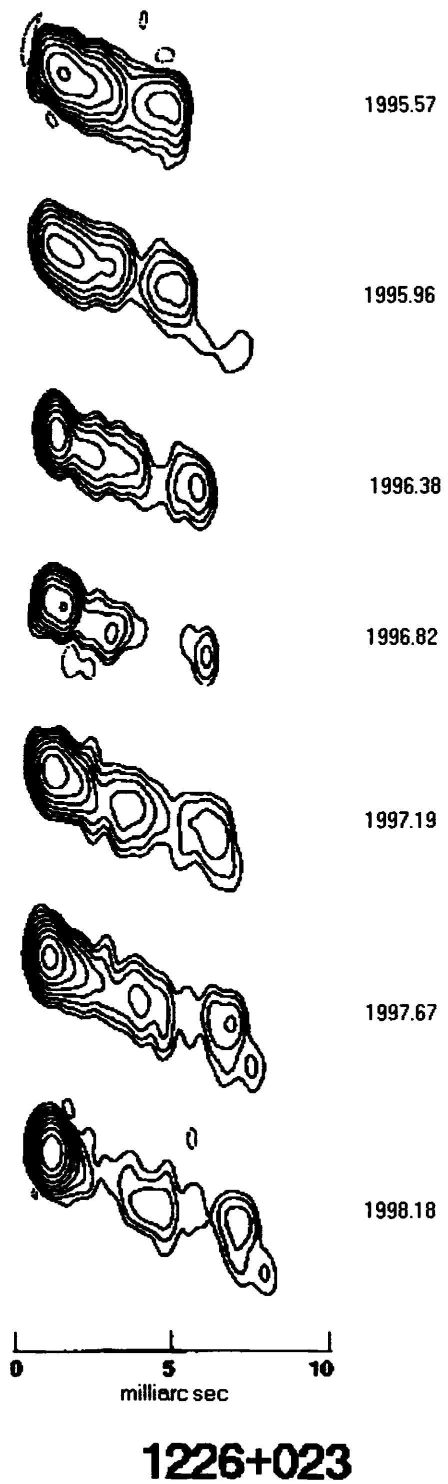
1995.57
1995.96
1996.38
1996.82
1997.19
1997.67
1998.18
0
5
10
milliarc sec
1226+023

Figure 1

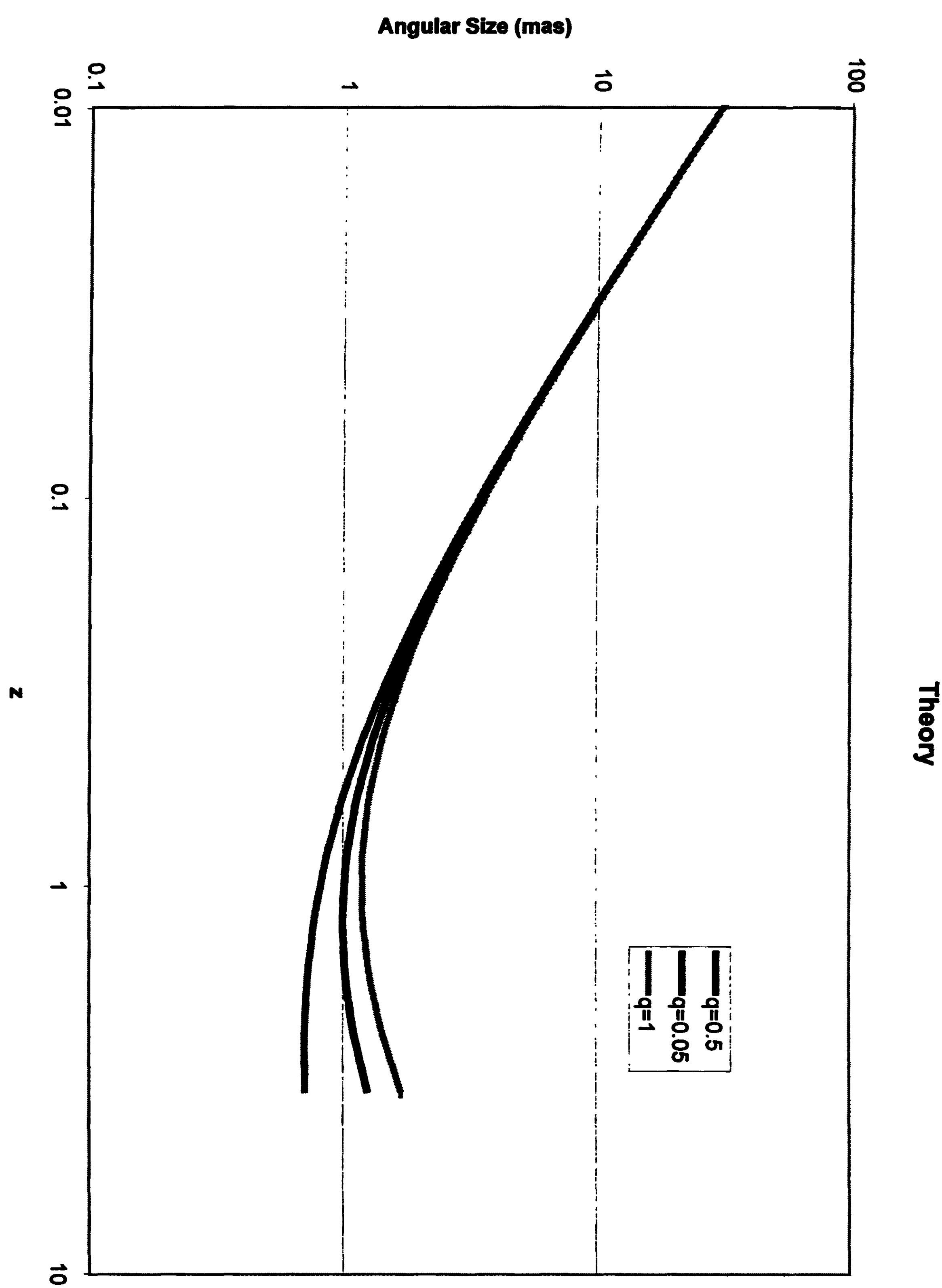


Figure 2

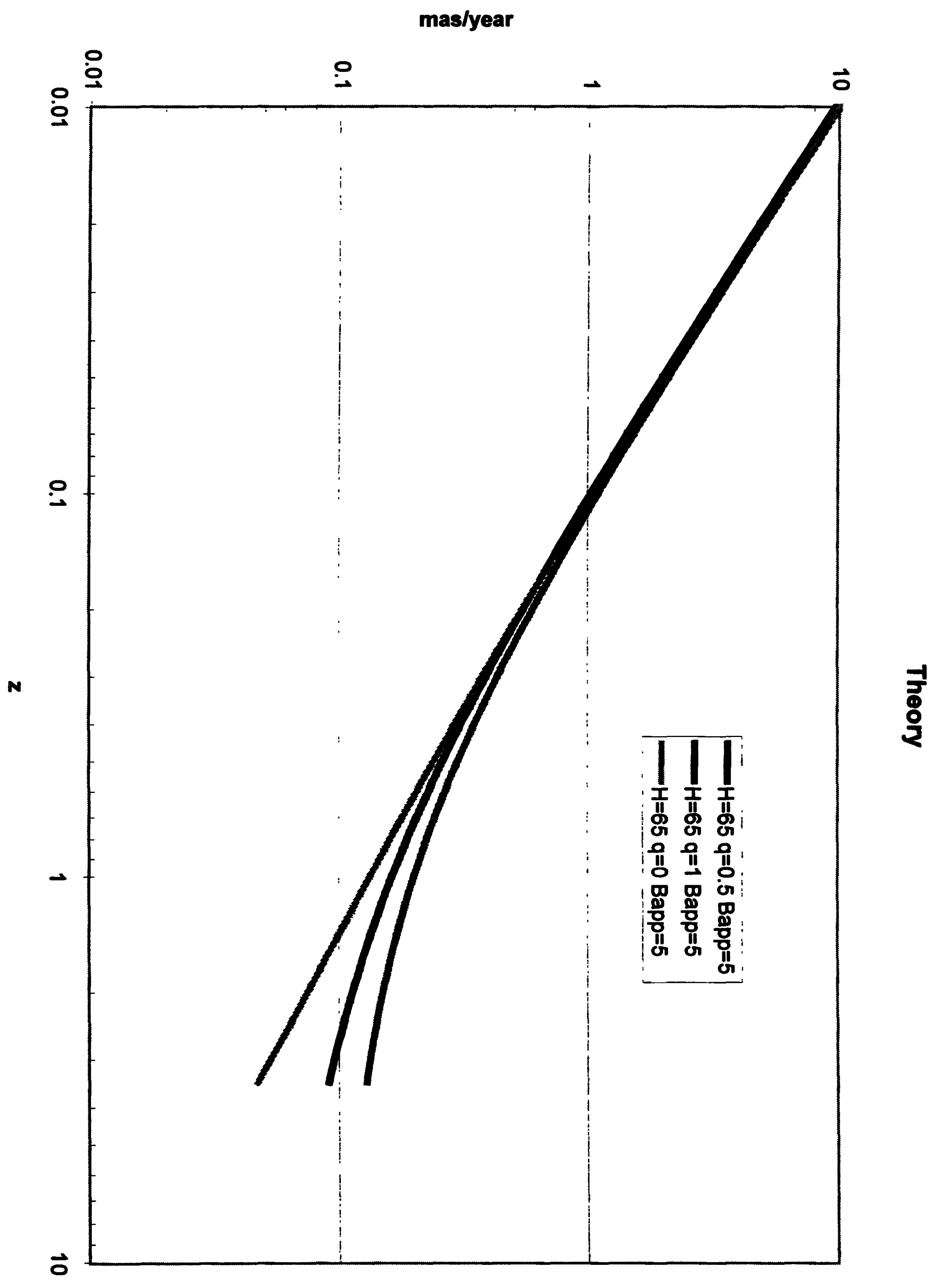
Theory
mas/year
z
H=65 q=0.5 Bapp=5
H=65 q=1 Bapp=5
H=65 q=0 Bapp=5
0.01
0.1
1
10
0.01
0.1
1
10

Figure 3

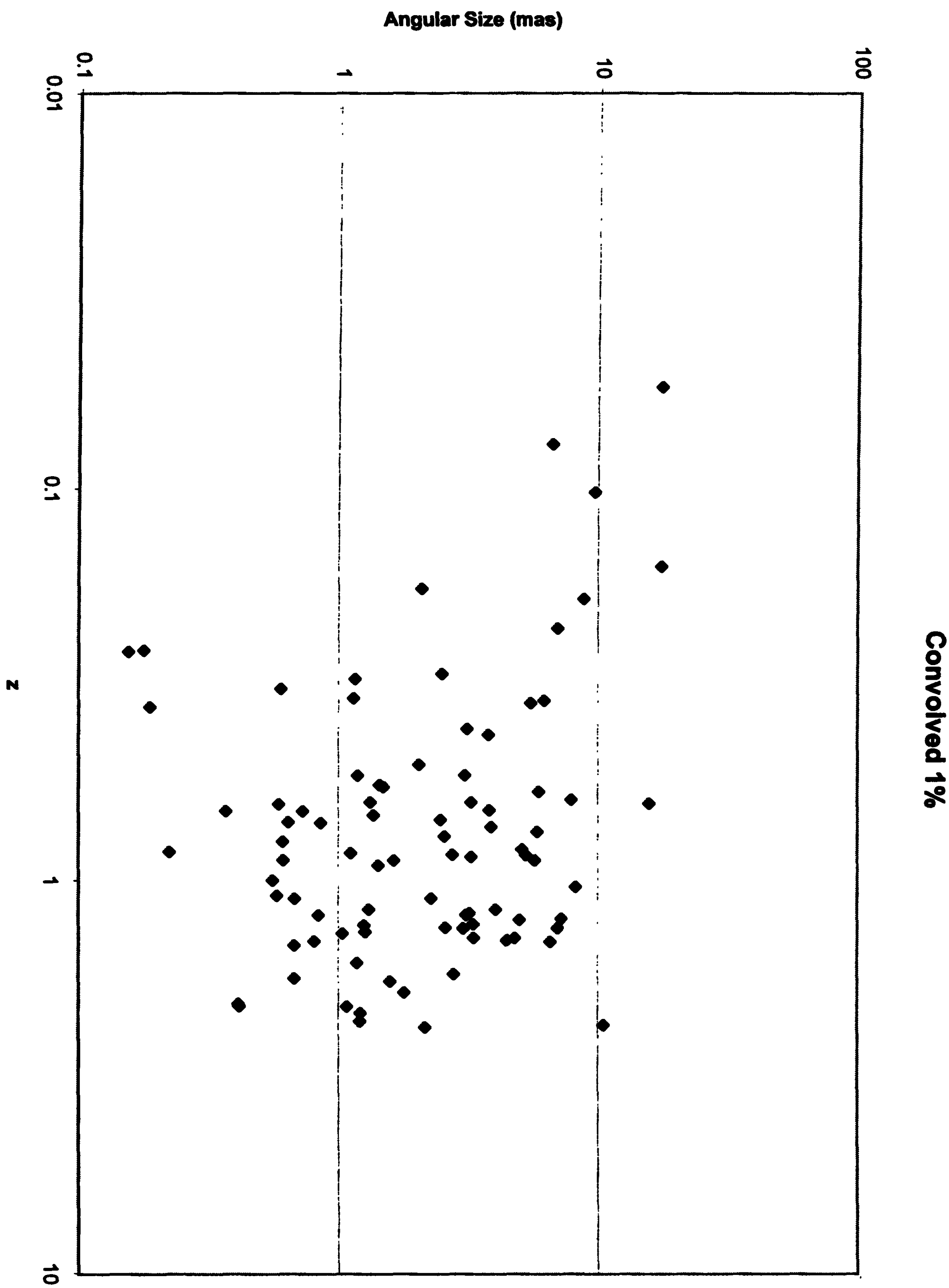


Figure 4

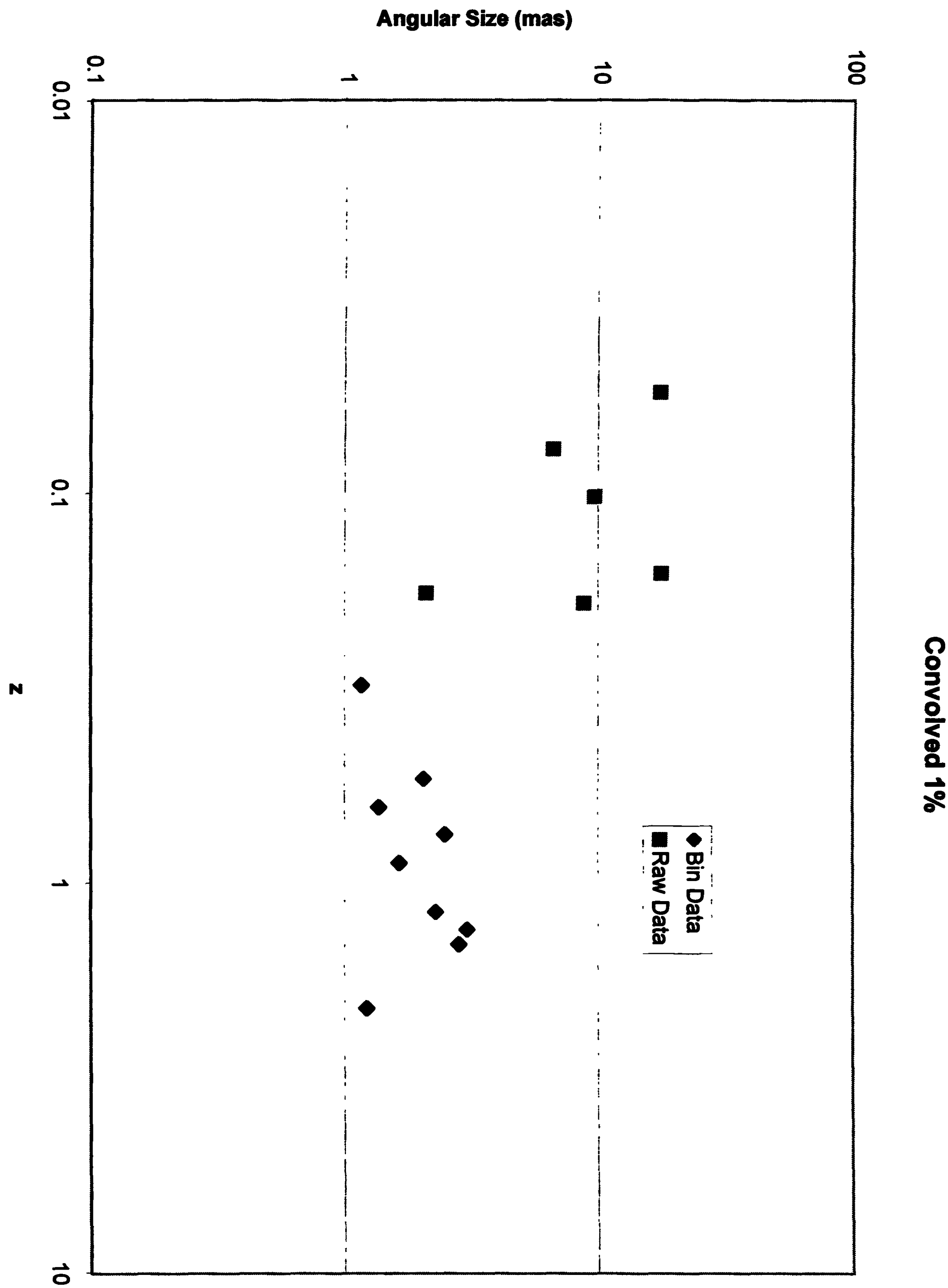
Convolved 1%
Angular Size (mas)
z
100
10
1
0.1
0.01
0.1
1
10
Bin Data
Raw Data

Figure 5

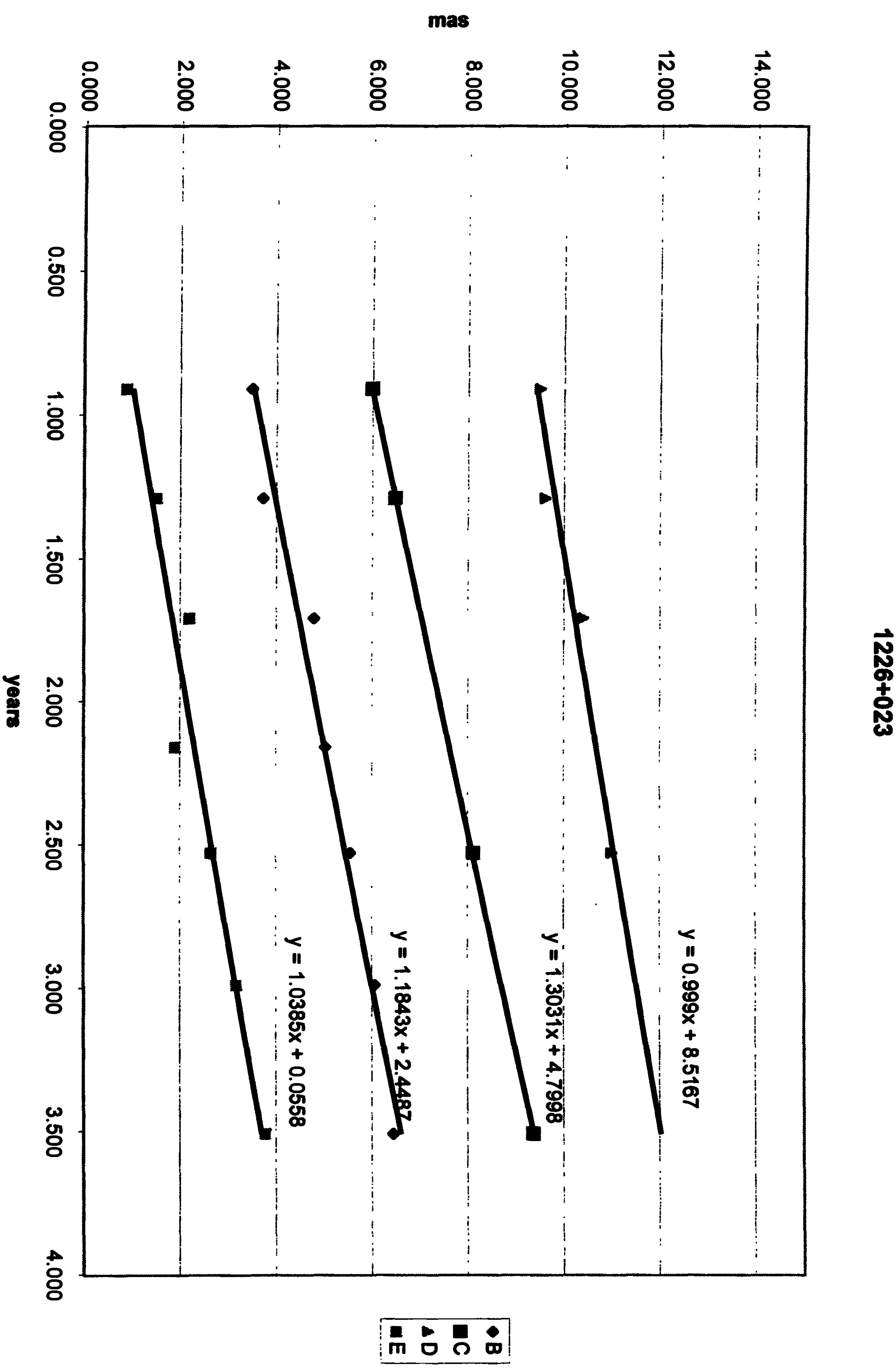

1226+023
mas
0.000
2.000
4.000
6.000
8.000
10.000
12.000
14.000
0.000
0.500
1.000
1.500
2.000
2.500
3.000
3.500
4.000
years
y = 0.999x + 8.5167
y = 1.3031x + 4.7998
y = 1.1843x + 2.4487
y = 1.0385x + 0.0558
B
C
D
E


Figure 6

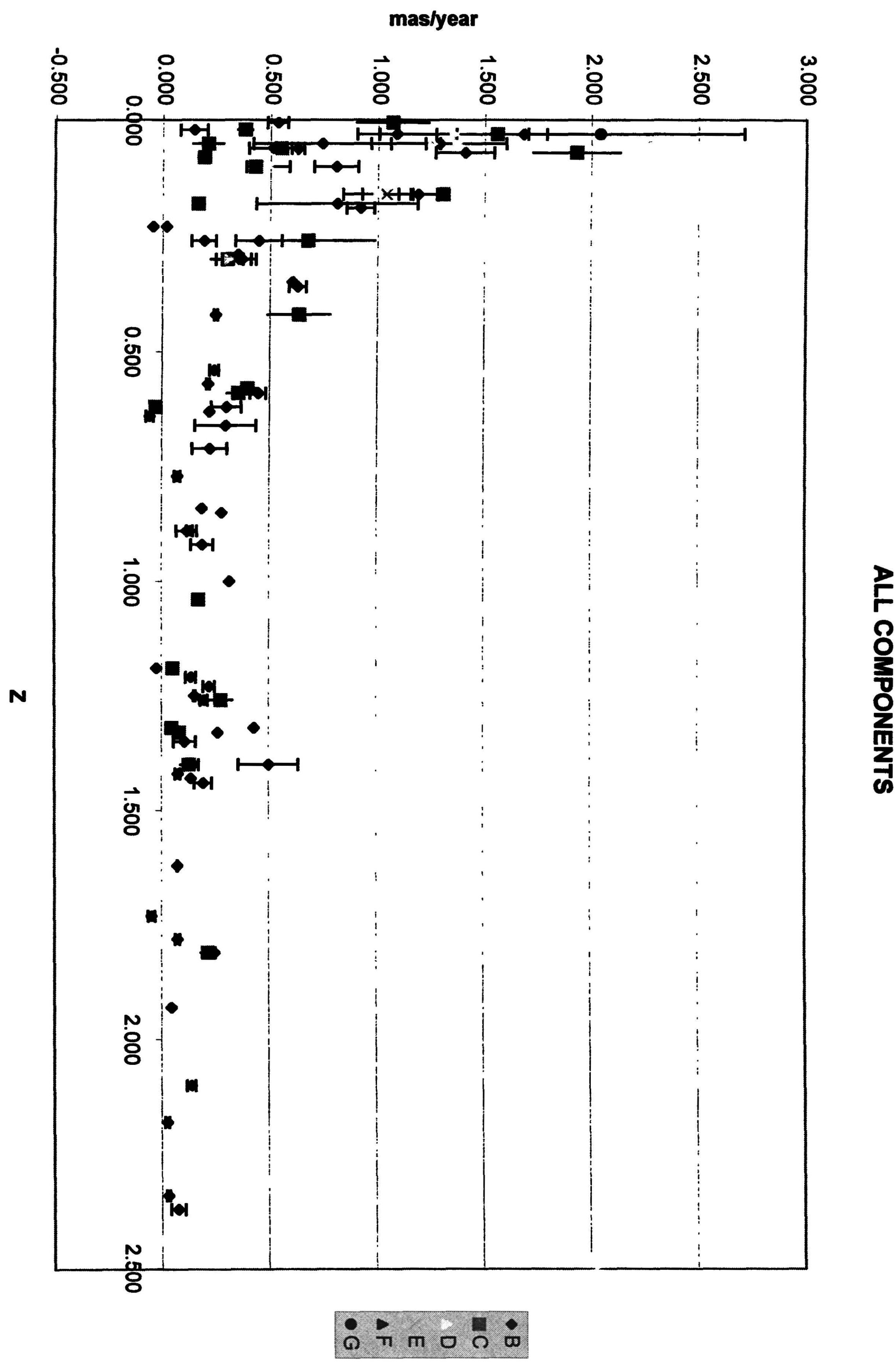
ALL COMPONENTS
mas/year
3.000
2.500
2.000
1.500
1.000
0.500
0.000
-0.500
0.000
0.500
1.000
1.500
2.000
2.500
Z
B
C
D
E
F
G

Figure 7

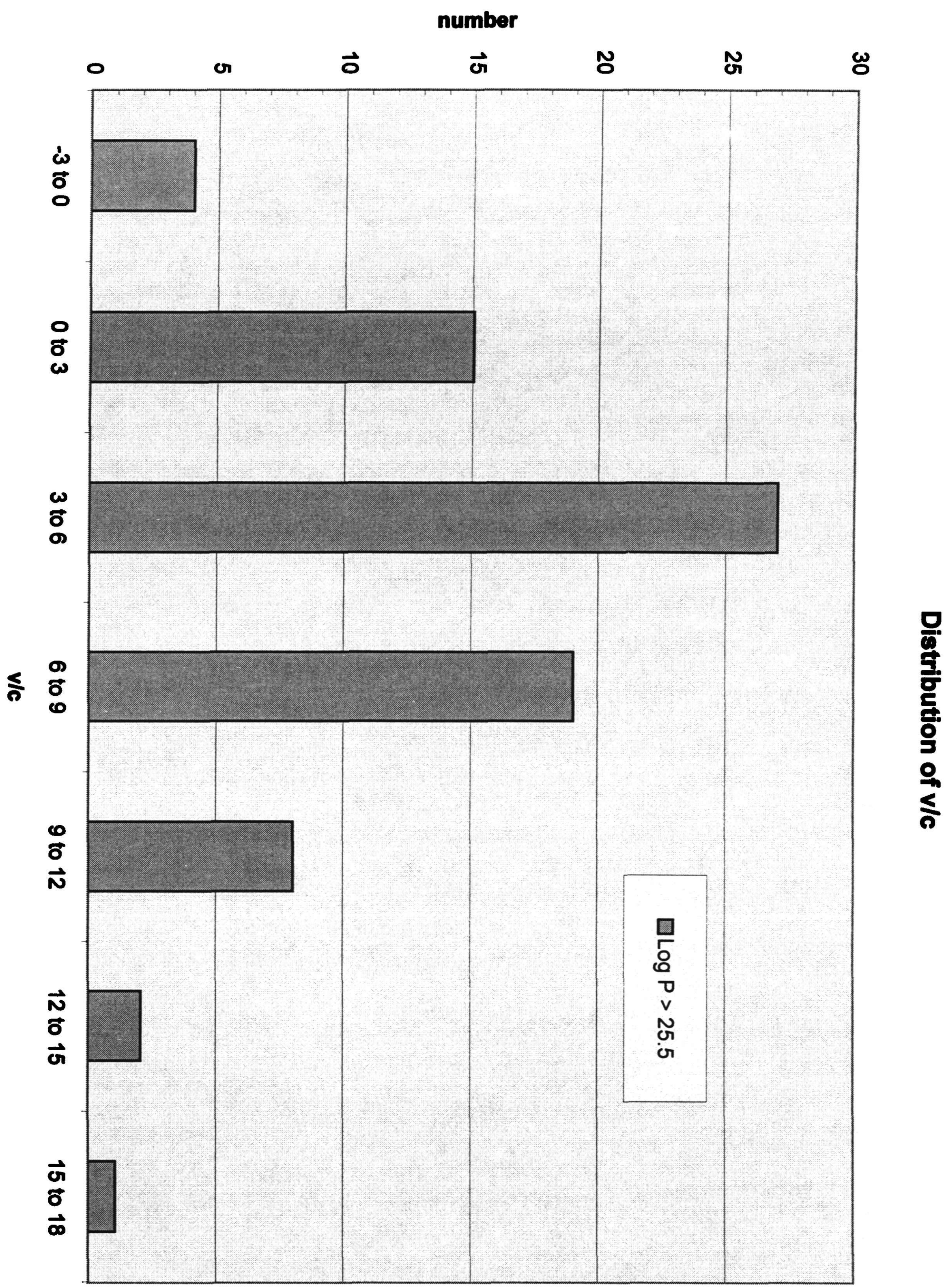
Distribution of v/c
number
0
5
10
15
20
25
30
-3 to 0
0 to 3
3 to 6
6 to 9
9 to 12
12 to 15
15 to 18
v/c
Log P > 25.5

Figure 8

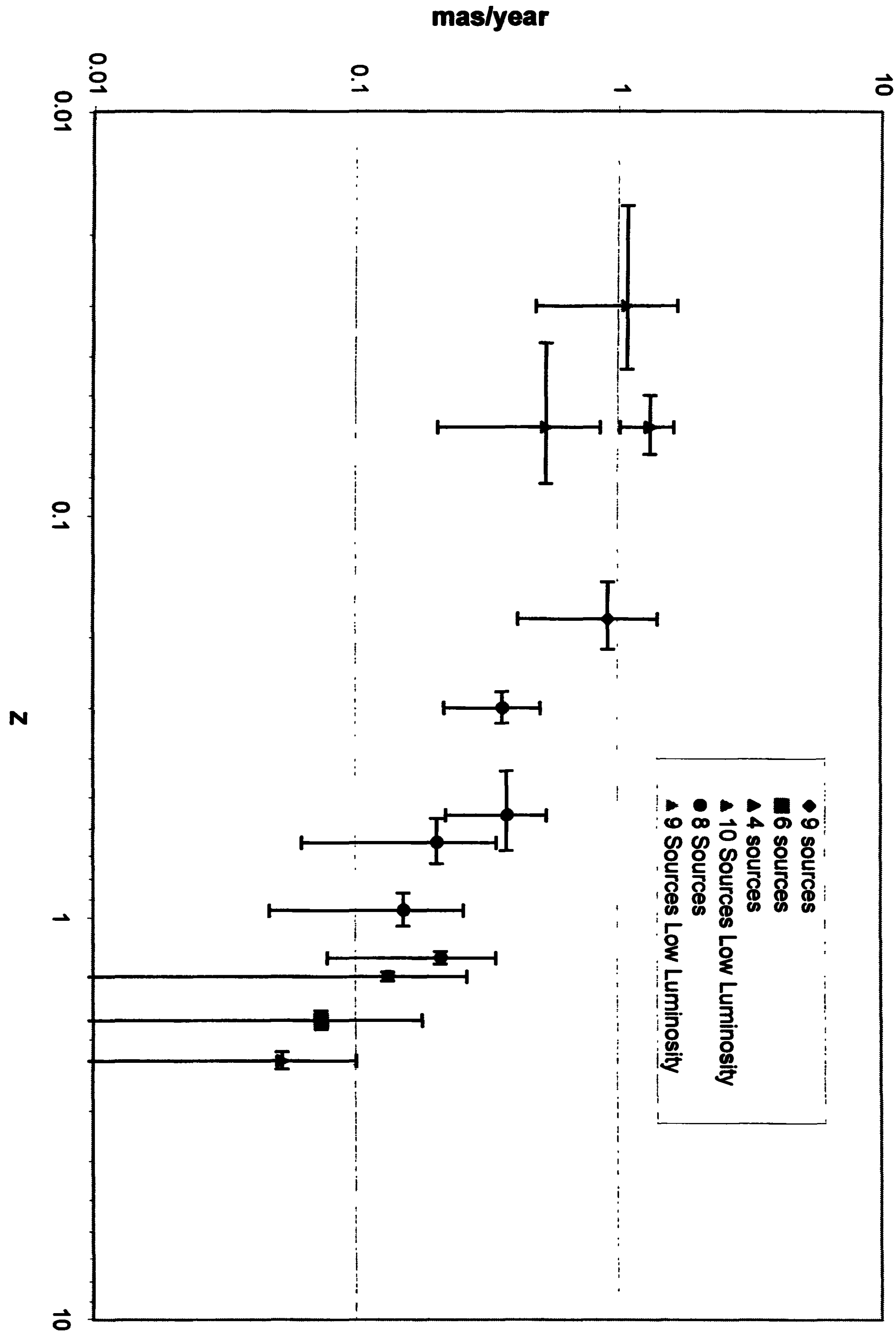
mas/year
Z
9 sources
6 sources
4 sources
10 Sources Low Luminosity
8 Sources
9 Sources Low Luminosity
0.01
0.1
1
10

Figure 9

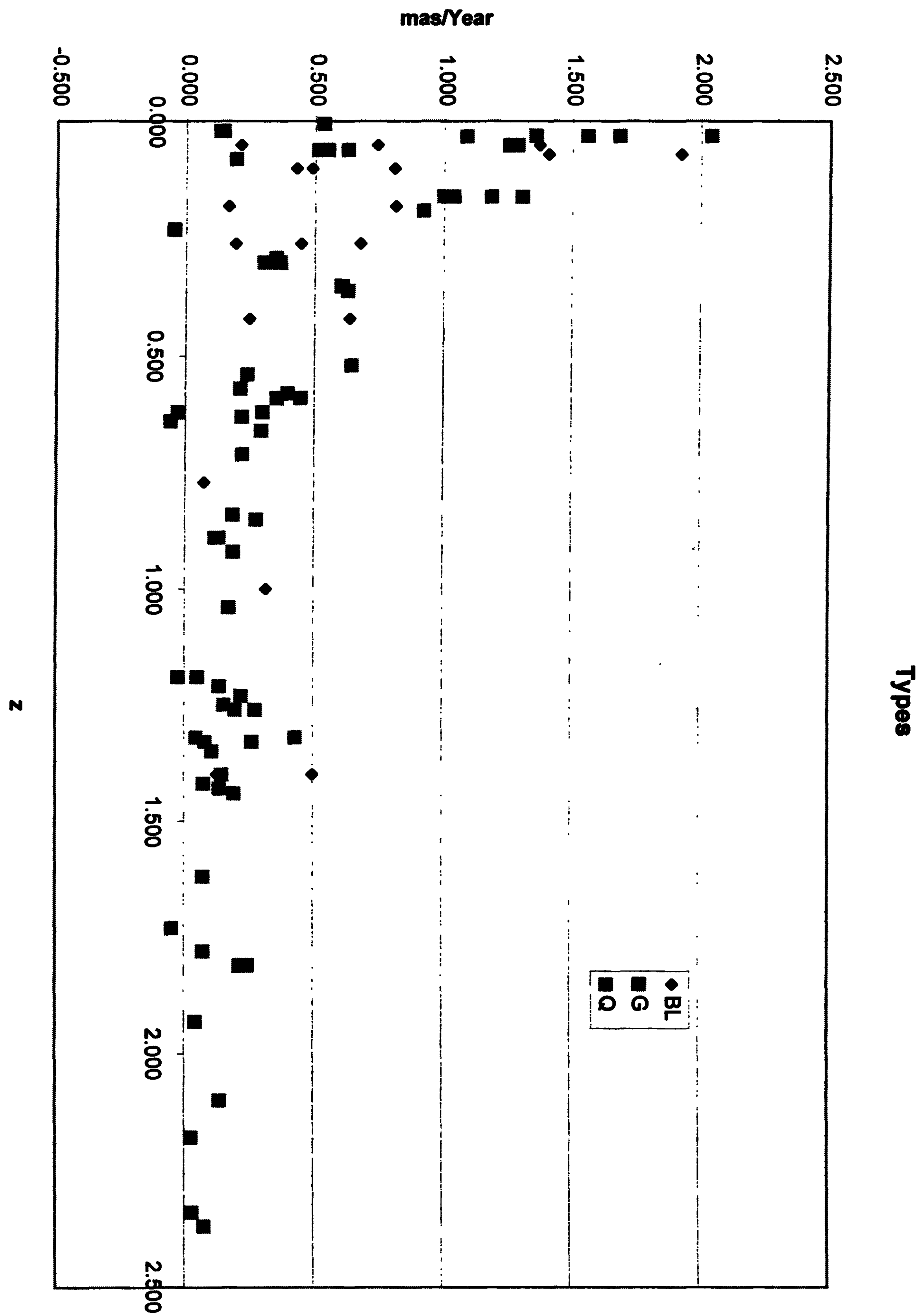
Types
mas/Year
2.500
2.000
1.500
1.000
0.500
0.000
-0.500
z
0.000
0.500
1.000
1.500
2.000
2.500
BL
G
Q

Figure 10

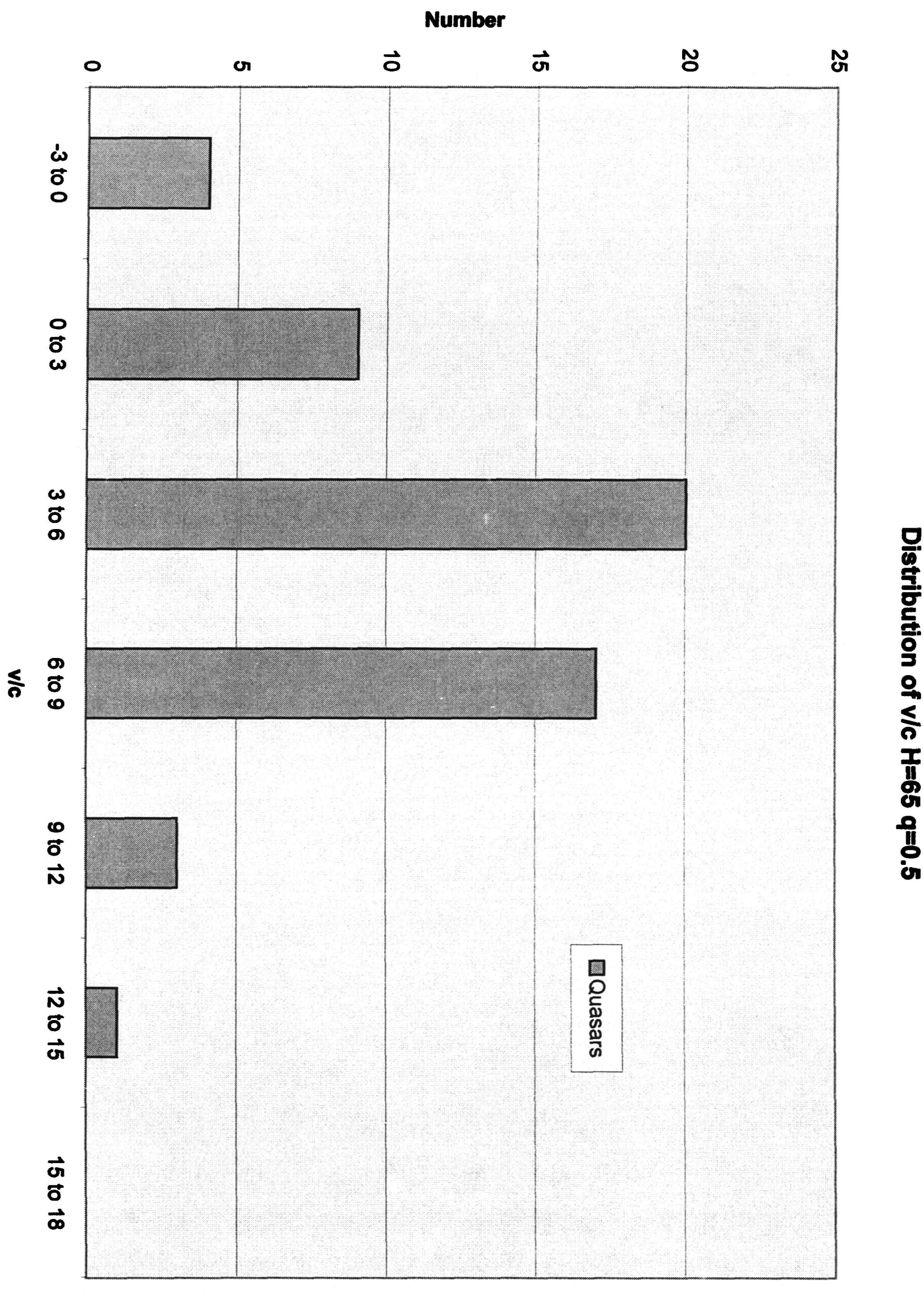
Distribution of v/c H=65 q=0.5
Number
0
5
10
15
20
25
-3 to 0
0 to 3
3 to 6
6 to 9
9 to 12
12 to 15
15 to 18
v/c
Quasars

Figure 11

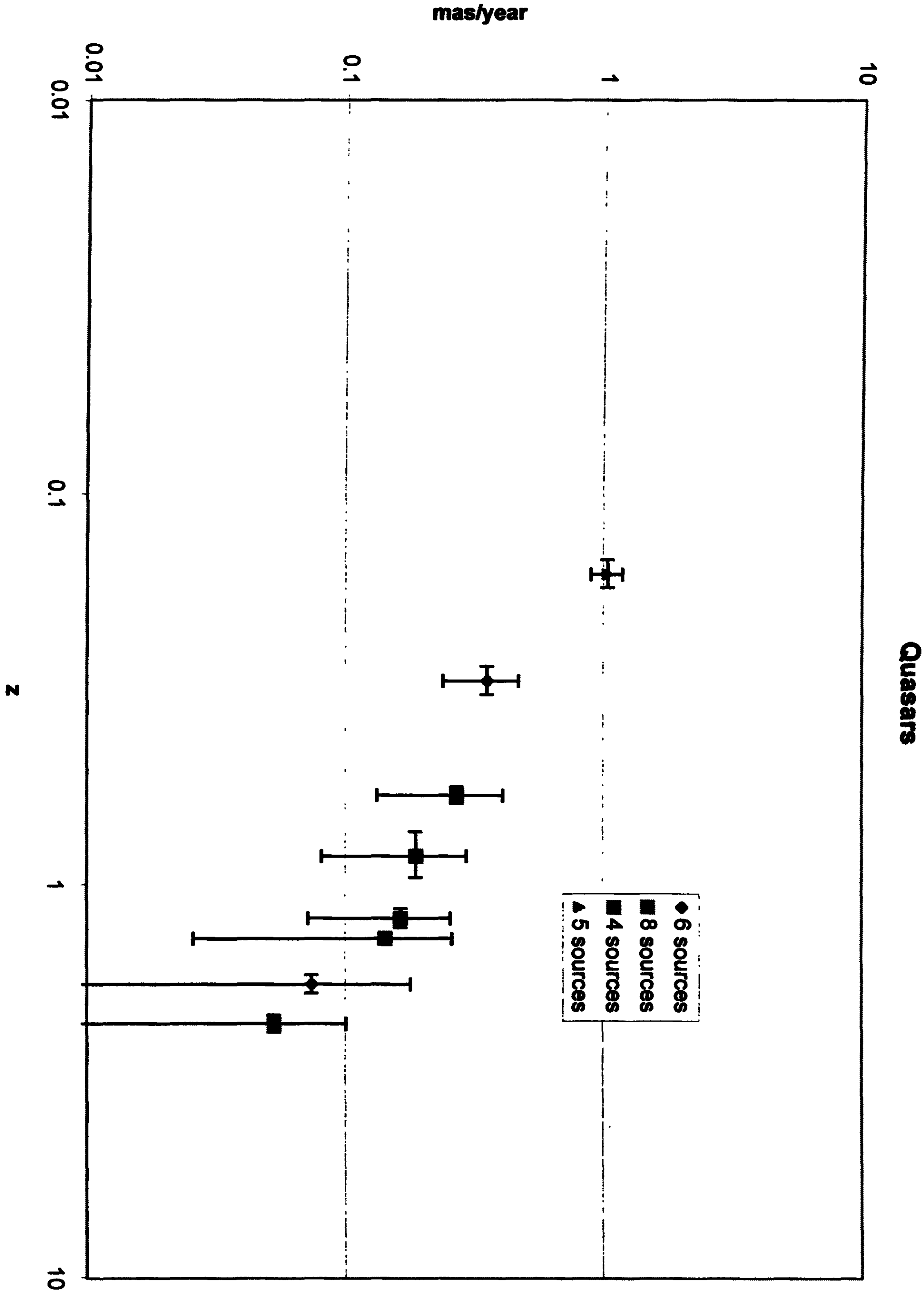
Quasars
mas/year
10
1
0.1
0.01
z
0.01
0.1
1
10
6 sources
8 sources
4 sources
5 sources

Figure 12

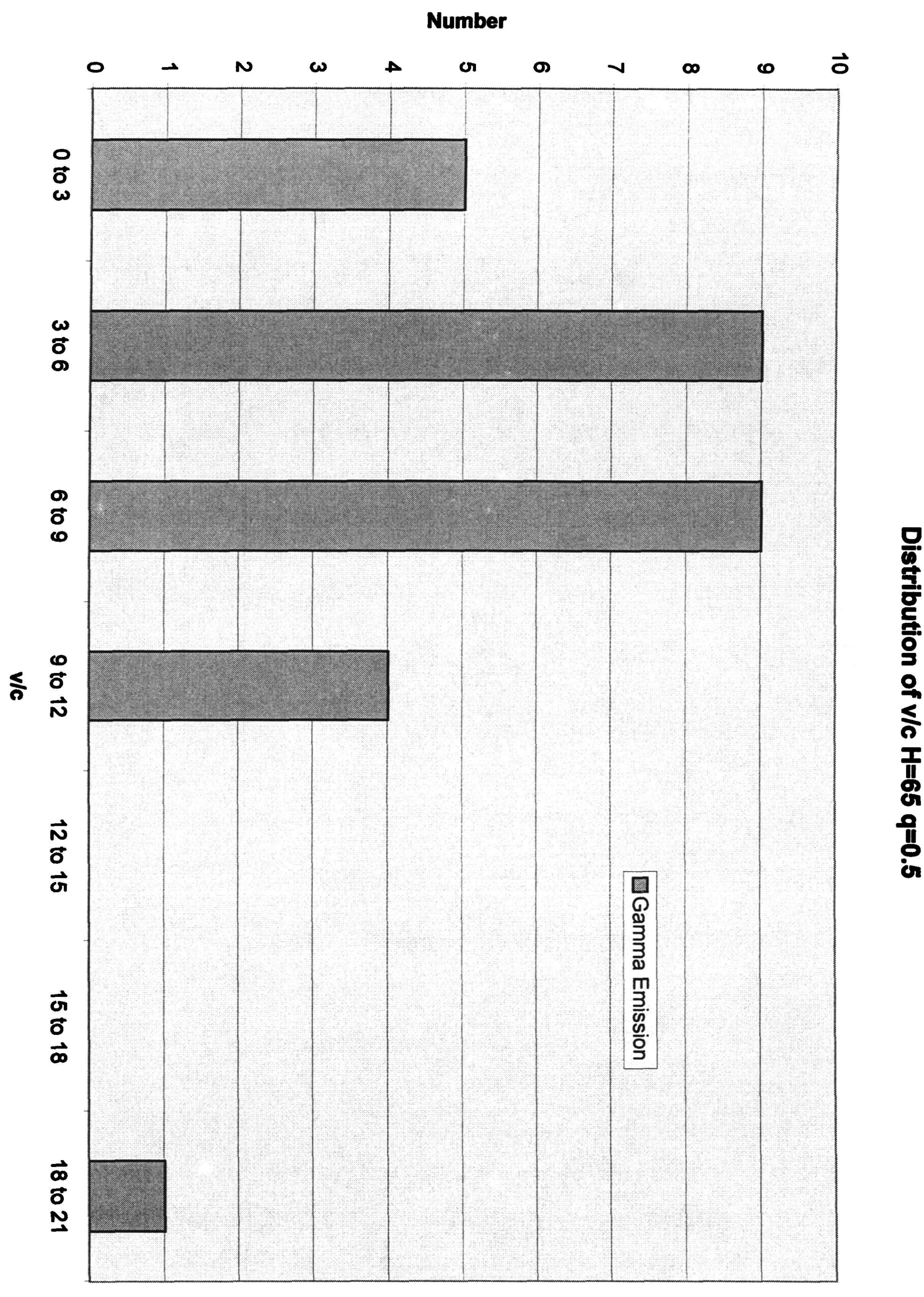
Distribution of v/c H=65 q=0.5
Number
0
1
2
3
4
5
6
7
8
9
10
0 to 3
3 to 6
6 to 9
9 to 12
12 to 15
15 to 18
18 to 21
v/c
Gamma Emission

Figure 13

# Papers to be Published

C. G. DePree, Melissa C. Nysewander and W. M. Goss, "NGC3576 and NGC3603: Two Luminous Southern HII Regions Observed at High Resolution with the Australia Telescope Compact Array." 1999 Astrophysical Journal, in press.

# NGC 3576 and NGC 3603: Two Luminous Southern HII Regions Observed at High Resolution with the Australia Telescope Compact Array

C. G. De Pree[1], Melissa C. Nysewander[1,2], W. M. Goss[2]

[1]Department of Physics & Astronomy, Agnes Scott College, 141 E. College Ave, Decatur, GA 30030

[2]National Radio Astronomy Observatory, P.O.Box 0, Socorro, NM 87801

## ABSTRACT

NGC 3576 (G291.28-0.71; $l$ = 291.3°, $b$ = -0.7°) and NGC 3603 (G291.58-0.43; $l$ = 291.6°, $b$ = -0.5°) are optically visible, luminous HII regions located at distances of 3.0 kpc and 6.1 kpc, respectively. We present 3.4 cm Australian Telescope Compact Array (ATCA) observations of these two sources in the continuum and the H90$\alpha$, He90$\alpha$, C90$\alpha$ and H113$\beta$ recombination lines with an angular resolution of 7$''$ and a velocity resolution of 2.6 km s$^{-1}$. All four recombination lines are detected in the integrated profiles of the two sources. Broad radio recombination lines are detected in both NGC 3576 ($\Delta V_{FWHM} \geq$ 50 km s$^{-1}$) and NGC 3603 ($\Delta V_{FWHM} \geq$ 70 km s$^{-1}$). In NGC 3576 a prominent N-S velocity gradient (~30 km s$^{-1}$ pc$^{-1}$) is observed, and a clear temperature gradient (6000 K to 8000 K) is found from east to west, consistent with a known IR color gradient in the source. In NGC 3603, the H90$\alpha$, He90$\alpha$ and the H113$\beta$ lines are detected from 13 individual sources. The $Y^+$ (He/H) ratios in the two sources range from 0.08±0.04 to 0.26±0.10. The H113$\beta$/H90$\alpha$ ratio in NGC 3576 is close to the theoretical value, suggesting that local thermodynamic equilibrium (LTE) exists. This ratio is enhanced for most regions in NGC 3603; enhanced $\beta/\alpha$ ratios in other sources have been attributed to high optical depth or stimulated emission. We compare the morphology and kinematics of the ionized gas at 3.4 cm with the distribution of stars, 10$\mu$m emission and $H_2O$, OH, and $CH_3OH$ maser emission. These comparisons suggest that both NGC 3576 and NGC 3603 have undergone sequential star formation.

*Subject headings:* HII regions: individual (NGC 3576, NGC 3603) – HII regions: kinematics and dynamics – ISM: abundances

## 1. Introduction

NGC 3576 (D = 3.0 ± 0.3 kpc) and NGC 3603 (D = 6.1 ± 0.6 kpc) are two of the highest luminosity optically visible HII regions in our Galaxy (Goss & Radhakrishnan, 1969). Indeed

NGC 3603 (with a bolometric luminosity of $10^7$ $L_\odot$) contains some $10^4$ $M_\odot$ of ionized gas, and aside from W49A, may be the most massive HII region in the Galaxy (Eisenhauer et al. 1998). Sources such as these are ideal laboratories to study the formation and evolution of massive stars and the initial mass function (IMF) of giant star forming regions. Similar regions that are visible with the Very Large Array (VLA) have been studied in detail. In particular, radio recombination line (RRL) studies of the Sgr B2 and W49A star forming regions with the VLA (Gaume et al. 1995; De Pree et al. 1995: Mehringer et al. 1995) have revealed small-scale outflows, very broad recombination lines ($\Delta V_{FWHM}$ ~80 km $s^{-1}$), expanding shells of ionized gas, and extremely compact structures. NGC 3576 and NGC 3603 appear to be similar regions in terms of luminosity, total mass and gas kinematics. Existing optical studies of NGC 3603, for example, have revealed broad emission lines and a stellar wind bubble, indicative of the early stages of a star forming region coming into equilibrium with its environment (Clayton 1986).

Though close in projection (~40′), the two regions are separated by about 30 km $s^{-1}$ in radial velocity as indicated by HI absorption (Goss & Radhakrishnan 1969) and hydrogen recombination line measurements (Wilson et al. 1970). Both regions are partially obscured by foreground dust, and studies of the kinematics of the associated ionized gas have been limited to optical wavelengths (Clayton 1986; Clayton 1990; Balick et al. 1980). Thus, existing velocity fields of the ionized gas are incomplete. The low resolution (4′) 6 cm image of Goss & Shaver (1970) shows that the radio emission associated with the two regions extends well beyond the detected H$\alpha$ emission. In both sources, however, it appears that the large scale ionized structures may be driven by energetic processes occuring near their cores. Evidence from a variety of wavelengths (including the radio line and continuum data from this study) indicate that both regions may have undergone sequential star formation, in NGC 3576 from east to west, and in NGC 3603 from north to south.

NGC 3603 and NGC 3576 have not been previously imaged with the Australia Telescope Compact Array (ATCA). Radio observations have been limited to low resolution line and continuum observations such as the ~1′ observations of Retallack & Goss (1980) at 21 cm. Thus, our radio frequency observations ($\theta_{FWHM}$ ~7″) improve by factors of ~10 the best spatial resolution radio observations of the ionized gas associated with NGC 3576 and NGC 3603. For both NGC 3576 and NGC 3603, we present high resolution radio continuum images and radio recombination lines. New kinematic distances which are in reasonable agreement with the previously derived spectroscopic distances are derived from the observed line velocities and a revised Galactic radius of $R_0$=8.5 kpc. We examine the ionized gas morphology and kinematics in the two sources, and possible star formation histories of these two regions. In addition, we derive electron temperatures, H113$\beta$/H90$\alpha$ ratios, helium abundances, and (where possible) carbon line strengths.

## 2. Observations and Data Reduction

Radio continuum and recombination line observations were made for NGC 3576 and NGC 3603 at the Australian Telescope Compact Array (ATCA) in the (750 m) B and (750 m) D configuration in two observing runs on the 13th and 19th of June in 1995 with a total of 24 hours of observing time. The observing frequency was 8.873 GHz, close to the the frequency of the H90$\alpha$ recombination line. The wide bandwidth (16 MHz) allowed the simultaneous observation of three additional recombination lines: He90$\alpha$, C90$\alpha$, and H113$\beta$. Detailed observing parameters are presented in Table 1. The initial calibrations were made using the AIPS (Astronomical Image Processing System) software distributed by NRAO. Each data set was flagged and the flagged continuum data were then calibrated using the observed phase and flux density calibrators. These flags and calibrations were copied to the line data, where a bandpass calibration was applied and the continuum was subtracted from the $u$-$v$ plane using the AIPS task UVLIN. Continuum images (with angular resolution of ~7″) were made from the line free channels for each source using the AIPS task IMAGR. This spatial resolution corresponds to a linear size of approximately 0.09 pc for NGC 3576 ($D$= 3.0 kpc) and approximately 0.21 pc for the more distant NGC 3603 ($D$= 6.1 kpc). The noise in the continuum images is dominated by the dynamic range limitations; thus the rms noise is significantly reduced in the continuum-subtracted line data.

After the initial data reduction in AIPS, the line and continuum data were analysed using GIPSY (the Groningen Image Processing System). Integrated line profiles were made for each pixel above a continuum cutoff level for both NGC 3576 ($5\sigma$ = 90 mJy beam$^{-1}$) and NGC 3603 ($5\sigma$ = 55 mJy beam$^{-1}$) using the GIPSY task PROFIL. Gaussian functions were then fitted to the spectral line data. The output from these fits are the line to continuum ratio ($T_L/T_C$), the integrated line strength, the central velocity ($V_{LSR}$) and the velocity full width at half maximum ($\Delta V_{FWHM}$) of the line emission in each region. The HII region NGC 3576 consists of a single extended source (containing several local bright spots) with an angular size of ~75″ (~0.7 pc). In NGC 3603, thirteen individual sources were observed above a $5\sigma$ level in the continuum image.

## 3. Results

### 3.1. 3.4 cm Continuum Emission

Continuum images at 3.4 cm were made for both NGC 3576 and NGC 3603 using the AIPS task IMAGR. Figure 1 is the resulting 3.4 cm continuum image for NGC 3576. The crosses in the plot indicate the positions of the 10 $\mu$m sources tabulated by Frogel & Persson (1974). Table 2 lists the continuum parameters for NGC 3576. These parameters include peak flux density ($S_{peak}$), integrated flux density ($S_{tot}$), angular diameter in arcseconds ($\theta$), and linear radius in pc ($r$). Using the Parkes 64-m telescope, McGee & Newton (1981) report a 14.7 GHz flux density of 97.8 Jy in NGC 3576. We detect about 73% of the single dish flux density, or 71±7 Jy. From the

13 sources in NGC 3603, we detect a total flux density of 25 Jy, or 38% of the reported single dish flux density of 65.9 Jy.

Figure 2 shows the 3.4 cm continuum image of NGC 3603. The crosses indicate the positions of the known 10 $\mu$m sources in NGC 3603 (Frogel et al. 1977). Each emission peak higher than the continuum $5\sigma$ cutoff (55 mJy beam$^{-1}$) has been designated as a separate region. The regions are labeled A to M, corresponding to increasing right ascension. The AIPS task JMFIT fitted two dimensional Gaussians to the individual continuum sources in NGC 3603. Table 2 presents continuum parameters for each region (A-M) in NGC 3603. These parameters include peak flux density ($S_{peak}$), integrated flux density ($S_{tot}$), deconvolved geometrical mean diameter in arcseconds ($\theta$), and the linear radius in pc ($r$). Table 3 presents derived physical parameters for the regions in NGC 3603. These calculated parameters include electron density ($n_e$), emission measure ($EM$), mass of ionized gas ($M_{HII}$), excitation parameter ($U$), Lyman continuum photon flux ($N_{LyC}$) and continuum optical depth ($\tau_c$). The continuum parameters were calculated assuming a uniform density, spherical, ionization bounded HII region, using the corrected formulae of Mezger & Henderson (1969). The calculated values are of course dependent on these assumptions. and in a complex region like NGC 3603, these assumptions may be overly simplistic. Figures 1 and 2 are plotted in B1950 coordinates. The last two figures in the paper (Figures 8 and 9) are plotted in J2000 coordinates to help in comparisons between the radio continuum emission and images at other frequencies, since images in the literature are shown in both epochs.

## 3.2. Radio Recombination Lines

### *3.2.1. NGC 3576*

A continuum-weighted, integrated line profile was generated for NGC 3576 using the GIPSY task PROFIL. The integrated profile was generated for all pixels above a continuum $5\sigma$ cutoff level. In addition, integrated profiles were generated for each pixel above the continuum $5\sigma$ level in a $7''\times7''$ box centered on each of the positions of the Irs sources tabulated by Frogel & Persson (1974). The integrated source profile, and the four profiles line profiles were then fitted with Gaussian functions using the GIPSY task PROFIT. Figure 3a presents the integrated line profile and model fit for NGC 3576. Each of the four lines (H90$\alpha$, He90$\alpha$, C90$\alpha$ and H113$\beta$) is clearly detected, and labeled in Figure 3a. The integrated spectra for the Irs sources (Irs1/2, Irs3. Irs4 and Irs5; Frogel & Persson 1974) in NGC 3576 are shown in Figures 4a-d. The spectra in Fig. 3a and Figs. 4a-d show the data (points), Gaussian fits (solid line), and the residuals (dotted line) for each recombination line. The parameters of Gaussian fits to the lines (V$_{LSR}$, $\Delta V_{FWHM}$, and T$_l$/T$_c$) are presented in Table 4.

¿From the integrated emission from NGC 3576, we determine a helium abundance of $Y^+$=0.09±0.01, and a H113$\beta$/H90$\alpha$ ratio close to the theoretically predicted value of 0.276 ($\beta/\alpha$=0.25±0.01). The electron temperature in NGC 3576 ($T_e^*$) is calculated assuming local thermodynamic equilibrium (LTE) from both the H90$\alpha$ and H113$\beta$ recombination lines (using equation [22] from Roelfsema & Goss [1992]):

$$T_e^* = (6943\nu^{1.1}\frac{T_c}{T_l \Delta V_{FWHM}}\frac{1}{1+Y^+})^{0.87}K, \tag{1}$$

with line width ($\Delta V_{FWHM}$) given in km s$^{-1}$and $\nu$ in GHz. These LTE temperatures are given in Table 4. An electron temperature ($T_e$) may also be calculated with corrections made for non-LTE effects (using Eq. [23] from Roelfsema & Goss [1992]):

$$T_e = T_e^*[b_n(1 - \frac{\beta_n \tau_c}{2})]^{0.87}K, \tag{2}$$

where $b_n$ and $\beta_n$ values are from the tables of Salem & Brocklehurst (1979).

For NGC 3576, a turbulent velocity ($v_{turb}$) and an electron temperature ($T_e$) are calculated by solving two equations for line width (Eq. 3) using the hydrogen and helium (H90$\alpha$ and He90$\alpha$) recombination line widths. The line width can be expressed as

$$< v_{turb}^2 >= \frac{3\Delta\ V_H^2}{8ln2} - \frac{3kT_e}{M} \tag{3}$$

where the $v_{turb}$ is the turbulent velocity in km s$^{-1}$, $k$ is the Boltzmann constant, $M$ is the mass of the atom, $T_e$ is the electron temperature, and $\Delta V_H$ is the line FWHM in km s$^{-1}$. Using this method for NGC 3576, we derive a turbulent velocity $v_{turb}$=17±1.0 km s$^{-1}$ and an electron temperature of (T$_e$) of 6100±200 K.

In order to examine the spatial variation in the H90$\alpha$ line parameters, single Gaussian fits were made to each pixel above the continuum 5$\sigma$ level in NGC 3576. The results of these point-to-point fits to the H90$\alpha$ line are presented in Figures 5a and 5b. Figure 5a shows the spatial variation in the the central line velocity ($V_{LSR}$), with continuum contours overlaid on the greyscale representation of the ionized gas velocity. Figure 5b shows the spatial variation in the linewidth ($\Delta V_{FWHM}$) of the H90$\alpha$ line. For NGC 3576, a map of the LTE electron temperature was also generated, using Equation 1 (above) for each point above 10$\sigma$ in the continuum image. The resulting LTE temperature image is shown in Figure 5c, indicating a clear E-W temperature gradient. This temperature gradient has also been plotted using the AIPS task IRING, which averages emission in concentric semicircles. The semicircles (with a thickness of ~7″), are centered on the continuum peak of NGC 3576 and extend to the east. A plot of temperature as a function of distance from the peak (in arcsec) is presented as Figure 6. The apparent temperature gradient is discussed in §4.2.1.

### *3.2.2. NGC 3603*

An integrated line profile was generated for the NGC 3603 region above a 5$\sigma$ cutoff in the continuum emission. Figure 3b presents the integrated line profile and model fit for NGC 3603.

Because of the large variation in line velocities across the source, the carbon line (apparent in some of the individual source profiles in NGC 3603) was fitted with the line width fixed at 10 km $s^{-1}$. Gaussian fits were made to the integrated profile, and the parameters of these fits are given in Table 5. Figures 7a-7m present the radio recombination line profiles and Gaussian fits for each of the thirteen subregions (A-M) in NGC 3603. For all 13 subregions, the signal-to-noise ratio is sufficiently high to fit the H90$\alpha$, He90$\alpha$, and H113$\beta$ lines. The C90$\alpha$ recombination line was successfully fit only in regions NGC 3603 B and H with a fixed carbon line width. Sources in which parameters were fixed and the fixed values are indicated parenthetically in Table 5. In a few cases, the fitted linewidth ($\Delta V_{FWHM}$) of the He90$\alpha$ line may be broad due to blending with the C90$\alpha$ line in the sources where a C90$\alpha$ line was not separately fitted. The line parameters from the Gaussian fits to the integrated emission from NGC 3603 and its 13 subregions are presented in Table 5. As with NGC 3576, the table also includes the LTE electron temperature ($T_e^*$), the corrected electron temperature ($T_e$), the ionized helium to hydrogen ratio ($Y^+$), and the H113$\beta$ to H90$\alpha$ ratio ($\beta/\alpha$), and the turbulent velocity ($v_{turb}$). For NGC 3603, the non-LTE electron temperature was calculated using Equation 2 (above). The turbulent velocity was calculated from the width of the H90$\alpha$ line and the non-LTE electron temperature using Eq. 3 (above). These temperatures and turbulent velocities are given in Table 5.

## 4. Discussion

### 4.1. Distances to NGC 3576 and NGC 3603

McGee & Newton (1981) detected recombination lines at 14.7 GHz from 25 high emission measure HII regions using the Parkes 64-m radio telescope. Both NGC 3576 (1109-610) and NGC 3603 (1112-610) were included in their survey. McGee & Newton detected the H76$\alpha$ line from NGC 3576 and NGC 3603 at -24.1±0.1 km $s^{-1}$ and 7.7±0.1 km $s^{-1}$ respectively. In addition to H76$\alpha$, McGee & Newton detected the He76$\alpha$ line toward both sources, and the carbon line toward NGC 3576. For NGC 3576, the detected line width in the H90$\alpha$ line ($\Delta V_{FWHM}$=28.7± 0.1) is in good agreement with the H76$\alpha$ line width published by McGee & Newton ($\Delta V_{FWHM}$=29.1±0.1). The integrated H90$\alpha$ line width for NGC 3603 ($\Delta V_{FWHM}$=36.9±0.25) is in reasonable agreement with the value for the H76$\alpha$ line given by McGee & Newton ($\Delta V_{FWHM}$=41.9±0.2).

The distance to NGC 3576 has been discussed at length in two papers, Goss & Radhakrishnan (1969), and Persi et al (1994). Goss & Radhakrishnan found a kinematic distance of 3.6 kpc, just beyond the tangential point of the Galaxy, using the Schmidt galactic model and a value of $R_0$ = 10 kpc. This distance is derived from a line center velocity of -23 km $s^{-1}$, and circular motion within the galaxy. This kinematic distance agrees well with the findings from Caswell & Haynes (1987). Our new observations, using a revised $R_0$ = 8.5 kpc, and a line velocity of -20.0 ± 0.1 km $s^{-1}$ suggest a distance of 3.0±0.3 kpc for NGC 3576. Because no ionizing cluster is optically visible, no reliable spectroscopic distance has been determined. Humphreys (1972), in a study of the effect of streaming in the Carina arm, determined a distance of 3.2 kpc for NGC 3576, and detected both velocity variations (~4 km $s^{-1}$ ) and a large spread in the individual velocities of early type stars in this direction. Persi et al. (1994) derive a distance based on the star HD 97499 (position plotted in Figure 8). However, the high resolution radio continuum image of the source (Fig. 8) shows that there may not be a direct association between HD 97499 and NGC 3576. HD 97499 (RA = 11 12 10.1, Dec = -61 18 45.1 J2000) is located ~2′ east of the peak in the 3.4 cm continuum emission. As a result, it is unlikely that HD 97499 contributes greatly to the ionization seen in NGC 3576. Finally, the stellar velocity of HD 97499 (-32 km $s^{-1}$ ± 11 km $s^{-1}$; Crampton, 1972) does not agree well with the observed velocities in the ionized gas (-23 km $s^{-1}$ [McGee & Gardner, 1968] and -25 km $s^{-1}$ [Caswell & Haynes, 1987]). Thus, distances associated with HD 97499 should not simply be applied to NGC 3576.

The determination of the distance to NGC 3603 is aided by the presence of an optically visible ionizing cluster. Distance estimates made from stellar observations can be compared to kinematic distances derived from the ionized gas. The earliest spectroscopic distance estimate was made by Sher (1965) at 3.5 kpc. Without a large number of faint stars visible, the spectroscopic distance estimate was admittedly crude. Shortly thereafter, Goss & Radhakrishnan (1969) found a distance of 8.4 kpc based on the observed line velocity of 10 km $s^{-1}$, using $R_0$ = 10 kpc. Caswell & Haynes (1987) also found a kinematic distance using $R_0$ = 10.5 kpc and $V$ = +11 km $s^{-1}$ of 8.6 kpc. McGee & Newton (1982) report an H76$\alpha$ line velocity of 7.7±0.1 km $s^{-1}$. Our velocity for the integrated line in NGC 3603 is $V_{LSR}$=9.1±0.1, consistent with previously reported values. The H90$\alpha$ velocities found for the thirteen individual regions range between −2 km $s^{-1}$ and 19 km $s^{-1}$. Using the velocity from the integrated line ($V_{LSR}$=9.1 km $s^{-1}$) and $R_0$ = 8.5 kpc, we determine a kinematic distance of 6.1±0.6 kpc.

*UBV* stellar photometry of NGC 3603 has resulted in distance estimates as low as 3.5 kpc (Sher, 1965) and as high as 8.1 kpc (Moffat, 1974). Melnick & Grosbøl (1982) derive a distance of 5.3 kpc. Moffat (1974), using the stars observed by Sher (1965) and a different reddening scale derive a distance of 8.1 ± 0.8 kpc. Finally, Melnick, Tapia & Terlevich (1989) use *UBV* photometry of the ionizing cluster of NGC 3603 to find a distance modulus of $(m - M)_0$=14.3, which corresponds to a distance of ~7.2 kpc. Their value is in good agreement with both Moffat (1974), and the kinematic distances of Goss & Radhakrishnan (1969), and Caswell & Haynes (1987), and in reasonable agreement with the distance derived from our integrated radio recombination line velocity. The smaller distances inferred from the measurements of Sher (1965) and Melnick & Grosbøl (1982) are likely the result of errors in photometry due to nebular contamination (Melnick, Tapia & Terlevich 1989).

### 4.2. NGC 3576

NGC 3576 has been extensively observed in the radio continuum (Goss & Shaver 1970) and in radio recombination lines (McGee & Gardner 1968, McGee & Newton 1981, Wilson et al. 1970).

Recombination line studies of the region show the line velocities to be centered at approximately $-23$ km s$^{-1}$. The core (diameter$\sim$1.5′) of NGC 3576 is the location of five identified infrared (10$\mu$m) sources (Frogel & Persson 1974), as well as $CH_3OH$ (Caswell et al. 1995) and $H_2O$ (Caswell et al. 1989) masers. The presence of bright 10$\mu$m emission, water masers and compact thermal radio emission are typical indications of the early stages of star formation and dense circumstellar environments.

Persi et al. (1994) have identified 135 individual stars with IR excess (to distinguish cluster stars from red field stars) in an extremely young galactic cluster associated with the HII region NGC 3576, using $JHK$ images and photometry. Approximately 40 of these IR sources are members of the cluster. In their $JHK$ images, Persi et al. (1994) detect a color gradient in the near-IR, indicating increasing extinction toward the western edge of NGC 3576. This gradient suggests that star formation may have progressed in NGC 3576 from east to west, with the youngest stars currently located at the western edge of the source.

In addition, Persi et al. (1994) provide a summary of existing studies of the region, and an overlay of the 21 cm continuum (Retallack & Goss 1980), the 10 $\mu$m continuum sources (Frogel & Persson 1974) and their K band mosaic of the region. The overlay (their Fig. 7) clearly shows that the radio continuum, near-IR continuum and 10$\mu$m continuum are all strongly peaked toward the western edge of the source. Our 3.4 cm radio continuum image (Fig. 1) improves significantly on the resolution of Retallack & Goss (1980), and shows that there is a coincidence between the location of the infrared sources (Irs1-Irs5) tabulated by Frogel & Persson (1974) and the extended ionized radio continuum emission. Figure 1 shows the 3.4 cm radio continuum with crosses and labels indicating the positions of the 10$\mu$m peaks (Frogel et al. 1977). All five sources are coincident with the ionized gas emission and are near local peaks in the radio continuum emission.

#### *4.2.1. Characteristics of the Ionized Gas*

Our radio recombination line observations have allowed us to examine in detail the variation in electron temperature and helium abundance in NGC 3576. Our results in both cases seem to strengthen the case for sequential star formation in that source. The LTE electron temperatures show a clear gradient from east to west, with temperature increasing with distance (east) from the continuum peak. The gradient is apparent in Figures 5c and 6. Figure 5c shows the spatial variation in electron temperature across the source. Figure 6 is a plot of temperature as a function of distance from the 3.4 cm continuum peak. The LTE electron temperature increases with distance from 6000 K to a maximum of $\sim$8,000 K, and then falls to lower levels in the more diffuse gas to the east. If the ionizing stars are those IR sources coincident with the radio continuum, this rising temperature signature is expected (Hjellming 1966). Lower energy photons on average would be absorbed first, with the higher energy photons penetrating deeper into the diffuse gas. Thus, the temperature gradient confirms a scenario in which the youngest, hottest stars in the HII region are located near the sharp western edge of the radio continuum.

Under LTE conditions, the theoretical value of the H113$\beta$ to H90$\alpha$ hydrogen ratio is 0.276 (Shaver & Wilson, 1979). Deviations from this theoretical ratio indicate local deviations from LTE, and the ratio can be used to correct the derived electron temperature. The H113$\beta$ to H90$\alpha$ ratio in NGC 3576 varies from ~0.25±0.05 to ~0.35±0.05, with the lowest values associated with the bright peak in the radio continuum along the western edge of the HII region. Pressure broadening can lower the $\beta/\alpha$ ratio from the theoretical value. When the $\beta/\alpha$ ratio is lower than the theoretical value, electron temperatures derived from the $\beta$ lines will of course be higher than those derived from $\alpha$ lines. In fact, for NGC 3576, the electron temperatures derived from the H113$\beta$ line are ~11 % higher than those derived from the H90$\alpha$ recombination line.

A small number of Galactic objects are known to have helium abundances in excess of 20%. Such elevated helium abundances have been reported in the W3 core (Adler, Wood & Goss 1996, Roelfsema, Goss & Mallik 1992), and are thought to be associated with the environments of evolved stellar objects that are rapidly losing mass. A small but significant positive gradient in helium abundance ($Y^+$) is detected from the western peak of the source ($Y^+ = 0.08 \pm 0.01$) to the more diffuse ionized gas to the east ($Y^+ = 0.14 \pm 0.03$). This range is consistent with the $Y^+$ value reported by McGee & Newton (1981) of $N(He^+)/N(H^+)=0.091$. The abundance gradient is consistent with the suggestion of Persi et al. (1994) who detect a color gradient in the near-IR indicating increasing extinction to the west of the source. Persi et al. (1994) propose that the youngest stars are located at the western edge of the ionized gas. The higher helium abundances found to the east of NGC 3576 may indicate the presence of a population of older stars and their associated mass loss.

### *4.2.2. Gas Kinematics in NGC 3576*

Figures 5a and 5b show that both broad lines and velocity gradients are present in the ionized gas associated with NGC 3576. Double-peaked emission lines are located over a ~15″ region at the northern edge of the source. In Fig. 5a, the double-peaked lines have been fitted with a single Gaussian with a $\Delta V_{FWHM}$ = 50 km s$^{-1}$. Closer inspection (see Figure 1 inset) shows that locally the lines are possibly double-peaked. The double-peaked recombination lines in this region have a velocity separation of ~25 km s$^{-1}$, and may be due to either the expansion of an ionized shell of gas, or the outflow of ionized gas from a local source. The broad line region is located to the east of the Irs1/Irs2 peak (Frogel & Persson 1974). The region of the broadest radio recombination lines corresponds spatially to a distinct gap in the 10 $\mu$m emission between Irs1/Irs2 and Irs5.

If the split lines are due to expansion, then the rate of expansion is ~13 km s$^{-1}$. Double-peaked lines with similar velocity separations have been seen in some of the compact HII regions in Sgr B2 North (De Pree et al. 1996). The spatial resolution of the current data is insufficient to determine whether an expanding shell of ionized gas is located at this position. Alternatively, the double-peaked lines may arise near the base of a large scale ionized outflow.

A large, approximately north-south velocity gradient of 30 km $s^{-1}$ $pc^{-1}$ is observed in the ionized gas, and is shown in Figure 5a. The velocity across the source varies from ~0 km $s^{-1}$ along the southern edge to ~-35 km $s^{-1}$ in the north. The gradient is not likely due to rotation in the ionized gas, since these rotational velocities would imply an approximate enclosed mass of $M=2\times10^5$ $M_\odot$. The gradient is more likely due to an ionized outflow, and may in fact be the base of a much larger scale outflow. A wide field of view optical image of the region (Fig. 8; Persi et al. 1994) shows several large loops and filaments of ionized gas extending several minutes of arc to the north of NGC 3576.

### *4.2.3. Sequential Star Formation in NGC 3576*

Figure 8 shows the positions of cluster members with infrared excess (crosses; Persi et al. 1994) overlaid on the 3.4 cm radio continuum. Approximately 40 infrared excess sources have been identified. Eight of the stellar positions are coincident with the radio continuum emission, with the majority of the sources located to the north, east and south of the radio continuum. Only a single infrared excess source is located to the west of the radio continuum peak. This spatial distribution would be expected if star formation were proceeding from east to west into the molecular cloud. Water ($H_2O$) and methanol ($CH_3OH$) maser emission (plotted) are located coincident with the peak in the radio continuum emission.

The location of molecular gas in NGC 3576 is also consistent with a triggered star formation scenario. The peak in the 1.0 mm dust continuum emission (Cheung et al. 1980) is located to the west of the bright radio continuum peak. The 1.0 mm emission traces the core of the molecular cloud located to the west of NGC 3576. Similar distributions of ionized and molecular gas are found near the Sgr B2 F HII regions (De Pree et al. 1996), G34.3 (Gaume et al. 1994), and others. In fact, the morphology of NGC 3576 is "cometary", and closely resembles a mirror image of the cometary source G34.3 (Gaume et al. 1994) in which a dense molecular cloud core is located at the eastern periphery of the ionized gas.

Taken as a whole, the radio, infrared, optical and molecular imaging of NGC 3576 suggest that the oldest ionizing sources are located to the east of the region, and the youngest ionizing sources to the west. The distribution of stars, ionized gas, molecular gas, and water masers in NGC 3576 is reminiscent of simple scenarios of sequential star formation. In this picture, the star formation process slowly "eats away" at a dense cloud, so that the most evolved stars are located far from the cloud core. The ionized gas is found at the periphery of the cloud, and the youngest sources (protostars) are still embedded in the nascent molecular material, but reveal their presence with water maser emission. In many such regions in the Galaxy, the stellar population is not observable. The ability to observe stars, ionized gas and molecular gas in this distant source make it unique in the Galaxy.

### 4.3. NGC 3603

NGC 3603 fills a gap in luminosity between a region like Orion, with ~1 O-type star, and R136 in 30 Doradus, with ~100 O-type stars (Eisenhauer et al. 1998). The ionizing core of NGC 3603 (HD 97950) consists of approximately 20 O-type and Wolf-Rayet stars (Moffat. 1983). ¿From photometric measurements, Melnick, Tapia & Terlevich (1989) have identified 181 sources (50 with $U$, $B$, and $V$ photometry) associated with the stellar cluster within NGC 3603. The authors found an average age of 2.5 ± 2 Myr and evidence that star formation propagated from north to south, ending at the bordering molecular cloud (Cheung 1980). Brandner et al. (1997) have identified a ring-shaped nebula and bipolar outflows from Sher 25, a cluster member of HD 97950. Sher 25 (a B1.5Iab supergiant) is located approximately ~20" north of the core of the cluster. Brandner et al. present evidence for association of this star with HD 97950 and compare the star to the progenitor of SN 1987A.

The initial mass function (IMF) of HD 97950, the stellar cluster associated with NGC 3603, has been discussed in recent articles by Moffat et al. (1994), Hofmann et al. (1995), Zinnecker (1995) and Eisenhauer et al. (1998). Because of the proximity of NGC 3603, high resolution, deep studies allow detailed counts of stellar mass distribution to be made. Moffat et al. (1994) observed the central cluster with the HST/PC, studying its dense stellar core and the population of Wolf-Rayet stars. Moffat et al. (1994) conclude that in terms of density and stellar population, NGC 3603 is a 'Galactic clone' of R136 in 30 Doradus. Hofmann et al. derive an IMF power law of $\Gamma = -1.4 \pm 0.6$ ($\xi \propto M^{\Gamma}$) for 30-60 $M_{\odot}$ which is similar to that of 30 Doradus. Using speckle masking techniques with the HST, Hofmann et al. (1995) found a similar slope for stellar masses of 15 to 50 $M_{\odot}$ of $\Gamma = -1.6 \pm 0.2$. Both Eisenhauer et al. and Zinnecker use adaptive optics to extend the IMF to stellar masses less than 1 $M_{\odot}$. Some theoretical and observational studies have claimed that starburst systems are deficient in low mass stars, but Eisenhauer et al. (1998) find that the IMF follows a Salpeter power law with an index of $\leq -0.73$, and that there does not appear to be a low mass truncation to the IMF down to the observational limit of 0.2 $M_{\odot}$. ¿From such properties of NGC 3603, it may be possible to extrapolate properties of larger extragalactic starbursts.

Sequential star formation has also been suggested in NGC 3603, proceeding from north to south (Melnick, Tapia & Terlevich 1989). The presence of evolved objects at the north end of the source and embedded IR sources and a molecular cloud to the south qualitatively confirms a sequential star formation scenario (Hofmann et al. 1995). Investigations of NGC 3603 have proceeded on two fronts: radio and optical observations of the ionized gas, and optical and infrared observations of the exciting stars. While the stars and gas in the giant HII region are visually observable, these high resolution radio observations present the first unobscured view of the ionized gas on small scales. Melnick, Tapia & Terlevich (1989) have tabulated the positions of 181 stars in NGC 3603 from their CCD $UBV$ photometry. The positions of the 50 cluster member stars for which $U$, $B$, and $V$ magnitudes are tabulated are shown in Figure 9. The figure shows the positions of these stars (crosses) plotted with the 3.4 cm radio continuum. Coordinates for the stellar positions were derived from pixel coordinates using the known position of the B1.5Iab supergiant (Sher 25) as given by Brandner et al. (1997).

Optical studies indicate both the presence of high velocity gas and of highly evolved stars. Clayton (1986) first investigated the velocity structure in the ionized gas located at the core of NGC 3603, and found both large scale motions (perhaps kinematic evidence of earlier supernovae) and two smaller shells, possibly wind-driven bubbles. The H$\alpha$ and [NII] line profiles were made along two lines across the core of NGC 3603. One possible explanation of the wind-driven bubbles was suggested by Moffat et al. (1994) who detected three Wolf-Rayet (WR) stars in their HST/PC observations of the cluster core. Hofmann et al. (1995) confirm the presence of three, perhaps four WR stars in the cluster core. Brandner et al. (1997) provide fascinating evidence that one of the sources believed to be an older member of the cluster (Sher 25, a B1.5Ia supergiant) is at the center of a clumpy ring of optical emission and a possible bipolar outflow. They compare the source to the progenitor of SN1987A.

Caswell & Haynes (1987) detected strong hydrogen radio recombination line emission from NGC 3603. The source was also included in the recombination line survey of McGee & Newton (1981), and both hydrogen and helium (at 14.7 GHz) were detected. Our integrated H90$\alpha$ line width ($\Delta V_{FWHM}$=36.9$\pm$0.25) is in reasonable agreement with the value for the H76$\alpha$ line given by McGee & Newton ($\Delta V_{FWHM}$=41.9$\pm$0.2).

The present study of the ionized gas in NGC 3603 addresses a number of the outstanding issues in this source:

1. Are there any regions of enhanced helium abundance, as might be expected in the presence of 3-4 WR stars?

2. Is there any evidence in the ionized gas emission of the bipolar outflow associated with the B1.5 supergiant Sher 25 (Brandner et al. 1997)?

3. How does the location of ionized gas compare to the known positions of infrared sources (Frogel et al. 1977), WR stars (Moffat et al. 1994 and references therein) and maser emission (Caswell et al. 1989, Caswell et al. 1998)?

### *4.3.1. Helium Abundance and $\beta/\alpha$ Ratios*

McGee & Newton (1981) derived a helium abundance in NGC 3603 of $Y^+$ =0.069 (no uncertainty given). Our calculated helium abundance from the integrated line profile is significantly higher ($Y^+$ =0.13$\pm$0.01), but in their notes on individual sources, McGee & Newton (1981) indicate that their He76$\alpha$ line profile was rather noisy.

Moffat et al. (1994) detect three prominent Wolf-Rayet stars in NGC 3603 in their narrowband HeII (4686 A) images. WR stars have been cited as the possible explanation of enhanced helium abundances (Adler, Wood & Goss 1996). It is certainly reasonable to look for evidence of such enhanced abundances in the vicinity of known WR stars. In fact, the highest helium abundances in NGC 3603 are detected in source C, which has a value of $Y^+ = 0.26 \pm 0.10$. Interpretation of this high value is complicated by the large uncertainty. The ionized gas in NGC 3603 is located on the periphery of the WR wind-blown bubble, so it is possible that ionized helium ($Y^+$) abundances are enhanced by the presence of an evolved star.

The observed H113$\beta$/H90$\alpha$ ratios for the 13 sources in NGC 3603 range from 0.29 $\pm$ 0.04 to 0.53 $\pm$ 0.12, all above the theoretical value ($\beta/\alpha$=0.276). Most detections are within $2\sigma$ of this theoretical value, but a few sources (NGC 3603 E, H, I, and K) exceed the theoretical value by more than $3\sigma$. Anomalously high $\beta/\alpha$ ratios were found from H92$\alpha$ and H115$\beta$ recombination line observations in two Galactic center regions (G0.18-0.04; the Sickle and the Pistol; Lang. et al., 1997). Thum et al. (1995) propose a model that can explain enhanced $\beta/\alpha$ ratios as the result of high continuum optical depth. However, NGC 3603 A-M appear to have high $\beta/\alpha$ ratios. and yet be low density ($n_e \leq 10^4$ cm$^{-3}$) regions with $\tau_c \leq 1$. Cersosimo & Magnani (1990) suggest that under such conditions, high $\beta/\alpha$ ratios may result from stimulated emission caused by a background source.

### *4.3.2. Ionized Gas Kinematics*

No ionized gas is detected above a $5\sigma$ continuum level at the location of Sher 25. The optical study of Clayton (1986) indicates clearly that there are both large scale and small scale motions in the ionized gas. Plate 1 of Clayton shows an H$\alpha$ image of the central 6′ of NGC 3603, and the positions of the two slit positions through the core. The bright ionized gas observed in our high resolution image (see Fig. 1b and Fig. 9) lies to the south of the cluster core. On scales probed by our high resolution observations, only one source (NGC 3603 F) has clearly double-peaked recombination line emission. Two Gaussians with velocities separated by ~29 km s$^{-1}$(V$_{LSR}$ =27.5 km s$^{-1}$ and $-1.1$ km s$^{-1}$) have been fitted to the H90$\alpha$ line in NGC 3603 F. The velocity separation is similar to that seen in other Galactic wind-driven bubbles and also in NGC 3576. In the radio continuum, source F is a relatively faint, marginally resolved source located near the western edge of the southern bright region. NGC 3603 F has a deconvolved diameter of $\theta_{FWHM}$ ~25″, giving the source a linear diameter of 0.5 pc (D = 6.1 kpc). Thus, source F may be an expanding shell of ionized gas. A small optically observable wind-driven "stellar bubble" with $r$ ~0.6 pc has been observed centered on the HD97950 star cluster in NGC 3603 (Balick, Boeshaar & Gull, 1980).

In NGC 3603, the individual source velocities (as derived from the H90$\alpha$ line) range from $-3.7\pm0.3$ km s$^{-1}$ in source A to to $15.9\pm0.2$ km s$^{-1}$ in source I. The broadest lines are detected in NGC 3603 F ($\Delta V_{FWHM}$=52.7$\pm$2.2 km s$^{-1}$). As indicated above, the broad lines in this source likely result from the double-peaked lines apparent in Fig. 7f. Broad lines can result from a variety of local conditions including pressure broadening or spatially unresolved velocity gradients. Given the relatively high frequency of the observations and other evidence for velocity gradients in the source, it is likely that the broad lines in source M (located to the north of the cluster core) are related to gas kinematics. NGC 3603 M has $v_{turb} \simeq 26 \pm 10$ km s$^{-1}$. Other localized regions in the source have very broad recombination line emission. Lines as broad as $\Delta V \sim 80$ km s$^{-1}$ are detected in the low surface brightness gas between sources NGC 3603 D and F. And in the bright core of NGC 3603 D ($\sim$0.07 pc in diameter) line widths approach $\Delta V \sim 75$ km s$^{-1}$. In a sequential star formation scenario, sources D and F are located at the boundary of the molecular cloud and the stellar cluster, and would be in the early stages of their evolution, perhaps still coming into equilibrium with their environment or photoevaporating material from the molecular cloud interface.

### *4.3.3. Evidence for sequential star formation in NGC 3603*

In Figure 2, the positions of ten 10$\mu$m sources (Frogel et al. 1977) are plotted over the 3.4 cm continuum. Figure 9 shows the positions of cluster stars and known maser emission. Error bars for the absolute positions of the IR sources are $\pm 10''$, and the size of the crosses in Fig. 2 indicates the absolute error in the positions of the infrared sources. In several cases (e.g. Irs 1, 2, 9, 14), the infrared sources are coincident with radio continuum sources.

Perhaps the clearest evidence for sequential star formation in NGC 3603 is the relative location of the radio emission from the ionized gas, the stellar positions, and the position of embedded infrared sources and maser emission. The distribution is very much like that observed in NGC 3576. The most evolved stars are located to the north, centered in what appears at many frequencies to be the wind-blown bubble resulting from the WR stars located there. The molecular cloud core is located farthest to the south, and the ionized gas emission (apparent at optical and radio frequencies) is located at the periphery between the stars and the cold gas.

## 5. Conclusions

Both NGC 3576 and NGC 3603 provide rare opportunities to study massive star formation in a variety of spectral regions. Massive star forming regions like W49A and Sgr B2 are impressive at radio frequencies, but the stellar populations are inaccessible in the infrared. In these two sources, high resolution stellar photometry and radio continuum and recombination line observations provide a more complete picture of the physical conditions and complex gas kinematics.

The following is a summary of our major conclusions:

(1) In these high resolution radio continuum and recombination line observations, we have identified a number of previously unresolved radio continuum sources, particularly in NGC 3603.

(2) The observed temperature gradient in NGC 3576 is in agreement with the known color

gradient in the source and supports a sequential star formation scenario that has been proposed for the region.

(3) We have detected several compact sources in NGC 3603 with broad recombination lines. One source (NGC 3603 F) has double peaked profiles, with the peaks separated by $\sim$30 km $s^{-1}$.

(4) The brightest radio continuum emission in NGC 3603 is located to the south of the core of the stellar cluster HD 97950. There is no radio continuum or line emission apparent at the position of Sher 25.

(5) Derived helium abundances and electron temperatures in NGC 3576 are in good agreement with values given in McGee & Newton (1981) while those in NGC 3603 are significantly higher.

(6) Enhanced helium abundances ranging in value from $Y^{+}$=0.16 to 0.26 are detected in NGC 3603 A-D and J. These regions may have had their helium abundance enriched by the 3 or 4 known WR sources located at the cluster core.

(7) In both sources, the relative positions of stars, ionized gas, molecular gas and masers is suggestive of a sequential star formation scenario. In NGC 3576 the star formation appears to have proceeded from east to west, in NGC 3603 from north to south.

C. G. De Pree gratefully acknowledges the support of an American Astronomical Society Small Research Grant. W. M. Goss would like to thank R. D. Ekers, J.B. Whiteoak, & D. McConnell for support during a sabbatical visit to the Australia Telescope Compact Array in 1996. The Australia Telescope is funded by the Commonwealth of Australia for operation as a National Facility operated by CSIRO. The National Radio Astronomy Observatory is a facility of the National Science Foundation, operated under cooperative agreement by Associated Universisites. Inc. The authors also thank H. Zinnecker, J. Caswell, W. Brandner, P. Palmer, D. Mehringer. L. Rodriguez, R. Gaume, M. Claussen and an anonymous referee for helpful discussions and comments.

## REFERENCES

Adler, D.S., Wood, D.O.S., Goss, W.M. 1996, ApJ, **471**, 871

Balick, B., Boeshaar, G.O., Gull, T.R. 1980, ApJ, **242**, 584

Brandner, W., Grebel, E.K., Chu Y., Weis, K. 1997, ApJ, **475**, L45

Caswell, J.L., 1998, MNRAS, 297, 215

Caswell, J.L., Vaile, R.A., Ellingsen, S.P., Whiteoak, J.B., Norris, R.P. 1995, MNRAS, 272, 96

Caswell, J.L., Haynes, R.F. 1987, A&A, **171**, 261

Caswell, J.L., Batchelor, R.A., Forster, J.R., Wellington, K.J. 1989, *Austral. J. Phys.*, **42**, 331

Caswell, J.L., Vaile, R.A., Ellingsen, S.P., Whiteoak, J.B., Norris, R.P., 1977, MNRAS, **272**, 96

Cersosimo, J.C., Magnani, L. 1990, A&A, **239**, 287

Cheung, L. H., Frogel, J. A., Hauser, M. G. & Gezari, D. Y. 1980, ApJ, 240, 74

Clayton, C.A. 1986, MNRAS, **219**, 895

Clayton, C.A. 1990, MNRAS, **246**, 712

Crampton, D. 1972, MNRAS, **158**, 85

De Pree, C.G., Mehringer, D. M. & Goss, W. M. 1997, ApJ, 482, 307

De Pree, C.G., Gaume, R. A., Goss, W. M. & Claussen, M.J., 1996, ApJ, 464, 788

De Pree, C.G., Gaume, R.A., Goss, W.M. & Claussen, M.J., 1995, ApJ, 451, 284

Eisenhauer, F., Quirrenbach, A., Zinnecker, H., and Genzel, R. 1998, ApJ, 498, 278

Frogel, J.A., Persson, S.E., Aaronson, M. 1977, ApJ, 213, 723

Frogel, J.A., Persson, S.E. 1974, ApJ, **192**, 351

Gaume, R.A., Fey, A.L. & Claussen, M.J. 1994, ApJ, 432, 648

Gaume, R.A., Claussen, M.J., De Pree, C.G., Goss, W.M. & Mehringer, D.M. 1995, ApJ, 449, 663

Goss, W.M., Radhakrishnan, V. 1969, Astrophys Letters, 4, 199

Goss & Shaver 1970, *Austral. J. Phys. Astroph. Suppl.*, 14, 133

Hjellming, R. 1966, ApJ, 143, 420

Hofmann, K.H., Seggewiss, W., Weigelt, G. 1995, A&A, **300**, 403

Humphreys, R.A. 1972, A&A, **20**, 29

Lang, C., Goss, W.M., Wood, D.O.S. 1997, ApJ, **474**, 275

Mehringer, D.M., De Pree, C.G., Gaume, R.A., Goss, W.M. & Claussen, M.J. 1995, ApJ, 442, L29

Mezger, P.G. & Henderson, A.P., ApJ, 147, 471

McGee, R.X., Gardner, F.F. 1968, *Austral. J. Phys.*, **21**, 149

McGee, R.X., Newton, L.M. 1981, MNRAS, **196**, 889

Melnick, J., Grosbøl, P. 1982, A&A. **107**, 23

Melnick, J., Tapia, M., Terlevich, R. 1989, A&A, **213**, 89

Moffat, A.F.J., 1974, A&A, **35**, 315

Moffat, A.F.J., 1983, A&A, **124**, 273

Moffat, A.F.J., Drissen, L., Shara, M.M. 1994, ApJ, **436**, 183

Norris, R. P., Caswell, J. L., Gardner, F. F., & Wellington, K. J. 1987, ApJ, 321, 159

Persi, P., Roth, M., Tapia, M., Ferrari-Toniolo, M., Marenzi, A.R. 1994, A&A, **282**, 474

Retallack, D.S., Goss, W.M., 1980, MNRAS, **193**, 261

Roelfsema, P.R., Goss, W.M., 1992, A&A Review, 4, 161

Roelfsema, P.R., Goss, W.M., & Mallick, 1992

Salem, M., & Brocklehurst, M. 1979, ApJS, 39, 633

Shaver, P.A., Wilson, T.L., 1979, A&A **79**, 312

Sher, D. 1965, MNRAS, **129**, 17

Thum, C., Strelninski, V.S., Martin-Pintado, J., Matthews, H.E., Smith, H.A. 1995, A&A, **300**, 643

Wilson, T. L., Mezger, P. G., Gardner, F. F., Milne, D. K. 1970, A&A, 6, 364

Zinnecker, H., 1995, 11th IAP Conference (Paris)

This preprint was prepared with the AAS LaTeX macros v4.0.

Table 1: Observational Parameters of NGC 3576 and NGC 3603

| Parameter | NGC 3576 | NGC 3603 |
|---|---|---|
| Date (configuration)........................ | 13 June 1995 (750m D) | 13 June 1995 (750m D) |
| | 19 June 1995 (750m B) | 19 June 1995 (750m B) |
| Total observing time (hr)................ | 12 | 12 |
| R.A. of field center (J2000)............. | $11^h\ 11^m\ 51.88^s$ | $11^h\ 15^m\ 02.6^s$ |
| Decl. of field center (J2000)............ | -61° 18′ 31″ | -61° 15′ 46″ |
| Major axis (″)................................ | 7.0″ | 7.0″ |
| Minor axis (″)................................ | 6.8″ | 6.9″ |
| Position angle (°)........................... | -9° | -13° |
| LSR central velocity (km $s^{-1}$).......... | -23 | 10 |
| Total bandwidth (MHz).................. | 16 | 16 |
| Number of channels......................... | 256 | 256 |
| Channel Separation (kHz, km $s^{-1}$)... | 62.5 (2.1) | 62.5 (2.1) |
| Spectral resolution (kHz, km $s^{-1}$)... | 75.6 (2.6) | 75.6 (2.6) |
| Continuum noise (mJy $beam^{-1}$)................ | 18 | 11 |
| Line noise (mJy $beam^{-1}$).......................... | 2.1 | 2.2 |

Table 2: Continuum Parameters for NGC 3576 and NGC 3603

| Source | RA (J2000) | Dec (J2000) | $S_{Peak}$ (Jy beam$^{-1}$) | $S_{Tot.}$ (Jy) | $\theta$ ($''$) | $r$ (pc) |
|---|---|---|---|---|---|---|
| NGC 3576 | $11^h\ 11^m\ 51.32^s$ | -61° 18′ 43.″5 | 4.1±0.4 | 71±7 | ~90 | 1.4 |
| | | | | | | |
| NGC 3603 A | $11^h\ 14^m\ 56.02^s$ | -61° 13′ 55.″8 | 0.10±0.01 | 1.3±0.3 | 24 | 0.52 |
| B | $14^m\ 56.51^s$ | 13′ 17.″0 | 0.08±0.01 | 2.5±0.4 | 38 | 0.80 |
| C | $15^m\ 00.90^s$ | 13′ 32.″7 | 0.06±0.01 | 0.85±0.3 | 24 | 0.52 |
| D | $15^m\ 01.99^s$ | 16′ 33.″0 | 0.11±0.01 | 1.2±0.3 | 22 | 0.46 |
| E | $15^m\ 02.62^s$ | 15′ 53.″8 | 0.40±0.02 | 1.9±0.2 | 13 | 0.28 |
| F | $15^m\ 06.13^s$ | 16′ 40.″5 | 0.12±0.01 | 1.7±0.3 | 25 | 0.52 |
| G | $15^m\ 08.76^s$ | 16′ 55.″7 | 0.30±0.01 | 4.4±0.3 | 26 | 0.54 |
| H | $15^m\ 09.45^s$ | 16′ 41.″4 | 0.23±0.01 | 4.6±0.3 | 30 | 0.64 |
| I | $15^m\ 10.36^s$ | 16′ 17.″4 | 0.25±0.02 | 1.3±0.2 | 14 | 0.30 |
| J | $15^m\ 14.24^s$ | 17′ 34.″0 | 0.11±0.01 | 2.2±0.3 | 30 | 0.65 |
| K | $15^m\ 18.75^s$ | 16′ 58.″1 | 0.08±0.01 | 1.2±0.3 | 25 | 0.53 |
| L | $15^m\ 24.20^s$ | 12′ 54.″0 | 0.06±0.01 | 0.94±0.3 | 29 | 0.61 |
| M | $15^m\ 31.59^s$ | 13′ 16.″7 | 0.06±0.01 | 1.1±0.3 | 26 | 0.55 |

Table 3: Derived Continuum Parameters for NGC 3603

| Source | $n_e$ ($10^3$ cm$^{-3}$) | $EM$ ($10^6$ pc cm$^{-6}$) | $M_{HII}$ ($M_\odot$) | $U$ (pc cm$^{-2}$) | $N_{LyC}$ ($10^{48}$ s$^{-1}$) | $\tau_c$ |
|---|---|---|---|---|---|---|
| A | 0.92 | 0.9 | 13 | 50 | 5.6 | 0.005 |
| B | 0.67 | 0.7 | 35 | 62 | 11 | 0.004 |
| C | 0.75 | 0.6 | 10 | 44 | 3.7 | 0.005 |
| D | 1.0 | 1.0 | 10 | 49 | 5.1 | 0.006 |
| E | 2.8 | 4.6 | 6 | 57 | 8.2 | 0.027 |
| F | 1.0 | 1.1 | 15 | 54 | 7.1 | 0.007 |
| G | 1.6 | 2.8 | 25 | 76 | 19 | 0.016 |
| H | 1.3 | 2.1 | 32 | 76 | 20 | 0.012 |
| I | 2.1 | 2.7 | 5 | 50 | 5.4 | 0.016 |
| J | 0.87 | 1.0 | 23 | 60 | 9.5 | 0.006 |
| K | 0.85 | 0.8 | 12 | 48 | 5.0 | 0.005 |
| L | 0.66 | 0.5 | 15 | 47 | 4.8 | 0.003 |
| M | 0.72 | 0.6 | 12 | 45 | 4.0 | 0.003 |

Table 4: Recombination Line Parameters and Derived Quantities for or NGC 3576

| | $V$ (km s$^{-1}$) | $\Delta V$ (km s$^{-1}$) | $T_l/T_c$ | T$_e$* (K) |
|---|---|---|---|---|
| H90$\alpha$ | -20.0±0.1 | 28.7±0.1 | 0.105±0.001 | 6300±700 |
| He90$\alpha$ | -19.3±0.4 | 24.8±0.8 | 0.011±0.001 | |
| C90$\alpha$ | -21.5±0.9 | 8.75±1.8 | 0.003±0.001 | |
| H113$\beta$ | -22.3±0.2 | 33.6±0.4 | 0.022±0.001 | 7100±800 |
| | | | | |
| H90$\alpha$ | | | | |
| *Irs1/Irs2* | -24.0±0.1 | 29.1±0.1 | 0.100±0.001 | 6500±700 |
| *Irs3* | -17.2±0.1 | 26.5±0.1 | 0.112±0.001 | 6400±700 |
| *Irs4* | -14.5±0.1 | 32.0±0.3 | 0.081±0.001 | 7200±800 |
| *Irs5* | -18.8±0.2 | 36.2±0.4 | 0.098±0.002 | 5500±600 |

Table 5: Recombination Line Parameters and Derived Quantities for NGC 3603

| Source | | $V$ (km s$^{-1}$) | $\Delta V$ (km s$^{-1}$) | $T_l/T_c$ | $T_e{}^*$ (K) | $T_e$ (K) | $Y^+$ | $\beta/\alpha$ | $V_{turb}$ |
|---|---|---|---|---|---|---|---|---|---|
| Total | H90$\alpha$ | 9.14±0.1 | 36.9±0.25 | 0.075±0.001 | 6600±500 | | | | 24±2 |
| | He90$\alpha$ | 8.9±1.0 | 38.9±2.6 | 0.009±0.001 | | | 0.13±0.01 | | |
| | C90$\alpha$ | 6.2±1.9 | 10.0 (fixed) | 0.002±0.001 | | | | | |
| | H113$\beta$ | 5.9±0.3 | 42.6±0.8 | 0.026±0.001 | 4800±400 | | | 0.39±0.01 | |
| A | H90$\alpha$ | 8.08±0.2 | 26.3±0.5 | 0.107±0.003 | 6300±1100 | 6700±1200 | | | 14±3 |
| | He90$\alpha$ | 4.0±1.3 | 25.0±3.1 | 0.019±0.003 | | | 0.17 ±0.03 | | |
| | H113$\beta$ | 2.5±0.8 | 31.6±1.9 | 0.033±0.003 | 4900±900 | 5200±1000 | | 0.31±0.03 | |
| B | H90$\alpha$ | -3.65±0.3 | 28.3±0.7 | 0.103±0.004 | 6300±1600 | 6400±1600 | | | 17±4 |
| | He90$\alpha$ | 0.9±2.0 | 28.8±4.8 | 0.016±0.004 | | | 0.16 ±0.04 | | |
| | C90$\alpha$ | -12.5±1.3 | 10 (fixed) | 0.015±0.003 | | | | | |
| | H113$\beta$ | -7.4±1.1 | 29.0±2.6 | 0.029±0.004 | 6000±1500 | 6100±1500 | | 0.29±0.04 | |
| C | H90$\alpha$ | 3.8±0.7 | 33.2±1.7 | 0.104±0.007 | 4300±1700 | 4200±1700 | | | 22±9 |
| | He90$\alpha$ | 9.1±4.3 | 44.1±10 | 0.020±0.006 | | | 0.26 ±0.10 | | |
| | H113$\beta$ | -5.2±4.1 | 49.1±10 | 0.023±0.006 | 4400±1700 | 4300±1700 | | 0.32±0.11 | |
| D | H90$\alpha$ | -0.80±0.4 | 35.9±1.1 | 0.078±0.003 | 6400±2000 | 6800±2100 | | | 23±7 |
| | He90$\alpha$ | 1.1±2.2 | 32.8±5.6 | 0.014±0.003 | | | 0.16 ±0.05 | | |
| | H113$\beta$ | -1.7±1.0 | 31.4±2.6 | 0.029±0.003 | 5700±1800 | 6100±1900 | | 0.33±0.05 | |
| E | H90$\alpha$ | 1.9±0.2 | 41.9±0.5 | 0.066±0.001 | 6700±600 | 8500±800 | | | 27±3 |
| | He90$\alpha$ | -2.2±1.5 | 36.9 (fixed) | 0.008±0.001 | | | 0.11±0.01 | | |
| | H113$\beta$ | -2.3±0.6 | 46.5±1.4 | 0.022±0.001 | 5300±500 | 6700±600 | | 0.36±0.02 | |
| F | H90$\alpha$ | 11.5±0.8 | 52.7±2.2 | 0.056±0.003 | 6500±3300 | 7000±3600 | | | 36±19 |
| | He90$\alpha$ | 27.6±2.7 | 22.7±6.9 | 0.011±0.005 | | | 0.08±0.04 | | |
| | H113$\beta$ | 5.9±2.4 | 59.9±6.8 | 0.020±0.003 | 4700±2400 | 5100±2600 | | 0.40±0.08 | |
| G | H90$\alpha$ | 15.5±0.4 | 25.6±1.0 | 0.115±0.006 | 6200±2200 | 7900±2800 | | | 13±5 |
| | He90$\alpha$ | 20.0±1.6 | 17.2±3.8 | 0.024±0.001 | | | 0.14±0.05 | | |
| | H113$\beta$ | 8.3±1.2 | 31.2±3.1 | 0.040±0.006 | 4400±1500 | 5600±1900 | | 0.43±0.07 | |
| H | H90$\alpha$ | 11.8±0.1 | 32.2±0.3 | 0.082±0.001 | 6900±1200 | 8300±1400 | | | 19±3 |
| | He90$\alpha$ | 12.4±0.9 | 29.3±2.2 | 0.011±0.001 | | | 0.12±0.02 | | |
| | C90$\alpha$ | 8.2±1.6 | 10.0 (fixed) | 0.003±0.001 | | | | | |
| | H113$\beta$ | 8.5±0.4 | 37.9±0.9 | 0.028±0.001 | 5100±900 | 6300±1100 | | 0.40±0.02 | |
| I | H90$\alpha$ | 15.9±0.2 | 34.8±0.6 | 0.068±0.002 | 7900±2200 | 9300±2600 | | | 21±6 |
| | He90$\alpha$ | 7.9±3.1 | 44.9±8.0 | 0.006±0.001 | | | 0.11±0.03 | | |
| | H113$\beta$ | 13.4±0.7 | 39.6±1.8 | 0.023±0.002 | 5900±1600 | 6800±1800 | | 0.39±0.03 | |
| J | H90$\alpha$ | 7.3±0.3 | 39.9±0.9 | 0.085±0.003 | 5700±1600 | 5800±1600 | | | 26±7 |
| | He90$\alpha$ | 2.9±3.6 | 59.0±9.7 | 0.011±0.003 | | | 0.18±0.05 | | |
| | H113$\beta$ | 5.3±1.2 | 47.8±2.9 | 0.031±0.003 | 3600±1000 | 3700±1000 | | 0.43±0.05 | |
| K | H90$\alpha$ | 5.5±0.3 | 40.8±0.7 | 0.093±0.002 | 5100±1000 | 5000±1000 | | | 28±6 |
| | He90$\alpha$ | 7.9±1.9 | 31.2±4.7 | 0.012±0.003 | | | 0.10±0.02 | | |
| | H113$\beta$ | 3.8±0.7 | 43.8±1.9 | 0.037±0.002 | 3600±700 | 3500±700 | | 0.43±0.03 | |
| L | H90$\alpha$ | 6.4±0.6 | 38.2±1.5 | 0.142±0.008 | 3800±1000 | 3700±1000 | | | 26±7 |
| | He90$\alpha$ | 5.7±4.5 | 35.0 (fixed) | 0.018±0.004 | | | 0.11±0.03 | | |
| | H113$\beta$ | 2.7±1.3 | 32.9±3.1 | 0.063±0.008 | 2900±800 | 2800±800 | | 0.37±0.07 | |
| M | H90$\alpha$ | 4.6±0.5 | 37.3±2.1 | 0.115±0.009 | 3600±1300 | 3500±1300 | | | 26±10 |
| | He90$\alpha$ | 8.5±6.3 | 33.8 (fixed) | 0.015±0.005 | | | 0.11±0.04 | | |
| | H113$\beta$ | 4.3±2.1 | 44.9±5.4 | 0.051±0.009 | 2600±1000 | 2500±1000 | | 0.53±0.12 | |

FIGURE CAPTIONS

**Fig. 1** The 3.4 cm continuum image of NGC 3576 is shown at a resolution of 7″ (0.09 pc at 3.0 kpc). The first positive and negative continuum contours are at $3\sigma$ (54 mJy beam$^{-1}$). Subsequent positive contours are 1.4, 2, 2.8, 4, 5.6, 8, 11.3, 16, 22.6, 32 and 45.3 times the $3\sigma$ level. The peak continuum flux density is 4.1 Jy beam$^{-1}$ The positions of the 10 $\mu$m sources (Frogel & Person 1974) are indicated with crosses. Errors in the absolute IR positions are $\pm 4''$(indicated by the cross size). The inset is an integrated profile made over a region of the source where broad recombination lines are detected. The best fit to the spectrum consists of two Gaussians separated by $\sim$ 25 km s$^{-1}$. Epoch is B1950.

**Fig. 2** The 3.4 cm continuum image of NGC 3603 with the 13 named sources (A to M in order of increasing RA). The continuum data has a spatial resolution of 7″ (0.21 pc at D = 6.1 $\pm$ 0.6 kpc). The first contour is at $5\sigma$ (55 mJy beam$^{-1}$) with subsequent levels at 1.4, 2, 2.8, 4, 5.6, 8. 11.3, 16, 22.6, 32 and 45.3 times the $5\sigma$ level. The peak continuum flux density is 0.47 Jy beam$^{-1}$. The positions of the 10 $\mu$m sources (Frogel et al. 1977) are indicated with crosses. Errors in the absolute IR positions from this later study are $\pm 10''$(indicated by the cross size). Epoch is B1950.

**Fig. 3** (a) The continuum weighted, integrated line profile for NGC 3576. The recombination lines shown (left to right) are H113$\beta$, C90$\alpha$, He90$\alpha$, and H90$\alpha$. The solid line is the Gaussian fit, the crosses are the data points, and the dashed line is the residual. The spectral resolution is 2.6 km s$^{-1}$. (b) The continuum weighted, integrated line profile for the bright southern region in NGC 3603. The recombination lines shown (left to right) are H113$\beta$, C90$\alpha$, He90$\alpha$, and H90$\alpha$. The solid line is the Gaussian fit, the crosses are the data points, and the dashed line is the residual. The spectral resolution is 2.6 km s$^{-1}$.

**Fig. 4** The continuum weighted, integrated line profiles for the Irs sources in NGC 3576 (Frogel & Persson 1974), indicated in Figure 1. The solid line is the Gaussian fit, the crosses are the data points, and the dashed line is the residual. The spectral resolution is 2.6 km s$^{-1}$. Figures show (a) Irs 1/2, (b) Irs 3, (c) Irs 4, (d) Irs 5.

**Fig. 5** Line parameters of the H90$\alpha$ line in NGC 3576 overlaid on the 3.4 cm continuum contours. Fits were made to each pixel above the $5\sigma$ level in the continuum. (a) The velocity ($V_{LSR}$) of the H90$\alpha$ line in NGC 3576 for each pixel is presented in grey-scale with the NGC 3576 3.4 cm continuum contours overlayed. The contour levels are as indicated in Figure 1. The grey scale velocity range is from -35 km s$^{-1}$ to 10 km s$^{-1}$. (b) The full width at half maximum ($\Delta V_{FWHM}$) of the H90$\alpha$ line in NGC 3576 for each pixel is presented in grey-scale with the NGC 3576 3.4 cm continuum contours overlayed. The contour levels are as indicated in Figure 1. The grey scale line width range is from 15 km s$^{-1}$ to 50 km s$^{-1}$. (c) The electron temperature calculated for each pixel in NGC 3576 above $10\sigma$ in the continuum image. The temperature (grey scale) ranges from 5000 to 12000 K. The contours start at 4000 K and rise linearly to 12000 K in increments of 1000 K.

**Fig. 6** The integrated electron temperature in NGC 3576 for 18 concentric semicircles (width of 4 pixels) centered on the peak in the 3.4 cm continuum image. Temperatures range from 6000 K to 9000 K across the source.

**Fig. 7** The integrated line profiles from the 13 individual HII regions in NGC 3603, as indicated in Figure 2. The recombination lines shown (left to right where detected) are H113$\beta$. C90$\alpha$, He90$\alpha$, and H90$\alpha$. The plot shows the Gaussian fit (solid line), data (crosses), and the residual (dashed line). The spectral resolution is 2.6 km s$^{-1}$. Figures 7a to 7m show the integrated profiles of sources NGC 3603 A-M respectively.

**Fig. 8** The 3.4 cm continuum contours for NGC 3576. The stellar positions of cluster member stars with infrared excess (Persi et al. 1994) are plotted as crosses. Also plotted are the positions of the star HD 97499 (diamond), and the $H_2O$ (triangle; Caswell 1989) and $CH_3OH$ (box; Caswell et al. 1995) maser positions. Continuum contours are as indicated in Figure 1. Epoch is J2000.

**Fig. 9** The 3.4 cm continuum contours in the vicinity of the known stellar cluster HD 97950. The positions of $\sim$50 cluster members with measured $U, B$, and $V$ magnitudes (Melnick, Tapia & Terlevich 1989) are plotted as crosses. Coordinates of the 50 stars were derived from pixel offsets from the known position of Sher 25 (a B1.5Iab supergiant) as given by Brandner et al (1997). Also indicated is the position of HD 97950 (diamond), and $H_2O$ (triangles; Caswell 1989) and OH (box; Caswell 1998) maser positions. Continuum contours are as indicated in Figure 2. Epoch is J2000.

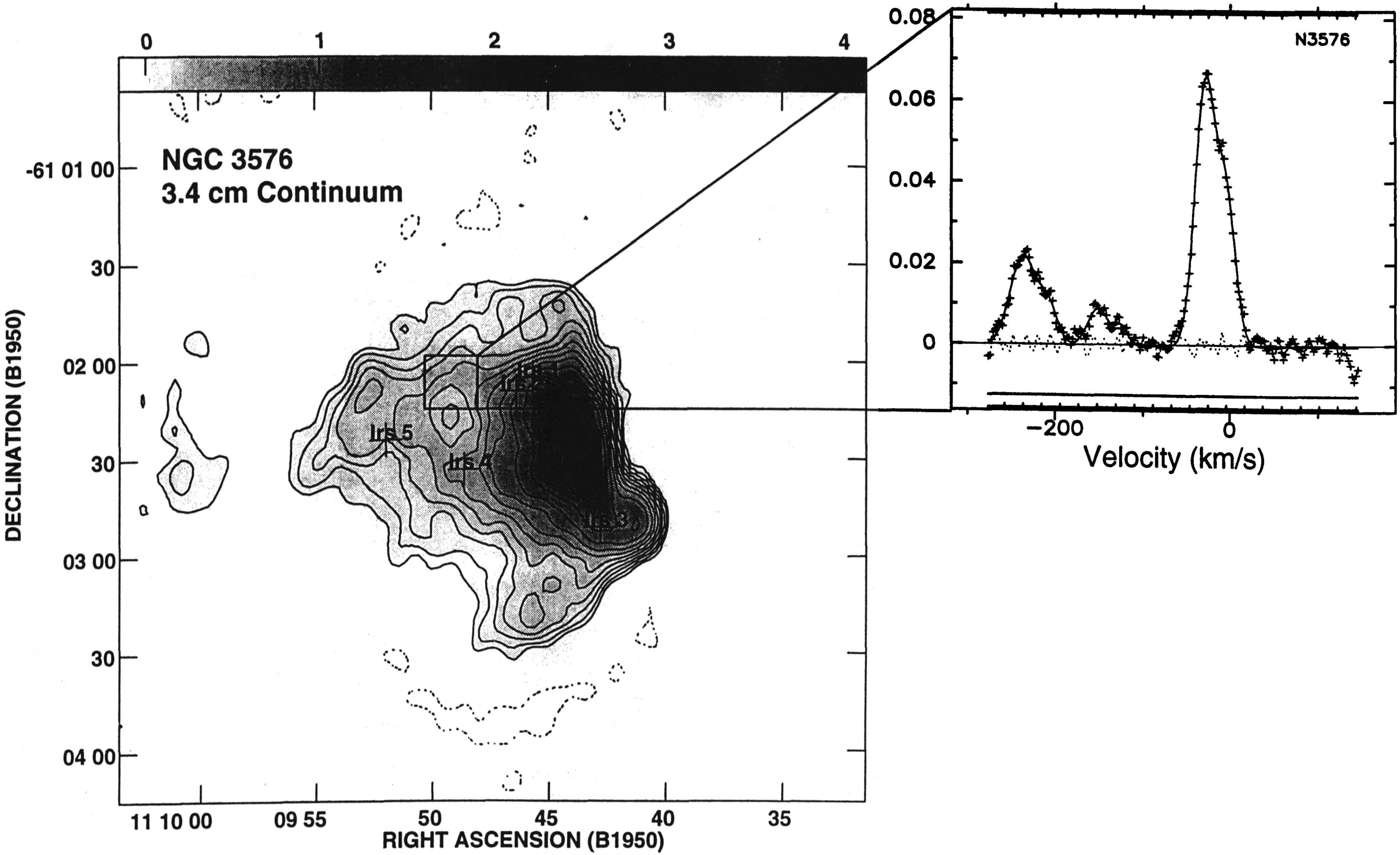
NGC 3576
3.4 cm Continuum
Irs 5
Irs 4
Irs 3
DECLINATION (B1950)
RIGHT ASCENSION (B1950)
N3576
Velocity (km/s)

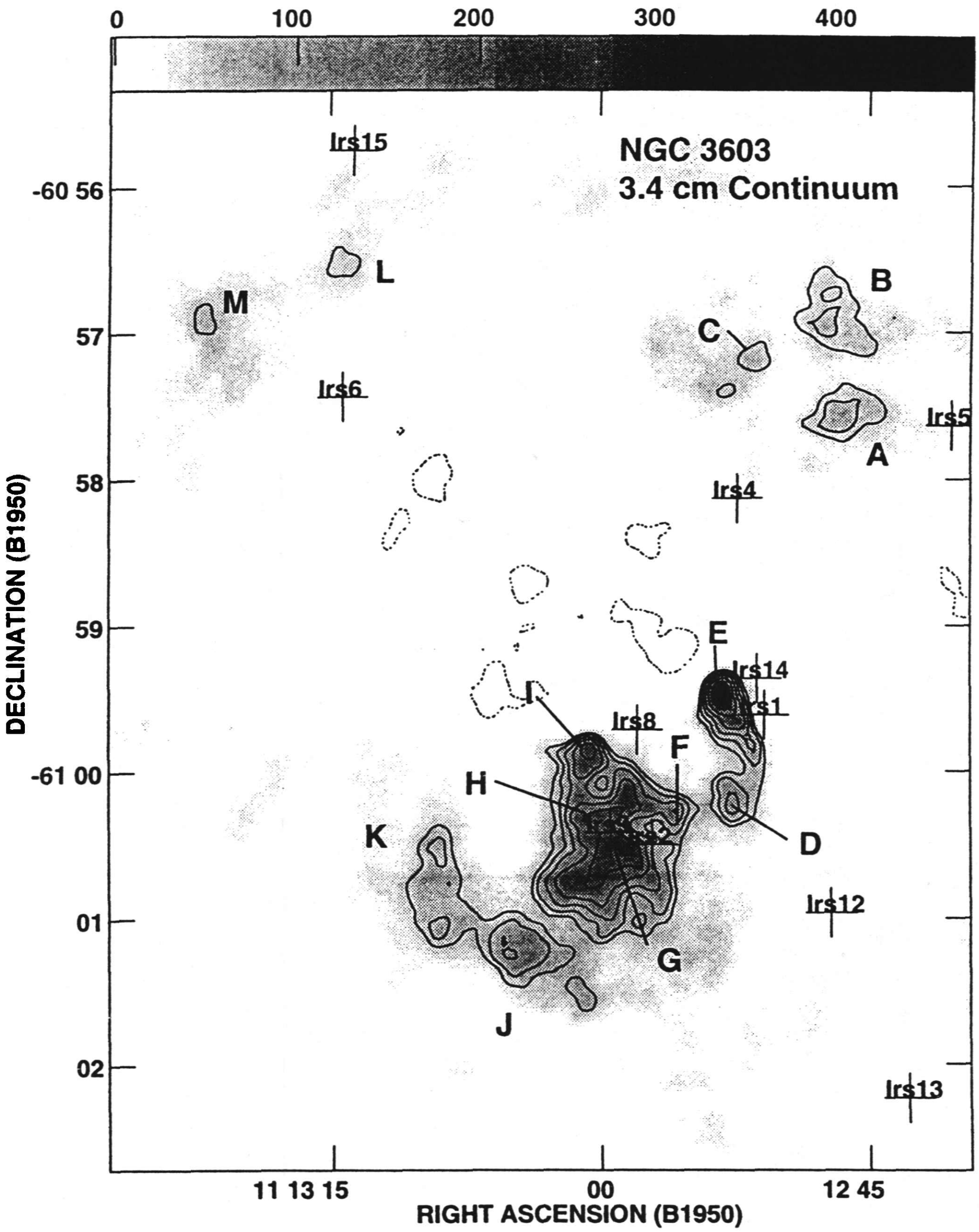

0
100
200
300
400
NGC 3603
3.4 cm Continuum
Irs15
Irs6
Irs5
Irs4
Irs8
Irs14
Irs1
Irs12
Irs13
A
B
C
D
E
F
G
H
I
J
K
L
M
-60 56
57
58
59
-61 00
01
02
DECLINATION (B1950)
11 13 15
00
12 45
RIGHT ASCENSION (B1950)

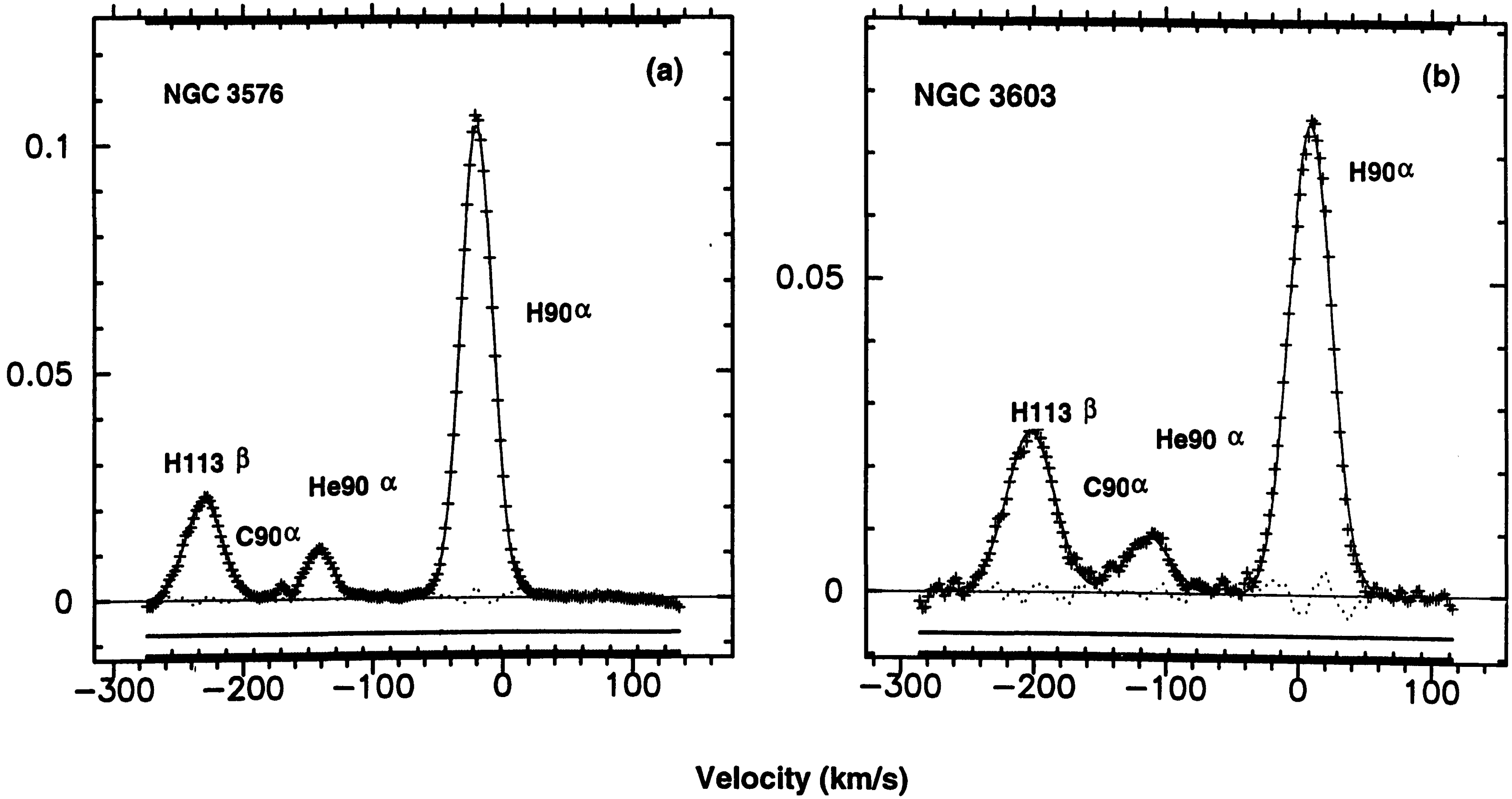
NGC 3576
(a)
H113 β
C90α
He90 α
H90α
0.1
0.05
0
−300
−200
−100
0
100
NGC 3603
(b)
H113 β
C90α
He90 α
H90α
0.05
0
−300
−200
−100
0
100
Velocity (km/s)

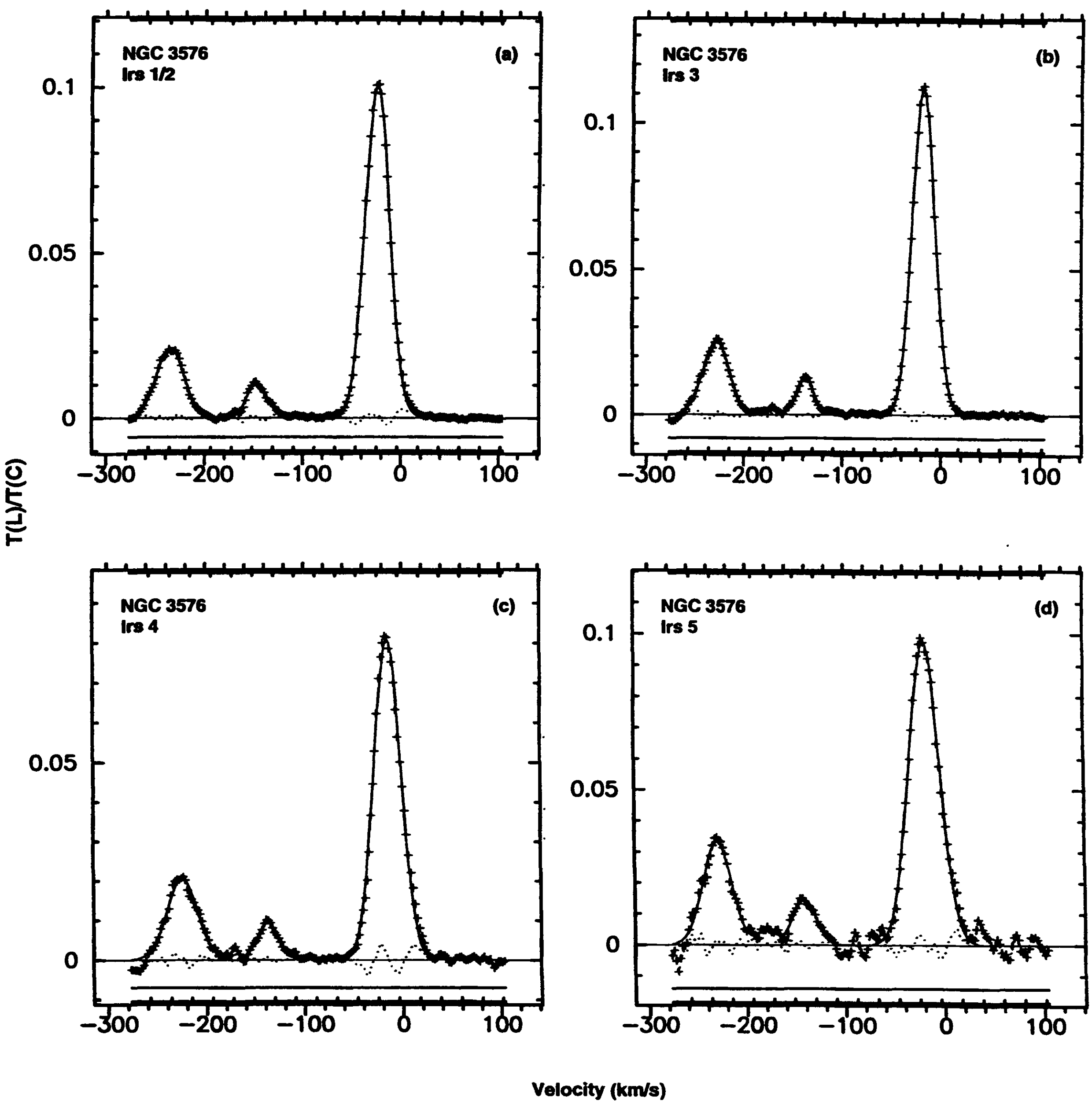
NGC 3576
Irs 1/2
(a)
NGC 3576
Irs 3
(b)
NGC 3576
Irs 4
(c)
NGC 3576
Irs 5
(d)
T(L)/T(C)
0.1
0.05
0
−300
−200
−100
0
100
Velocity (km/s)

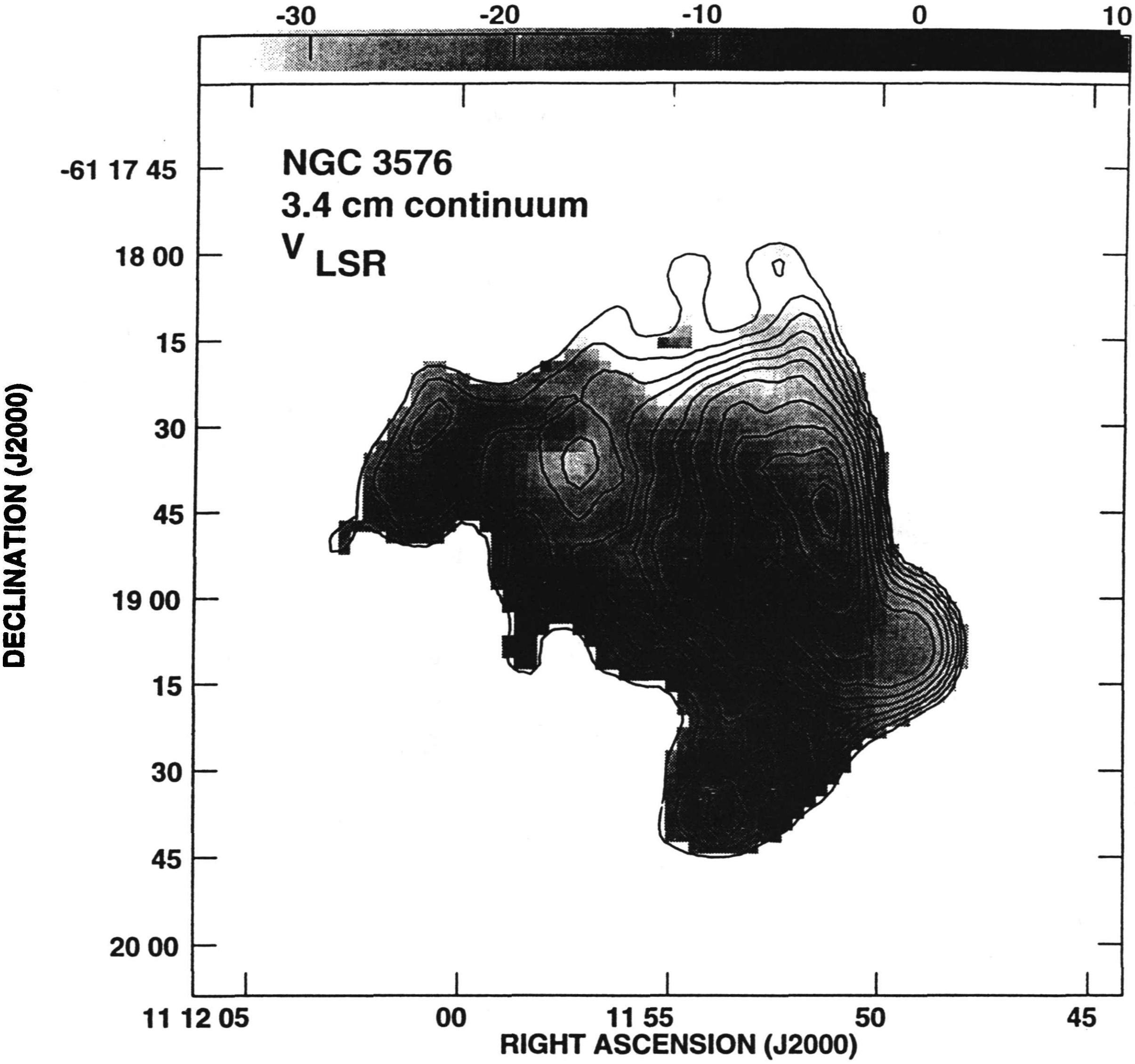

-30
-20
-10
0
10
NGC 3576
3.4 cm continuum
V LSR
-61 17 45
18 00
15
30
45
19 00
15
30
45
20 00
DECLINATION (J2000)
11 12 05
00
11 55
50
45
RIGHT ASCENSION (J2000)

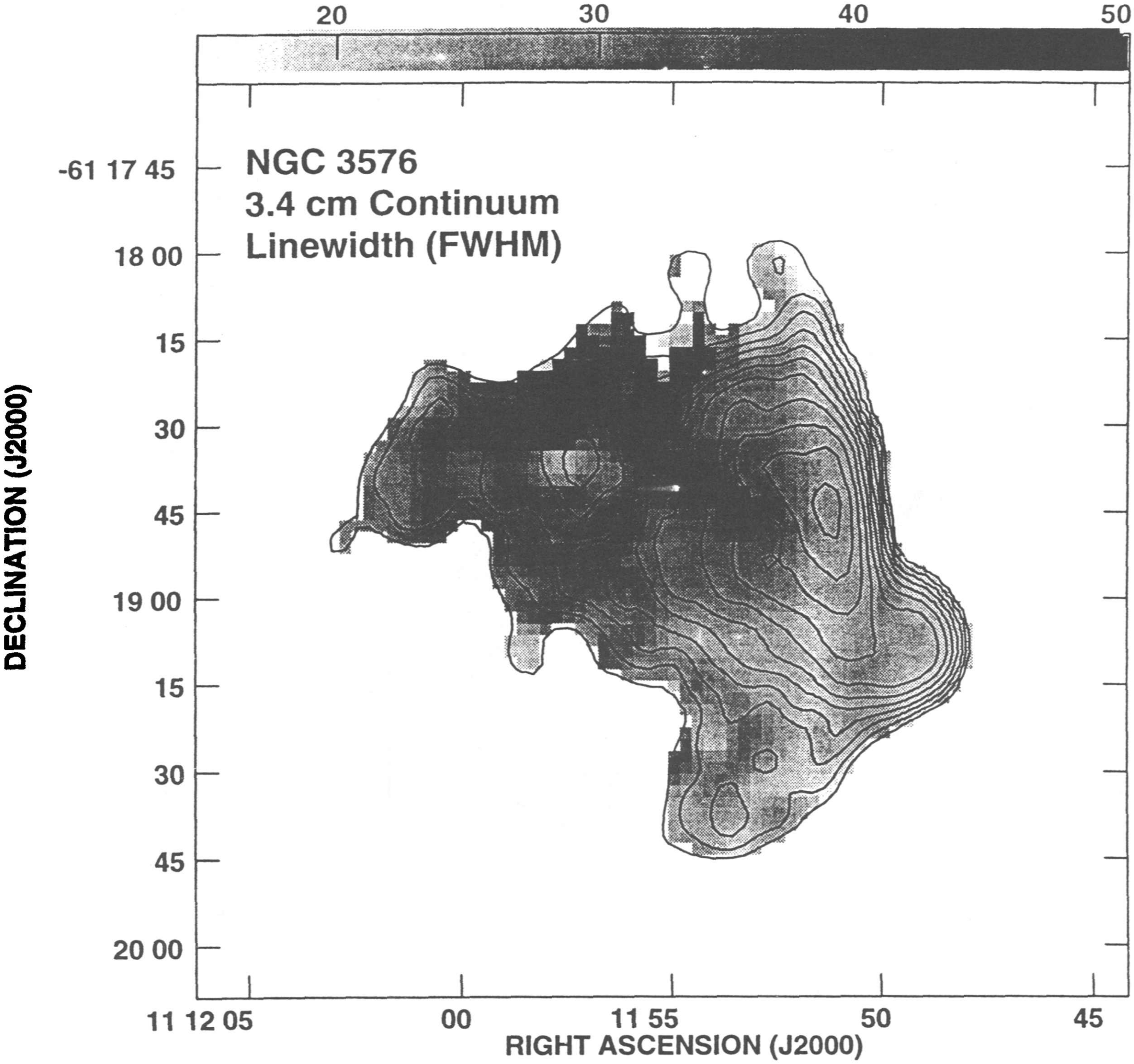

20
30
40
50
NGC 3576
3.4 cm Continuum
Linewidth (FWHM)
-61 17 45
18 00
15
30
45
19 00
15
30
45
20 00
DECLINATION (J2000)
11 12 05
00
11 55
50
45
RIGHT ASCENSION (J2000)

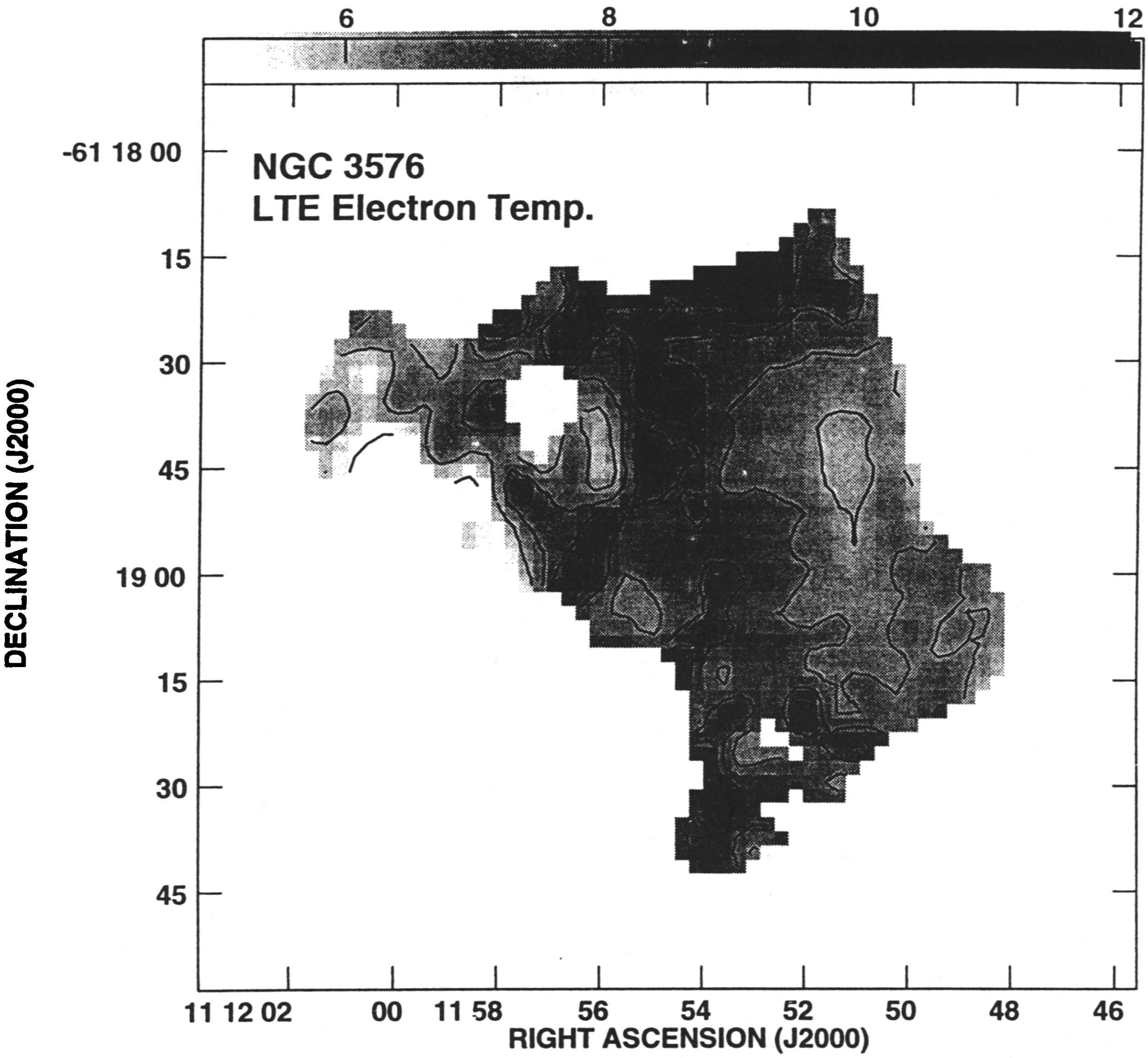

6
8
10
12
NGC 3576
LTE Electron Temp.
-61 18 00
15
30
45
19 00
15
30
45
DECLINATION (J2000)
11 12 02
00
11 58
56
54
52
50
48
46
RIGHT ASCENSION (J2000)

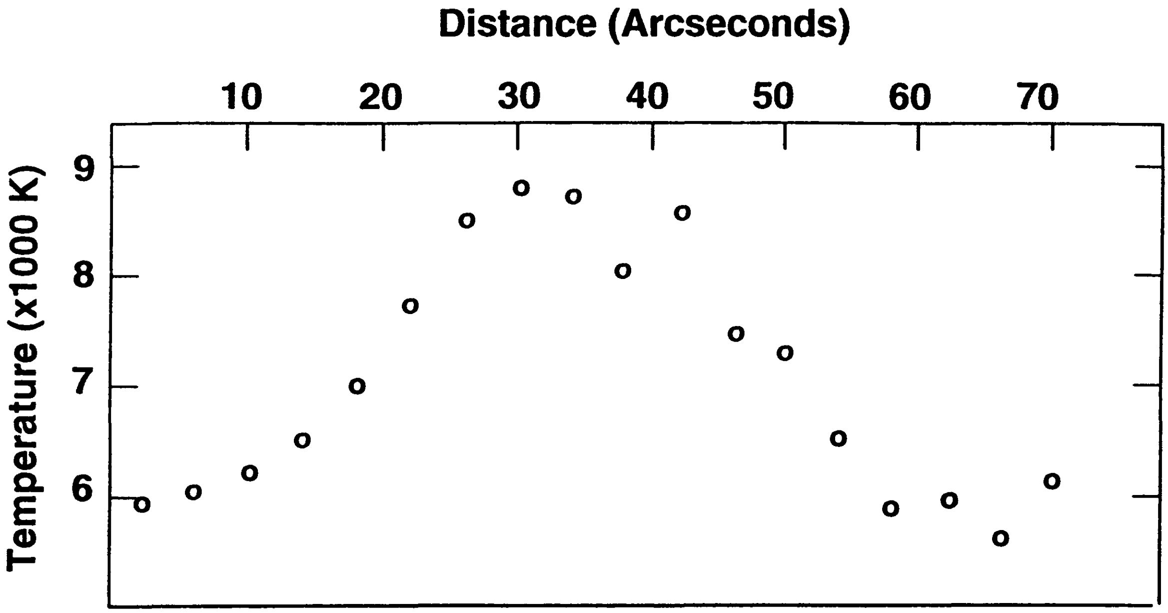

Distance (Arcseconds)
10
20
30
40
50
60
70
Temperature (x1000 K)
9
8
7
6

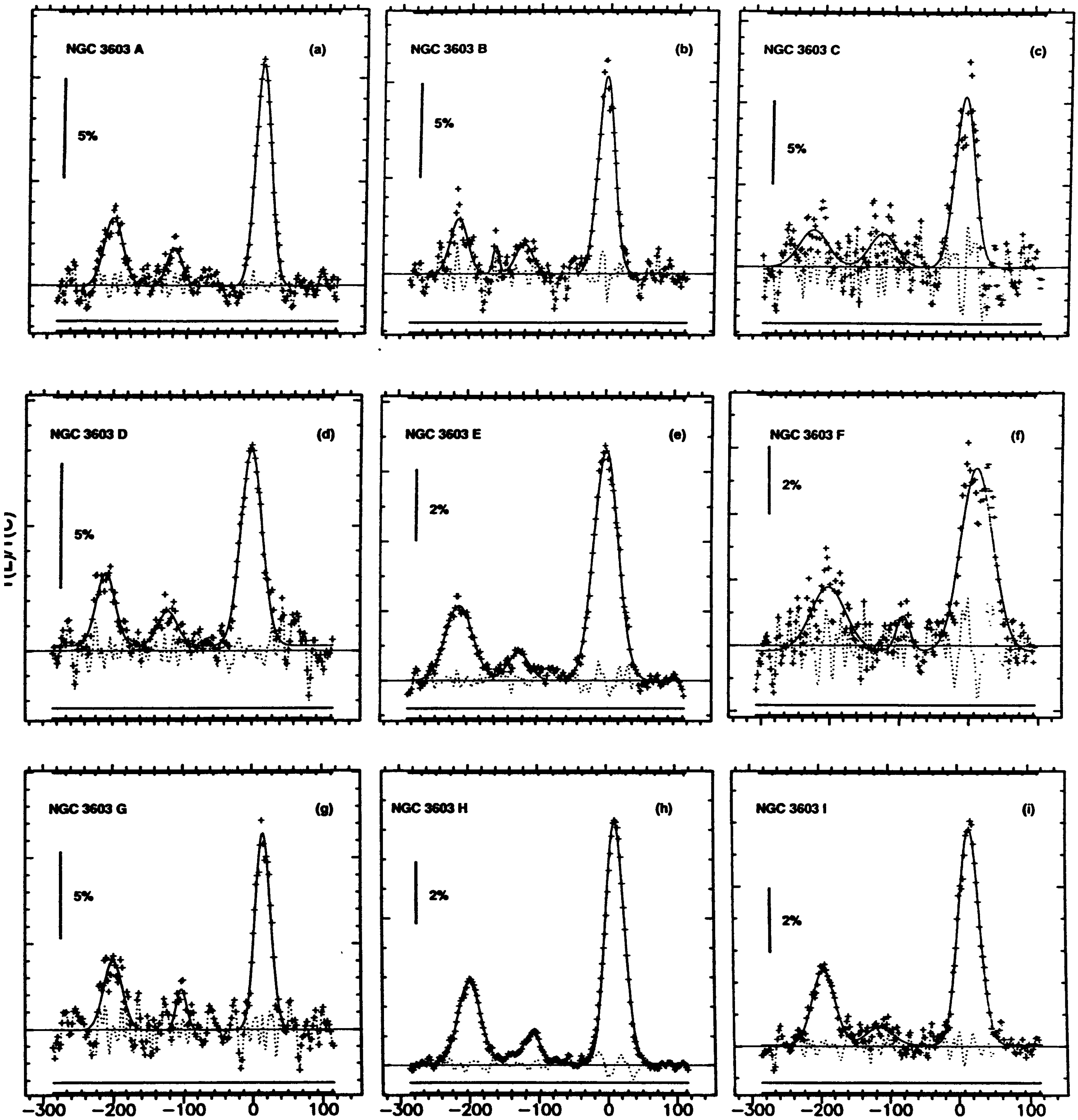

NGC 3603 A
(a)
5%
NGC 3603 B
(b)
5%
NGC 3603 C
(c)
5%
NGC 3603 D
(d)
5%
NGC 3603 E
(e)
2%
NGC 3603 F
(f)
2%
NGC 3603 G
(g)
5%
NGC 3603 H
(h)
2%
NGC 3603 I
(i)
2%
−300 −200 −100 0 100
Velocity (km/s)

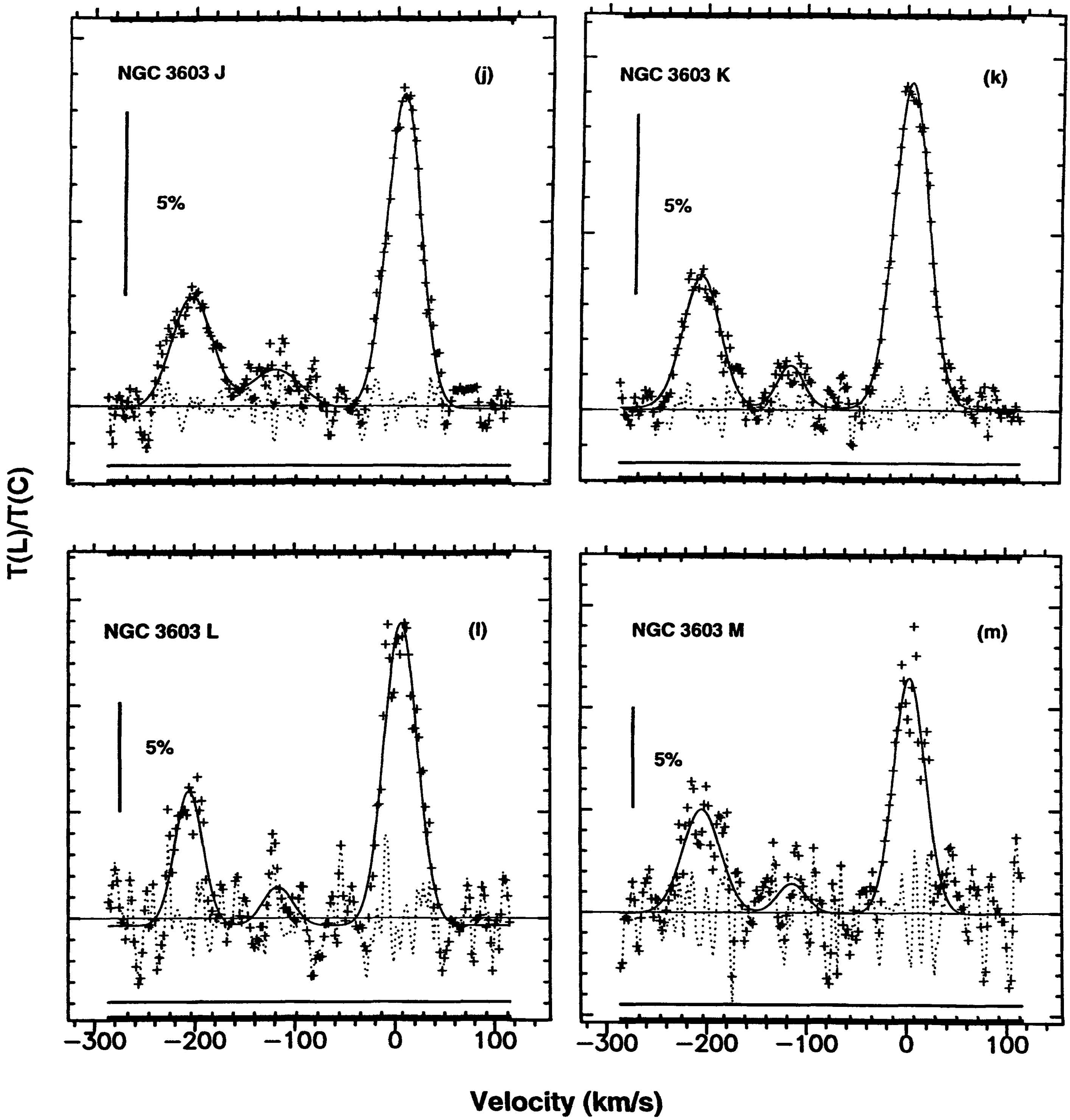
NGC 3603 J
(j)
5%
NGC 3603 K
(k)
5%
NGC 3603 L
(l)
5%
NGC 3603 M
(m)
5%
T(L)/T(C)
−300
−200
−100
0
100
Velocity (km/s)

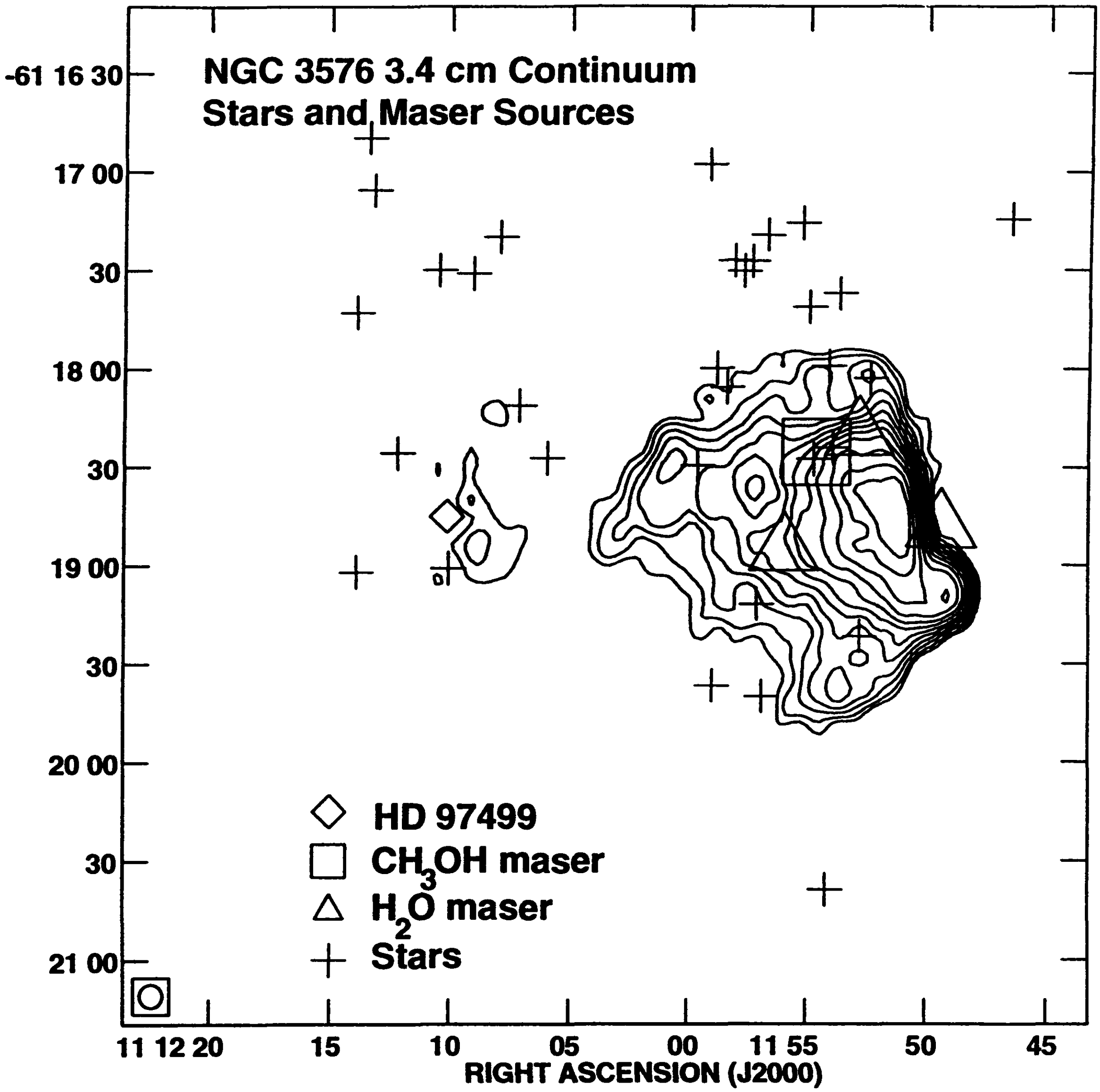
NGC 3576 3.4 cm Continuum
Stars and Maser Sources
-61 16 30
17 00
30
18 00
30
19 00
30
20 00
30
21 00
HD 97499
CH3OH maser
H2O maser
Stars
11 12 20
15
10
05
00
11 55
50
45
RIGHT ASCENSION (J2000)

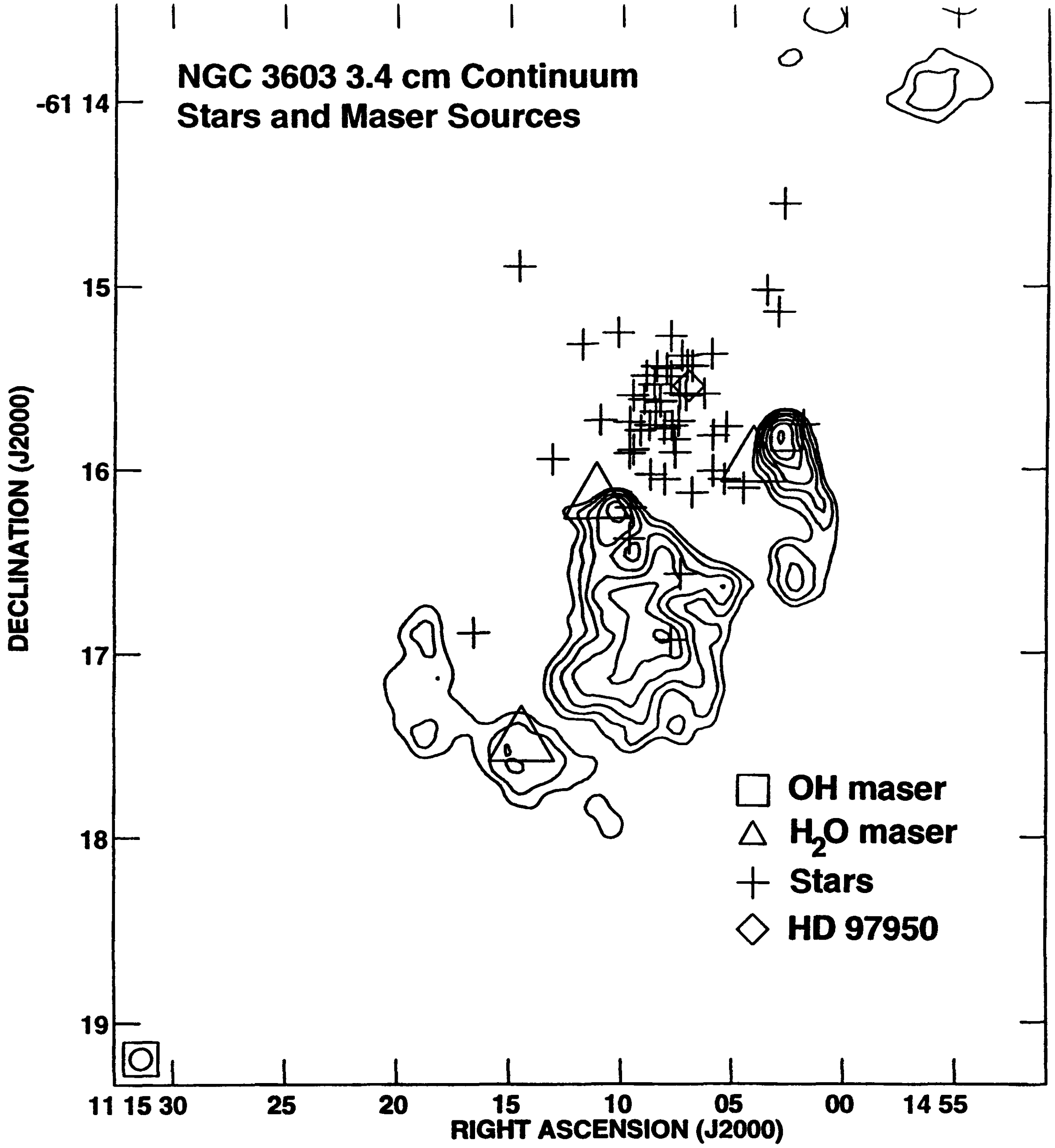
NGC 3603 3.4 cm Continuum
Stars and Maser Sources
-61 14
15
16
17
18
19
DECLINATION (J2000)
11 15 30
25
20
15
10
05
00
14 55
RIGHT ASCENSION (J2000)
OH maser
H2O maser
Stars
HD 97950

# Student Questionnaires 1999
# (GB and CV Students)

# NATIONAL RADIO ASTRONOMY OBSERVATORY
## MEMORANDUM

DATE: August 4, 1998
TO: Summer Students
FROM: Ron Maddalena
SUBJECT: Questionnaire

Before you leave us we would appreciate you filling out and returning to me the following questionnaire. We will use your responses to improve the program for next year. Feel free to use the back of this sheet if you need more room for your responses. Thanks!

- **How did you find out about the NRAO-REU program?**

  Off of the internet and by talking to my professors at school.

- **What is your overall reaction to the program?**

  I loved it! I learned a lot and the resources here are great.

- **How have your career decisions been influenced by you experiences at NRAO?**

  Yes - I have a much stronger interest in radio astronomy and electrical engineering. I for sure want to go into this field for grad school.

- **Have you previously been an REU student at another institution? If so, how do your NRAO experiences compare with your experiences elsewhere?**

  Nope But if I did, they couldn't compare to NRAO.

- **In what ways could we improve your stay at NRAO?**

  More seminars and talks would be nice. Maybe a group project we could all work on. Something short-term.

- **What changes would you like to see in the NRAO-REU program?**

  ? Can't think of any

- **Do you and your mentor plan to publish results of your summer research, or to present the results at a professional meeting (the REU program can pay most of your costs)?**

  Somtime in the future - maybe in a year We will see about a AAS meeting.

**NATIONAL RADIO ASTRONOMY OBSERVATORY**
MEMORANDUM

DATE: August 4, 1998
TO: Summer Students
FROM: Ron Maddalena
SUBJECT: Questionnaire

Before you leave us we would appreciate you filling out and returning to me the following questionnaire. We will use your responses to improve the program for next year. Feel free to use the back of this sheet if you need more room for your responses. Thanks!

- How did you find out about the NRAO-REU program?

  from my astronomy advisor at my school - he gave me a large list of REU possibilities in all areas of astronomy (planetary, optical, etc)

- What is your overall reaction to the program?

  I love it! I want more! I want more! NRAO has not only been helpful, but respectful towards me and the other students - a quality hard to find in undergraduate progra

- How have your career decisions been influenced by you experiences at NRAO?

  yes - more like career ideas than decision, but certainly influentaal

- Have you previously been an REU student at another institution? If so, how do your NRAO experiences compare with your experiences elsewhere?

  no

- In what ways could we improve your stay at NRAO?

  would've liked an introduction/expectations talk a little sooner

- What changes would you like to see in the NRAO-REU program?

  maybe let the students adjust to living here for a week before they start working; otherwise it takes a lot longer to "get into the GB groove" and work most efficiently

- Do you and your mentor plan to publish results of your summer research, or to present the results at a professional meeting (the REU program can pay most of your costs)?

  yes - plan to publish

# NATIONAL RADIO ASTRONOMY OBSERVATORY
## MEMORANDUM

DATE: August 20, 1998
TO: Summer Students
FROM: Ron Maddalena
SUBJECT: Questionnaire

Before you leave us we would appreciate you filling out and returning to me the following questionnaire. We will use your responses to improve the program for next year. Feel free to use the back of this sheet if you need more room for your responses. Thanks!

- How did you find out about the NRAO-REU program?

  I live locally and have worked in maintenance for 3 summers.

- What is your overall reaction to the program?

  It was a great experience and will be an asset to my career.

- How have your career decisions been influenced by you experiences at NRAO?

  My experiences here have shown me that I have chosen the right career.

- Have you previously been an REU student at another institution? If so, how do your NRAO experiences compare with your experiences elsewhere?

  No

- In what ways could we improve your stay at NRAO?

  I was satisfied with every thing.

- What changes would you like to see in the NRAO-REU program?

  I am satisfied with the program as it is now.

- Do you and your mentor plan to publish results of your summer research, or to present the results at a professional meeting (the REU program can pay most of your costs)?

  My results will be Archived for future students to look at and to continue to build on.

# NATIONAL RADIO ASTRONOMY OBSERVATORY
## MEMORANDUM

DATE: August 4, 1998
TO: Summer Students
FROM: Ron Maddalena
SUBJECT: Questionnaire

**Before you leave us we would appreciate you filling out and returning to me the following questionnaire. We will use your responses to improve the program for next year. Feel free to use the back of this sheet if you need more room for your responses. Thanks!**

- **How did you find out about the NRAO-REU program?**

  info sent to the department at school

- **What is your overall reaction to the program?**

  nice. I liked it. Lots of astronomy is fun.

- **How have your career decisions been influenced by your experiences at NRAO?**

  not too much. perhaps I'll think about working more closely w/ research institutions (as opposed to Universities) in the future but I'd already planned on a career in astronomy. Maybe I'll try to do more radio work in the future, too.

- **Have you previously been an REU student at another institution? If so, how do your NRAO experiences compare with your experiences elsewhere?**

  yes. last summer the program seemed more organized (there were 24 students!) but my project/mentor was less organized & had less time for me. It was nice to have more [illegible] last [illegible] but I got more out of my project [illegible]

- **In what ways could we improve your stay at NRAO?**

  hmm... take the rent directly out of my paycheck so I don't have to pay taxes on it? Umm... can't think of much, really... The house was kinda crowded for a while.

- **What changes would you like to see in the NRAO-REU program?**

  well... not many. Perhaps there don't need to be quite so many talks. I mean, they were all great, but I feel like I wasn't getting any work done after a while. But... no, they were all worthwhile. Never mind.

- **Do you and your mentor plan to publish results of your summer research, or to present the results at a professional meeting (the REU program can pay most of your costs)?**

  Yup, I think so. He said it'd go to a journal.

  I wanna go to AAS, too.

Oh, ma[illegible] more abo[illegible] usi[illegible] the [illegible] I wan[illegible] liked [illegible] [illegible]

# NATIONAL RADIO ASTRONOMY OBSERVATORY
# MEMORANDUM

DATE: August 4, 1998
TO: Summer Students
FROM: Ron Maddalena
SUBJECT: Questionnaire

Before you leave us we would appreciate you filling out and returning to me the following questionnaire. We will use your responses to improve the program for next year. Feel free to use the back of this sheet if you need more room for your responses. Thanks!

- How did you find out about the NRAO-REU program?

Department Email at school

- What is your overall reaction to the program?

Great learning experience. Ideal environment.

- How have your career decisions been influenced by you experiences at NRAO?

I am definately more directed.

- Have you previously been an REU student at another institution? If so, how do your NRAO experiences compare with your experiences elsewhere?

No

- In what ways could we improve your stay at NRAO?

Make a more organised method of getting equipment, computers, office space. Each student needs different things.

- What changes would you like to see in the NRAO-REU program?

- Do you and your mentor plan to publish results of your summer research, or to present the results at a professional meeting (the REU program can pay most of your costs)?

Before you leave us we would appreciate you filling out and returning to me the following questionnaire. We will use your responses to improve the program for next year. Feel free to use the back of this sheet if you need more room for your responses. Thanks!

- How did you find out about the NRAO-REU program?

NSF web page and Bruce Partridge at Haverford.

- What is your overall reaction to the program?

It was an excellent experience. I have been introduced to research and scientists ~~that~~ are unique

- How have your career decisions been influenced by you experiences at NRAO?

I am still excited about continuing in Astronomy but I don't think I could do research 100% of the time.

- Have you previously been an REU student at another institution? If so, how do your NRAO experiences compare with your experiences elsewhere?

N/A

- In what ways could we improve your stay at NRAO?

Something to make housing easier would be great. It was tough to find, especially if you arrive mid-late July.

- What changes would you like to see in the NRAO-REU program?

I can't think of anything

- Do you and your mentor plan to publish results of your summer research, or to present the results at a professional meeting (the REU program can pay most of your costs)?

Ken has tallked about going to the AAS meeting perhaps to present a poster. I am not sure what the status is now. I don't know about a paper.

# 1998 Summer Research Symposium
# Program (CV)

1998 Summer Research Symposium

Friday, 14 August 1998

12:00 noon NRAO Conference Room

"Exploring the Hearts of Monsters:
Compact Extragalactic Radio Sources"
Andrew West, Haverford College

"HI in Elliptical Galaxies"
Kjersten Bunker, North Carolina State University

"Beyond Toomre and Toomre"
Greg Stinson, Carleton College